

Modeling and Analysis of Almost Unidirectional Flows in Porous Media

Von der Fakultät für Mathematik und Physik der Universität Stuttgart
zur Erlangung der Würde eines Doktors der Naturwissenschaften (Dr. rer. nat.)
genehmigte Abhandlung

Vorgelegt von

Alaa Armiti

aus Nablus (Palestine)

Hauptberichter: Prof. Dr. Christian Rohde
Mitberichter: Prof. Dr. Sorin Pop
Prof. Dr. Dominik Göttsche

Tag der mündlichen Prüfung: 11.10.2017

Institut für Angewandte Analysis und Numerische Simulation, Universität Stuttgart
2017

D93

Acknowledgements

At the end of PhD journey, I would like to thank all people who supported me to make this thesis possible. First and foremost, I would like to express my deepest sense of gratitude to my advisor Professor Dr. Christian Rohde for giving me the opportunity to work in his research group. I thank him for the guidance and great effort he put into training me in the scientific field. I also deeply appreciate his support since the days I arrived Germany.

I am thankful and proud to be a graduate student of the University of Stuttgart. I would like to express my deepest gratitude to the Deutscher Akademischer Austauschdienst (DAAD) for the financial support.

I would like to thank the Non-linearities and Upscaling in Porous Media (NUPUS) for giving me the opportunity to participate in several events and lectures that enriched my knowledge in porous media.

I would like to thank Prof. Sorin Pop, Prof. Dominik Goddeke and Prof. Guido Schneider for reviewing this thesis and taking the time for my exam.

My thanks to all my colleges at the IANS in Stuttgart for the great time and all kinds of help. Especially, I would like to thank Dr. Jan Giesselmann and Dr. Iryna Rybak for proofreading the thesis and the helpful discussions. My special appreciation to my friend Emna Mejri from the IWS in Stuttgart for all kinds of support and the careful reading of the thesis.

My steadfast husband, Ayser. Your continued love, faith in me, and sharing my dream made the completion of thesis possible. You helped me to keep focused at times I thought that it is impossible to continue. My sons, you have inspired me with your love and patience. Thank you Mohammed and Abdulrahman for being such great boys.

My mother and father, you dreamed and believed that I will succeed in this task since I was a young girl. Your love and countless prayers guided me all the time to make this thesis possible.

Contents

Acknowledgements	iii
Abstract	ix
Zusammenfassung	xi
1 Introduction	1
1.1 Modeling Fluid Flows in the Subsurface	3
1.2 Well-Posedness of Mathematical Models	4
1.3 Objectives	5
1.4 Challenges	5
1.5 Contributions	6
1.6 Structure of the Thesis	7
2 Model Problems and Mathematical Preliminaries	9
2.1 The Two-Phase Flow Model	9
2.1.1 Physical Properties and Relationships	9
2.1.2 The Two-Phase Flow Model	14
2.1.3 Fractional Flow Formulation	15
2.2 Sobolev Spaces and Compactness Theorems	16
2.2.1 Sobolev Spaces	16
2.2.2 Bochner Spaces	17
2.2.3 Compactness Theorems	18
2.2.4 Inequalities	19

3	The Vertical Equilibrium Model	21
3.1	Problem Description and Related Work	22
3.2	Background	23
3.2.1	The Two-Phase Flow Model	24
3.2.2	The Vertically Integrated Model (VI-Model)	25
3.2.3	The Multiscale Model	27
3.3	The Vertical Equilibrium Model (VE-Model)	29
3.3.1	Dimensionless Two-Phase Flow Model	30
3.3.2	Asymptotic Analysis	32
3.4	Models Comparison	34
3.4.1	Finite-Volume Scheme	35
3.4.2	VE-Model vs. Two-Phase Flow Model	39
3.4.3	VE-Model vs. VI-Model	41
3.4.4	VE-Model vs. Multiscale Model	46
3.5	Reduced Regularity of the VE-Model	51
3.6	Conclusion	52
4	The Brinkman Vertical Equilibrium Model	55
4.1	Brinkman Two-Phase Flow Model	56
4.2	The Brinkman VE-Model	58
4.2.1	Dimensionless Model	59
4.2.2	Asymptotic Analysis	62
4.3	Numerical Results	64
4.3.1	Brinkman VE-model vs. Brinkman Two-Phase Flow Model .	66
4.3.2	Brinkman VE-model vs. VE-model	74
4.4	Conclusion	79
5	Well-posedness of the Brinkman Vertical Equilibrium Model	81
5.1	Preliminaries and Assumptions	83

5.2	A priori Estimates	89
5.3	Convergence Analysis	91
5.4	Boundedness of Weak Solutions in $L^\infty(\Omega_T)$	99
5.5	Uniqueness of Weak Solutions	103
5.6	Conclusion	107
6	Gravity-Driven Water Infiltration into Unsaturated Zone	109
6.1	Background	110
6.1.1	Richards' model	110
6.1.2	Fourth-Order Model of Cueto-Felgueroso and Juanes	111
6.2	The Fourth-Order Model	112
6.3	Preliminaries and Assumptions	114
6.4	Well-posedness of the Transformed Fourth-Order Model	116
6.4.1	A Priori Estimates	119
6.4.2	Convergence Results	122
6.4.3	Uniqueness	127
6.5	Regularity	130
6.6	Well-posedness of the Fourth-Order Model	133
6.7	Conclusion	135
7	Summary and Outlook	137
7.1	Summary	137
7.2	Outlook	139
	Bibliography	141

Abstract

For many environmental and industrial applications, such as aquifers purification and extraction of fossil fuels from reservoirs, it is crucial to study fluid flows in porous media and the phenomenon of saturation overshoots. Typically, mathematical models are used to describe and predict such flows. These models are often coupled systems of nonlinear differential equations. As a result, exact solutions are hard to obtain and only numerical simulations are feasible where two issues must be tackled. First, it is necessary to prove the well-posedness of these models as a validating criterion of the simulations. Second, such simulations have high computational complexity depending on the number of unknowns, the effective forces, and media's volume. In this thesis, we contribute to three aspects of modeling transport processes in the subsurface: first, reducing models' complexity based on natural properties, second, describing more physical phenomena like saturation overshoots, and third, proving models' well-posedness.

In saturated media, such as aquifers and reservoirs, fluid flows are modeled using the two-phase flow model, which is a coupled system of two unknowns. Applying this model in such large media might lead to very high computational complexity. However, transport processes in saturated media are in general almost horizontal, such as the flow of extracted oil. This natural property has been utilized to reduce model's complexity. Of specific interest is the approach proposed by Yortsos (1995), which reduces the number of unknowns. In this thesis, we perform several numerical examples to analyze the validity and numerical efficiency of this approach. We also extend it to describe almost horizontal flows in media with high porosity as well as macroscopically heterogeneous media, where fluids velocity is often modeled using Brinkman's equations instead of Darcy's law. Our extended approach leads to a third-order pseudo-parabolic differential equation of saturation only. We provide various numerical tests to show the computational efficiency of the extended model. Additionally, these tests show the ability of the model to

describe the phenomenon of saturation overshoots. Finally, we investigate the well-posedness of the extended model, where we prove the existence of weak solutions and the uniqueness for a special case of it.

In unsaturated soils, the vertical infiltration processes are modeled using Richards' equation, which is a second-order parabolic equation of saturation. This equation is unable to describe saturation overshoots, as it satisfies the maximum principle. Therefore, different higher-order extensions have been suggested. We propose a nonlinear fourth-order extension of Richards' equation. We investigate the well-posedness of this model by applying Kirchhoff's transformation to linearize the higher-order terms. Then, we prove the well-posedness of the transformed equation. Finally, we use the inverse of Kirchhoff's transformation to prove the well-posedness of the original equation.

Zusammenfassung

Für viele umwelt- und industrielle Anwendungen, wie beispielweise die Abwasserreinigung und die Gewinnung von fossilen Brennstoffen aus Reservoirs, ist es entscheidend, Flüssigkeitsströme in porösen Medien und das Phänomen der Sättigungsüberschüsse zu untersuchen. Typischerweise werden mathematische Modelle verwendet, um solche Ströme zu beschreiben und vorherzusagen. Diese Modelle sind oft gekoppelte Systeme von nichtlinearen Differentialgleichungen. Infolgedessen gibt es selten exakte Lösungen und es sind nur numerische Simulationen möglich, bei denen zwei Fragen angegangen werden müssen. Erstens ist es notwendig die Wohlgestelltheit dieser Modelle als ein Validierungskriterium der Simulationen zu beweisen. Zweitens haben solche Simulationen eine hohe Rechenkomplexität, die von der Anzahl der Unbekannten, den effektiven Kräften und dem Volumen der Medien abhängig ist. In dieser Arbeit tragen wir zu drei Aspekten der Modellierung von Transportprozessen im Untergrund bei: Erstens, Komplexitätsreduktion der Modelle auf der Grundlage natürlicher Eigenschaften, zweitens, Beschreibung von mehreren physikalischen Phänomenen wie Sättigungsüberschüsse und drittens, der Beweis der Wohlgestelltheit der Modelle.

In gesättigten Medien, wie Aquiferen und Reservoirs, werden Fluidströmungen mit dem zweiphasigen Strömungsmodell modelliert, welches ein gekoppeltes System von zwei Unbekannten ist. Die Anwendung dieses Modells in so großen Medien kann zu einer sehr hohen Rechenkomplexität führen. Allerdings sind die Transportprozesse in gesättigten Medien im Allgemeinen fast horizontal, wie der Fluss von extrahiertem Öl. Diese natürliche Eigenschaft wurde genutzt, um die Komplexität des Modells zu reduzieren. Von besonderem Interesse ist der von Yortsos (1995) vorgeschlagene Ansatz, der die Anzahl der Unbekannten reduziert. In dieser Arbeit führen wir mehrere numerische Beispiele durch, um die Gültigkeit und die numerische Effizienz dieses Ansatzes zu analysieren. Wir erweitern es auch, um fast horizontale Strömungen in Medien mit hoher Porosität

sowie in makroskopisch heterogenen Medien zu beschreiben, in welchen die Fluidgeschwindigkeit oft mit Brinkman Gleichungen anstelle des Darcy-Gesetzes modelliert wird. Unser erweiterter Ansatz führt zu einer pseudo-parabolischen Differentialgleichung dritter Ordnung, die nur von der Sättigung abhängig ist. Wir liefern verschiedene numerische Tests, um die rechnerische Effizienz des erweiterten Modells zu zeigen. Zusätzlich zeigen diese Tests die Fähigkeit des Modells, das Phänomen der Sättigungsüberschüsse zu beschreiben. Schliesslich untersuchen wir die Wohlgestelltheit des erweiterten Modells, für welches wir die Existenz von schwachen Lösungen und die Eindeutigkeit in einem Sonderfall beweisen.

In ungesättigten Böden werden die vertikalen Infiltrationsprozesse unter Verwendung der Richards-Gleichung modelliert, die eine parabolische Gleichung zweite Ordnung der Sättigung ist. Diese Gleichung ist nicht in der Lage, Sättigungsüberschüsse zu beschreiben, da sie das Maximumprinzip erfüllt. Daher wurden verschiedene Erweiterungen höherer Ordnung vorgeschlagen. Wir schlagen eine nichtlineare Erweiterung vierter Ordnung der Richards-Gleichung vor. Wir untersuchen die Wohlgestelltheit dieses Modells, indem wir die Kirchhoff Transformation anwenden, um die Terme höherer Ordnung zu linearisieren. Anschließend beweisen wir die Wohlgestelltheit der transformierten Gleichung. Schliesslich verwenden wir die Inverse Kirchhoff Transformation, um die Wohlgestelltheit der ursprünglichen Gleichung zu beweisen.

Chapter 1

Introduction

Understanding fluid flows and transport phenomena in porous media is important for many fields and applications. For example, in environmental fields, understanding the infiltration process of contaminants into water aquifers is crucial to predict and improve underground water purification. In saline aquifers, studying the flow of sequestered CO_2 helps to decrease the effect of global climate warming. In petroleum applications, fluid flows are of high importance to optimize the process of extracting fossil fuels, like oil or gas, from reservoirs. In addition to this, industrial applications extensively study processes in porous media to improve the production of paper, filters, napkins, and fuel cells. Finally, understanding the flow of blood or drugs in the living organisms is of high importance to improve medical solutions.

Recent experiments show that fluids naturally flow in preferential flow paths having the shape of fingers with different widths and velocities [19, 34]. This flow behavior is connected to the phenomenon of fluid higher concentration at the wetting front, called saturation overshoots [19, 21, 22]. Figure 1.1 illustrates these two phenomena in an unsaturated domain, where the driving force is gravity. This flow behavior encourages the flowing fluid to channelize in the fingers with highest speed. This has crucial impact on the fields and applications mentioned in the upper paragraph. For example, the required time for a contaminant to reach water aquifers or for sequestered CO_2 to remain captured is reduced [22]. In addition, such a flow behavior decreases the efficiency of oil recovery [23]. For these reasons and many more, studying these two phenomena has been of special interest for many researchers, such as [32, 19, 46].

Empirical experiments are a main tool for observing and understanding fluid dynamics in porous media. However, the efficiency of such experiments is often limited. For example, physical experiments require very long time, sometimes

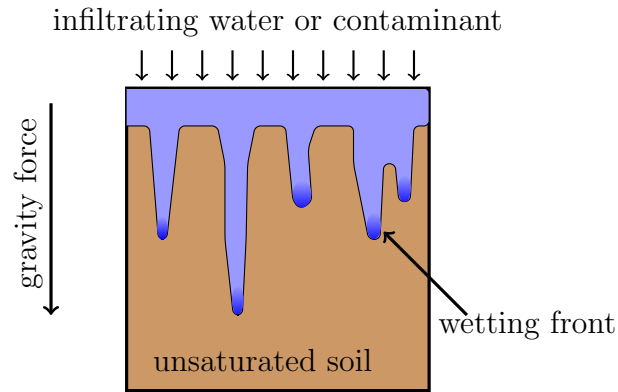


Figure 1.1: Infiltrating fluid in preferential flow paths (fingers) with saturation overshoots at the wetting front.

years, to be finished, like the process of oil recovery or CO_2 sequestration. In industrial and medical applications, experiments are often very expensive and sometimes dangerous to conduct. Therefore, mathematical models have been used to describe fluid dynamics and predict future informations. These models are, in general, coupled systems of nonlinear differential equations. Due to their complexity, exact solutions of these models are hard to obtain. Hence, different numerical methods have been developed to provide approximated solutions.

Our main interest in this thesis is fluid dynamics in the subsurface, where porous media are very large and fluids flow under the effect of different forces, like gravity, viscous, capillary, and shear stress forces. According to the geometrical properties, the subsurface consists of two main parts: the unsaturated and the saturated zones. The unsaturated zone is the upper part (soil), where fluids infiltrate vertically. The saturated zone is the lower part containing aquifers and reservoirs, where fluids flow almost horizontally. Modeling fluid dynamics varies depending on the zone of interest, where the main effective forces and the number of unknowns differ.

This chapter is structured as follows: Section 1.1 introduces the main features of modeling fluid flows in saturated and unsaturated zones in the subsurface. Section 1.2 discusses the importance of proving well-posedness for mathematical models describing fluid flows in the subsurface. Our objectives of the thesis are presented in Section 1.3 and the challenges we had to deal with are summarized in Section 1.4. Then, we give a list of our contributions in Section 1.5. Finally, we show the structure of the thesis in Section 1.6.

1.1 Modeling Fluid Flows in the Subsurface

The first part of the thesis studies fluid flows in the saturated zone, where porous media are very large with high heterogeneities. In this zone, fluid flows are described using the **two-phase flow model** [5, 33], which is a coupled system of nonlinear differential equations with two unknowns. Under these conditions, approximate solutions up to a limited tolerance require conducting complex numerical methods in very large domains. Hence, different approaches have been developed to reduce the complexity of the model:

- One approach is to neglect forces with less effect on the flow, like shear stress, capillary, and sometimes gravity forces. This simplifies the mathematical model and consequently decreases the computational complexity. However, it has a negative impact as it might lead to ill-posed models and/or reduce the ability of models to describe physical phenomena, like saturation overshoots.
- A second approach that has been widely used is to reduce the spatial dimensionality of mathematical models describing fluid flows in porous media with specific geometrical properties. For example, aquifers and reservoirs are flat domains with small thickness, where fluids spread almost horizontally. Mathematical models for such media are usually averaged over the vertical direction [13, 28, 29, 39, 43]. This reduces the spatial dimensionality of models, but might lead to over-estimating the spreading speed of the flowing fluids.
- A third approach is to decrease the number of unknowns in the two-phase flow model for flat media with a small thickness [53]. This simplifies the required numerical methods and provides better estimations on the spreading speed compared to the second approach, as it accounts for fluid movements in the vertical direction.

There exist different mathematical models that combine the first approach with the second or the third. We focus in the first part of the thesis on a model that combines the first and the third approach. This is a model proposed by Yortsos [53] that has a reduced number of unknowns and accounts for the viscous force only, which we call the **vertical equilibrium model**. On one hand, this model has many numerical advantages over other widely used models. For example, standard numerical methods, like finite difference and finite-volume schemes, are sufficient to provide approximate solutions with a well estimated speed of displacement. On the other hand, a well-posedness proof of the model is still lacking and the model

is unable to describe the phenomenon of saturation overshoots using the standard numerical methods.

The second part of the thesis studies vertical infiltration of fluids through the unsaturated zone and the formation of saturation overshoots. Fluid flows in this zone are described using Richards' equation [6], which is a second-order nonlinear parabolic differential equation with one unknown. It accounts for capillary and gravity forces, but is unable to describe saturation overshoots or fingering, see [24, 50] and the references therein. Therefore, several extensions of Richards' equation have been proposed [7, 17, 32, 46]. One extension is a fourth-order model proposed by Cueto-Felgueroso and Juanes [17], for which numerical experiments show the ability to describe saturation overshoots. We consider a fourth-order extension of Richards' equation, related to their model, but allows applying the Kirchhoff transformation. This transformation linearizes the higher order terms in the model, which is an important step to prove the well-posedness of the model.

1.2 Well-Posedness of Mathematical Models

One of the main advantages of using mathematical models to describe fluid flows in the subsurface is their ability to provide fast predictions and numerical simulations. This is possible by applying different numerical methods to the models, like finite-difference, finite-volume, finite-element, and many others. However, studying the well-posedness of the mathematical models is necessary as a validating criterion on the resulting numerical solutions. Precisely defined, a well-posed mathematical model is a model that has a unique solution satisfying the model at each point in the domain, which is called the strong solution.

Throughout the thesis we investigate the well-posedness of mathematical models describing fluid flows in saturated and unsaturated media in the subsurface. However, strong solutions for models like transport equations do not exist globally in time, as shocks might develop. In addition to this, investigating the existence of strong solutions is often unfeasible due to the strong nonlinearities in the models. For these reasons, the concept of weak solutions had been introduced. Investigating the existence of such solutions is relatively easier. Moreover, regularity of such solutions in the case of nonlinear elliptic and parabolic equations might be improved such that weak solutions satisfy the definition of strong solutions.

1.3 Objectives

Mathematical models are a key tool for fast and efficient numerical simulations and predictions of many natural and industrial processes. This emphasizes the necessity of validating criteria on these simulations.

Our main objective in this thesis is investigating the validity of different mathematical models that describe fluid dynamics in the subsurface, both numerically and analytically. For the saturated zone, we consider the vertical equilibrium model [53] that describes fluid flows in flat porous media with a small thickness. On one side, we establish numerical tests on the model to confirm its validity and numerical efficiency. On the other side, we show that weak solutions in the distributional sense cannot be defined for this model.

We propose an extension of the vertical equilibrium model for regimes of high porosity and porous media that are macroscopically nonhomogeneous. We provide numerical tests that emphasize the numerical validation and efficiency of the model. We also prove the existence of weak solutions of the model and the uniqueness of a special case of it.

For the unsaturated zone, we prove the well-posedness of a fourth-order extension of Richards' equation.

1.4 Challenges

Mathematical models provide high efficiency in analyzing, simulating, and predicting fluids movements in porous media. However, these models are in general very complex, mainly, from the analytical point of view. In the following, we summarize the main challenges we faced during investigating the well-posedness:

1. Our proposed extension of the vertical equilibrium model is a third-order pseudo-parabolic differential equation. Since the convective term in the model is not Lipschitz continuous, the conditions of the Nonlinear Lax-Milgram theorem that provides the well-posedness of the time-discrete model are not satisfied.
2. The convective term of our proposed extension of the vertical equilibrium model is of second order such that the regularization theory in [30, 38] is not applicable. This provides difficulties in proving the uniqueness of weak solutions for the model.

3. Mathematical models describing fluid flows in the subsurface have strong nonlinearities that require special techniques to extract their convergences.

1.5 Contributions

In this thesis, we propose mathematical models, design numerical tests and prove well-posedness of different models describing fluid flows in saturated and unsaturated domains in the subsurface. The main contributions of the thesis are summarized as follows:

The Vertical Equilibrium Model

We investigate the numerical efficiency and validity of the vertical equilibrium model [53] by designing different numerical tests comparing it to other widely used models in the same field. These models include the two-phase flow model, a vertically integrated two-phase flow model, and a multiscale model by Guo *et al.* [31]. In addition to the numerical tests, we prove that the vertical equilibrium model is equivalent to the multiscale model.

The Brinkman Vertical Equilibrium Model

We propose an extension of the vertical equilibrium model that describes fluid flows in regimes of high porosity, where Darcy's law can be replaced by Brinkman's equations. To do this, we follow [53] and apply asymptotic analysis to the two-phase flow model with Brinkman's equations replacing Darcy's law. This leads to a third-order pseudo-parabolic differential equation of saturation alone, which we call the **Brinkman vertical equilibrium model**. This model can also be adopted to describe fluid flows in macroscopically nonhomogeneous porous media. We design different numerical tests on the proposed model and conclude the following:

1. Numerical solutions of the two-phase flow model with Brinkman's equations converge to the corresponding solution of the Brinkman vertical equilibrium model as the geometrical ratio of the domain's width to the length tends to zero.
2. The computational complexity of the Brinkman vertical equilibrium model is much less than that of the two-phase flow model with Brinkman's equations.
3. Including Brinkman's equations in the two-phase flow model, and thus in the Brinkman vertical equilibrium model, allows describing the phenomenon of saturation overshoots.

4. Decreasing the ratio of a domain's width to length increases the vertical mixing at the wetting front. This, consequently, decreases saturation at the front such that the phenomenon of saturation overshoots is less likely to occur.

Well-posedness of the Brinkman Vertical Equilibrium Model

We prove the existence of weak solutions for the Brinkman vertical equilibrium model. To do this, we first approximate the time derivatives in the model using the backwards difference quotient, then apply Galerkin's method to the approximated equation. After that, we prove a set of a priori estimates on the sequence of approximate solutions that are essential for the convergence arguments. Finally, we show that the limit of the sequence is a weak solution for the model.

We prove the uniqueness of weak solutions for the Brinkman vertical equilibrium model in the case that the fractional flow function and the horizontal velocity are linear functions of saturation.

Gravity-Driven Water Infiltration into Unsaturated Zone

We consider a fourth-order extension of Richards' model to describe fluid flows in unsaturated porous media and the formation of saturation overshoots. This model is related to the fourth-order extension proposed in [19], but allows applying the Kirchhoff transformation to linearize the higher order terms. We prove the well-posedness of the transformed model. Then, we prove the well-posedness of the original fourth-order model using the inverse of the Kirchhoff transformation.

1.6 Structure of the Thesis

The thesis has the following structure: Chapter 2 provides an overview on the two-phase flow model and the essential mathematical knowledge for establishing the analysis. Chapter 3 presents the vertical equilibrium model [53] and provides a comparison study that shows the numerical efficiency of the model over other models in the field. In Chapter 4, we propose the Brinkman vertical equilibrium model as an extension of the vertical equilibrium model and design a set of numerical tests to show its numerical efficiency. In Chapter 5, we prove the existence of weak solutions for the Brinkman vertical equilibrium model and the uniqueness for a special case of it. In Chapter 6, we prove the well-posedness of a fourth-order extension of Richards' equation. In Chapter 7, we summarize our accomplishments in the thesis and give a list of ideas for future work.

Chapter 2

Model Problems and Mathematical Preliminaries

This chapter provides an overview on the mathematical modeling of fluid flows in the subsurface following [5, 33]. It also gives a short introduction into Sobolev spaces and compactness theorems following [1, 25].

2.1 The Two-Phase Flow Model

In this section, we consider the case of two fluids flowing through a porous medium and introduce the main model concepts and physical properties. Throughout the thesis, we restrict ourselves to isothermal flows, and therefore, neglect the energy balance equations. The two-phase flow model is then a combination of the conservation laws of mass and momentum (Darcy's law).

2.1.1 Physical Properties and Relationships

A phase is a volume of a material with homogeneous physical properties. Different phases are separated by interfaces, across which fluid physical properties change. A porous medium is a solid phase with a certain amount of pores that are occupied by one or more fluid phases. We consider media with connected pores allowing the flow of fluids. The number of fluid phases flowing through a porous medium determines whether we have a one-phase, two-phase, or multi-phase flow.

The subsurface consists of two zones: saturated and unsaturated, as illustrated in Figure 2.1. In the unsaturated zone or the vadose zone (soil), pores are occupied with water, gas and/or contaminants, such that the gas phase is connected to the atmosphere. Driven by gravity, fluids infiltrate through the unsaturated zone into

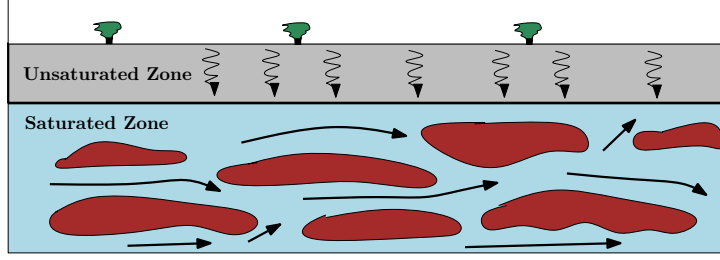


Figure 2.1: An illustration of saturated and unsaturated zones in the subsurface.

aquifers. Saturated zones, like water aquifers and oil reservoirs, are usually wide domains with a small thickness compared to the horizontal directions. In this zone, fluids spread almost horizontally, mainly, under the effect of viscous forces.

In a two-phase flow situation, one of the fluid phases is more attracted to the surface of the solid matrix under the effect of the adhesion forces. This fluid phase is called the wetting phase, denoted by w , and the other is called the nonwetting phase, denoted by n . For example, in the unsaturated zone, water is usually the wetting phase and air is the nonwetting phase.

It is impossible to describe fluid flows in the subsurface on the micro scale due to two main reasons: the unknown distribution of pores and the domains' huge sizes. To overcome these difficulties, fluid flows are studied on the macro scale (continuum scale), such that physical properties of the phases are averaged over an appropriate control volume V_0 , the representative elementary volume (REV). The REV has to be large enough such that the averaged quantities are independent of V_0 . Figure 2.2 illustrates the necessary properties of the REV for the porosity. If the REV is very small, then it covers either solid or pore space. Increasing the control volume causes oscillations in the porosity up to an ideal volume, where the porosity is constant and independent of the control volume. The REV is then the smallest volume for which the physical properties are constant. A further enlargement of the control volume leads to new oscillations due to the heterogeneity of the porous medium.

On the continuum scale, all phases are allowed to exist at the same point simultaneously, as illustrated in Figure 2.3. Moreover, new equations (like Darcy's equation) with new parameters (like saturation and porosity) are created.

In a porous medium $\Omega \subset \mathbb{R}^3$, the porosity $\phi : \Omega \rightarrow [0, 1]$ at a point $\mathbf{x} \in \Omega$ is the ratio of the pore space in the REV, corresponding to that point, to the volume of the REV. The saturation $S_\alpha : \Omega \rightarrow [0, 1]$ of a phase $\alpha \in \{w, n\}$ at a point $\mathbf{x} \in \Omega$ is the ratio of the volume occupied with phase α in the REV to the volume of the

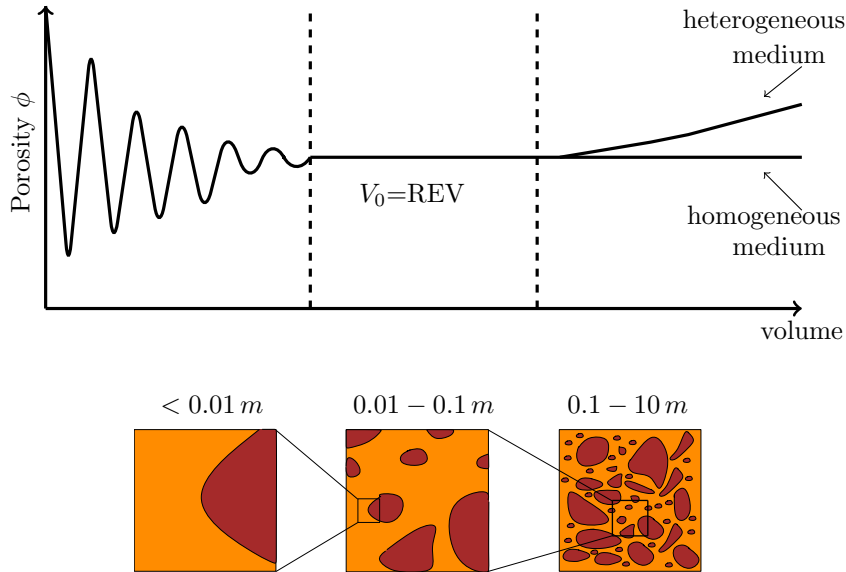


Figure 2.2: Definition of the representative elementary volume.

pore space. In saturated media, we have the closure relation

$$S_w + S_n = 1. \quad (2.1)$$

The intrinsic permeability \mathbf{K} [m^2] of a porous medium $\Omega \subset \mathbb{R}^3$ is a symmetric, positive definite tensor that describes the pore network within a porous medium. If the intrinsic permeability is independent of the spatial variables, then the porous medium is called homogeneous. Otherwise, it is called heterogeneous. Using a principal axis transformation, the intrinsic permeability tensor can be represented by the diagonal tensor

$$\mathbf{K} = \begin{pmatrix} K_1 & 0 & 0 \\ 0 & K_2 & 0 \\ 0 & 0 & K_3 \end{pmatrix}, \quad (2.2)$$

where K_1 , K_2 , K_3 are the permeabilities in the principal directions of the flow. A porous medium is called isotropic, if $K_1 = K_2 = K_3$. Otherwise, it is called anisotropic.

If two or more fluids flow through a porous medium at the same time, the presence of one of these fluids influence the flow behavior of the others. The relative permeability $k_{r\alpha} : [0, 1] \rightarrow [0, 1]$ of a phase α is a function of the phase saturation S_α measuring the influence on its flow behavior. The typical parameterizations of $k_{r\alpha}$ are given by Brooks and Corey [11] and van Genuchten [51]. For mathematical purposes, we use the quadratic relative permeabilities, depending on the wetting

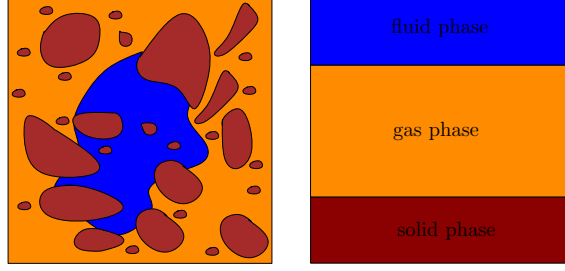


Figure 2.3: Transition from the micro scale (left) to the continuum scale (right).

phase saturation $S = S_w$. These are given as

$$\begin{aligned} k_{rw}(S) &= S^2, \\ k_{rn}(S) &= (1 - S)^2. \end{aligned} \quad (2.3)$$

The hydraulic conductivity $[\frac{m}{s}]$ is the ease with which a fluid phase α flows through a porous medium

$$\mathbf{K}_f = \mathbf{K} k_{r\alpha} \frac{\rho_\alpha g}{\mu_\alpha}, \quad (2.4)$$

where $\rho_\alpha [\frac{kg}{m^3}]$ and $\mu_\alpha [\text{Pa}\cdot\text{s}]$ are the density and the dynamic viscosity of a phase $\alpha \in \{n, w\}$, respectively, and $g [\frac{m}{s^2}]$ is the gravitational acceleration.

Definition 2.1. The **mobility** $\lambda_\alpha : [0, 1] \rightarrow [0, \infty)$ of a phase α is the ratio of the relative permeability $k_{r\alpha}$ to the dynamic viscosity μ_α of that phase

$$\lambda_\alpha(S) = \frac{k_{r\alpha}(S)}{\mu_\alpha}. \quad (2.5)$$

The **total mobility** $\lambda_{tot} : [0, 1] \rightarrow (0, \infty)$ is defined as $\lambda_{tot}(S) = \lambda_w(S) + \lambda_n(S)$.

Definition 2.2. The **fractional flow function** $f : [0, 1] \rightarrow [0, 1]$ of the wetting phase $\alpha = w$ is the ratio of the phase mobility to the total mobility. For the saturation of the wetting phase, $S = S_w$, it is given as

$$f(S) = \frac{\lambda_w(S)}{\lambda_{tot}(S)}. \quad (2.6)$$

The **diffusion function** $\bar{\lambda} : [0, 1] \rightarrow [0, \infty)$ is defined as

$$\bar{\lambda}(S) = f(S)\lambda_n(S) = \frac{\lambda_w(S)\lambda_n(S)}{\lambda_{tot}(S)}. \quad (2.7)$$

Figure 2.4 illustrates the shape of the fractional flow function and the total mobility using the quadratic relative permeabilities (2.3) and viscosities $\mu_w = 1$, $\mu_n = 2$. The diffusion function $\bar{\lambda}$ is illustrated in Figure 2.5.

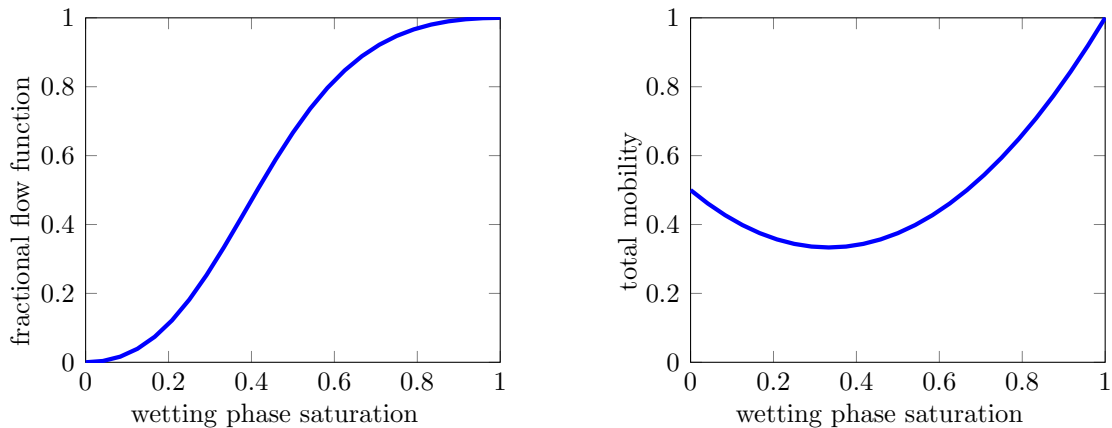


Figure 2.4: Fractional flow function f (left) and total mobility λ_{tot} (right) using the quadratic relative permeabilities and viscosities $\mu_w = 1$, $\mu_n = 2$.

Definition 2.3. The *capillary pressure* p_c on the continuum scale is the phases pressure difference

$$p_c = p_n - p_w, \quad (2.8)$$

where p_n, p_w are the averaged pressures of the nonwetting and wetting phases in the REV, respectively.

According to the empirical relations by Brooks and Corey [11] and van Genuchten [51], capillary pressures $p_c : [0, 1] \rightarrow [0, \infty)$ is a function of saturation $p_c = p_c(S)$ (Figure 2.5). Under the assumption of negligible residual saturations, the parameterization of van Genuchten [51] is given as

$$p_c(S) = \frac{1}{\alpha} (S^{-1/m} - 1)^{1/n}, \quad (2.9)$$

where $\alpha, n > 0$ are empirical parameters characterizing the pore space geometry and $m = 1 - \frac{1}{n}$.

Throughout the thesis, the following assumptions are imposed to hold:

- Assumption 2.4.**
1. There exist constants $m, M > 0$ such that the permeability functions $K_i, i \in \{1, 2, 3\}$, in equation (2.2), satisfy $0 < m \leq K_i \leq M \leq \infty$ for almost all $x \in \Omega$ and $K_1 = K_3$.
 2. The total mobility function $\lambda_{tot} \in C^2([0, 1])$ is strictly positive.
 3. The fractional flow function $f \in C^2([0, 1])$ is monotone increasing.
 4. The capillary pressure function $p_c \in C^2([0, 1])$ is nonnegative.

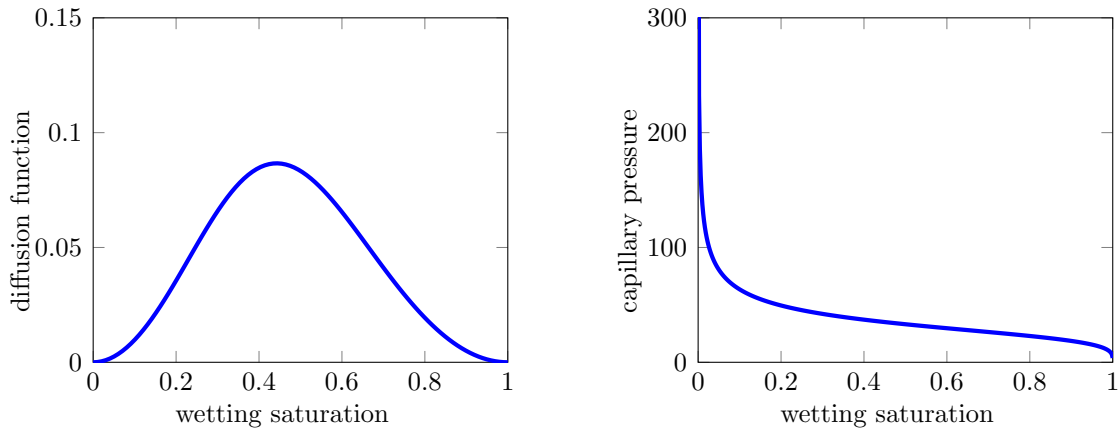


Figure 2.5: Diffusion function $\bar{\lambda}$ for $\mu_w = 1$, $\mu_n = 2$ (left) and capillary pressure (2.9) for $\alpha = 0.37$ and $n = 4.37$ (right).

2.1.2 The Two-Phase Flow Model

The two-phase flow model is a coupled system of the mass conservation equation and Darcy's law. Assuming incompressible fluids in a nondeformable porous medium Ω , the **mass conservation equation** (the continuity equation) for each phase is

$$\phi \partial_t S_\alpha + \nabla \cdot \mathbf{v}_\alpha = 0 \quad \text{in } \Omega \times (0, T), \quad (2.10)$$

where $T > 0$ is the end time and \mathbf{v}_α is the averaged velocity of the phase α through the porous medium.

Darcy's Law states that the averaged velocity \mathbf{v}_α of a phase α is proportional to the potential gradient $\nabla \Phi_\alpha$ applied on the flow in a porous medium, where the flow potential Φ_α comprises the pressure potential p_α and the gravity potential $\rho_\alpha g z$,

$$\mathbf{v}_\alpha = -\frac{k_{r\alpha}(S)}{\mu_\alpha} \mathbf{K} \nabla \Phi = -\frac{k_{r\alpha}(S)}{\mu_\alpha} \mathbf{K} \nabla (p_\alpha - \rho_\alpha g z) \quad \text{in } \Omega \times (0, T), \quad (2.11)$$

for both phases $\alpha \in \{n, w\}$ where $S := S_w$. It is found upon the measurements by Henry Darcy in 1856, but can also be derived from the Stokes equations using the method of homogenization [6]. In terms of the hydraulic conductivity \mathbf{K}_f , Darcy's law can be reformulated as:

$$\mathbf{v}_\alpha = -\mathbf{K}_f(S) \nabla \left(\frac{p_\alpha}{\rho_\alpha g} - z \right). \quad (2.12)$$

2.1.3 Fractional Flow Formulation

In saturated domains $\Omega \subset \mathbb{R}^3$, the closure relation $S_w + S_n = 1$ holds. Summing the continuity equation (2.10) for both phases yields the incompressibility relation

$$\nabla \cdot \mathbf{v} = 0, \quad (2.13)$$

where $\mathbf{v} = \mathbf{v}_w + \mathbf{v}_n$ is the total velocity. Substituting equation (2.5) and (2.8) into Darcy's equation (2.11) for both phases yields

$$\begin{aligned} \mathbf{v}_w &= -\lambda_w(S) \mathbf{K} (\nabla p_w - \rho_w g \mathbf{e}_3), \\ \mathbf{v}_n &= -\lambda_n(S) \mathbf{K} (\nabla p_w + \nabla p_c - \rho_n g \mathbf{e}_3), \end{aligned} \quad (2.14)$$

where $\mathbf{e}_3 = (0, 0, 1)^T$. Reformulating the second equation in (2.14) as $(-\mathbf{K} \nabla p_w = \frac{\mathbf{v}_n}{\lambda_n(S)} + \mathbf{K} \nabla p_c - \mathbf{K} \rho_n g \mathbf{e}_3)$, then substituting it into the first equation yields

$$\mathbf{v}_w = \frac{\lambda_w(S)}{\lambda_n(S)} \mathbf{v}_n + \mathbf{K} \lambda_w(S) (\nabla p_c - \rho_n g \mathbf{e}_3 + \rho_w g \mathbf{e}_3).$$

Using the relation $\mathbf{v}_n = \mathbf{v} - \mathbf{v}_w$, we have

$$\left(1 + \frac{\lambda_w(S)}{\lambda_n(S)}\right) \mathbf{v}_w = \frac{\lambda_w(S)}{\lambda_n(S)} \mathbf{v} + \mathbf{K} \lambda_w(S) (\nabla p_c + (\rho_w - \rho_n) g \mathbf{e}_3).$$

Thus, equation (2.6), (2.7), and (2.9) lead to

$$\mathbf{v}_w = f(S) \mathbf{v} + \bar{\lambda}(S) \mathbf{K} (\nabla p_c(S) + (\rho_w - \rho_n) g \mathbf{e}_3). \quad (2.15)$$

Substituting (2.15) into the continuity equation (2.10) for $\alpha = w$ gives

$$\phi \partial_t S + \nabla \cdot (f(S) \mathbf{v} + \bar{\lambda}(S) \mathbf{K} (\nabla p_c(S) + (\rho_w - \rho_n) g \mathbf{e}_3)) = 0. \quad (2.16)$$

Definition 2.5. *Neglecting capillary and gravity forces, equations (2.15) and (2.16) reduce to the **Buckley-Leverett problem***

$$\begin{aligned} \phi \partial_t(S) + \nabla \cdot (\mathbf{v} f(S)) &= 0, \\ \mathbf{v} &= -\lambda_{tot}(S) \mathbf{K} \nabla p, & \text{in } \Omega \times (0, T), \\ \nabla \cdot \mathbf{v} &= 0, \end{aligned}$$

and f is now called the *Buckley-Leverett flux function*. The unknowns in this system are saturation $S = S(x, y, z, t) \in [0, 1]$, total velocity $\mathbf{v} = \mathbf{v}(x, y, z, t) \in \mathbb{R}^3$, and pressure $p = p(x, y, z, t) \in \mathbb{R}$ which coincides with phases pressure.

2.2 Sobolev Spaces and Compactness Theorems

This section presents definitions and properties of Sobolev and Bochner spaces of integer order in a domain $\Omega \subset \mathbb{R}^n$ following [1, 25]. It also provides a set of compactness theorems and inequalities that will be repeatedly used throughout the thesis.

2.2.1 Sobolev Spaces

Definition 2.6. Assume that $u, v \in L^1_{loc}(\Omega)$ and β is a multi-index. Then, v is called the β^{th} -**weak partial derivative** of u , written

$$D^\beta u = v,$$

provided that

$$\int_{\Omega} u D^\beta \phi \, dx = (-1)^{|\beta|} \int_{\Omega} v \phi \, dx$$

holds for all test functions ϕ in the space $C_c^\infty(\Omega)$ consisting of all compactly supported functions that are infinitely many times continuously differential.

Definition 2.7. For any $1 \leq p \leq \infty$ and $k \in \mathbb{Z}^+$, the **Sobolev space** $W^{k,p}(\Omega)$ is defined as

$$W^{k,p}(\Omega) = \{u \in L^p(\Omega) \mid D^\beta u \in L^p(\Omega) \text{ for } 0 \leq |\beta| \leq k\}. \quad (2.17)$$

Definition 2.8. If $u \in W^{k,p}(\Omega)$, then its **Sobolev norm** $\|\cdot\|_{W^{k,p}(\Omega)}$ is defined as

$$\|u\|_{W^{k,p}(\Omega)} := \begin{cases} \left(\sum_{|\beta| \leq k} \int_{\Omega} |D^\beta u|^p \right)^{1/p}, & 1 \leq p < \infty, \\ \sum_{|\beta| \leq k} \text{ess sup}_{\Omega} |D^\beta u|, & p = \infty. \end{cases}$$

Definition 2.9. The Sobolev space $W_0^{k,p}(\Omega)$ is the closure of $C_c^\infty(\Omega)$ in $W^{k,p}(\Omega)$. In other words, $u \in W_0^{k,p}(\Omega)$ if and only if there exists a sequence $\{u_i\}_{i=1}^\infty \subset C_c^\infty(\Omega)$ such that $u_i \rightarrow u$ in $W^{k,p}(\Omega)$.

The space $W_0^{k,p}(\Omega)$ is also associated with the Sobolev norm $\|\cdot\|_{W^{k,p}(\Omega)}$.

Theorem 2.10. For any $1 \leq p \leq \infty$ and $k \in \mathbb{Z}^+$, the Sobolev space $W^{k,p}(\Omega)$ is a Banach space.

Remark 2.11. If $p = 2$, then $W^{k,2}(\Omega)$ is a Hilbert space, and we use the notation

$$H^k(\Omega) = W^{k,2}(\Omega), \quad \forall k = 0, 1, 2, \dots$$

The n -dimensional Lebesgue measure of the boundary $\partial\Omega$ of a domain $\Omega \subset \mathbb{R}^n$ is zero. To give a meaning for the values of a function $u \in W^{k,p}(\Omega)$ at the boundary $\partial\Omega$, the notion of the trace operator $T : W^{k,p}(\Omega) \rightarrow L^p(\partial\Omega)$ is introduced.

Theorem 2.12 (Trace Theorem). *Let Ω be a bounded domain with the boundary $\partial\Omega$ is C^1 . Then, there exists a bounded linear operator $T : W^{1,p}(\Omega) \rightarrow L^p(\partial\Omega)$ such that*

1. $Tu = u|_{\partial\Omega}$ if $u \in W^{1,p}(\Omega) \cap C(\bar{U})$.
2. $\|Tu\|_{L^p(\partial\Omega)} \leq C\|u\|_{W^{1,p}(\Omega)}$, for any $u \in W^{1,p}(\Omega)$, where the constant C depends on p and Ω only.

Theorem 2.13 (Zero Traces in $W^{k,p}(\Omega)$). *Let $\Omega \subset \mathbb{R}^n$ be a bounded domain with the boundary $\partial\Omega$ is C^k . Then, a function $u \in W^{k,p}(\Omega)$ belongs to $W_0^{k,p}(\Omega)$ if and only if*

$$T(D^\beta u) = 0 \quad \text{on } \partial\Omega, \quad \text{for all } 0 \leq |\beta| \leq k-1.$$

Definition 2.14. *For any $1 \leq p \leq \infty$, the **dual space** to $W_0^{k,p}(\Omega)$, denoted by $W^{-k,p^*}(\Omega)$, is the space of all bounded linear functionals L on $W_0^{k,p}(\Omega)$, equipped with the norm,*

$$\|L\|_{W^{-k,p^*}(\Omega)} = \sup \left\{ L(u) \mid u \in W_0^{k,p}(\Omega), \|u\|_{W_0^{k,p}(\Omega)} \leq 1 \right\},$$

where $p^* := \frac{p}{p-1}$.

2.2.2 Bochner Spaces

Bochner spaces are Sobolev spaces that map time into Banach spaces. They are essential for defining weak solutions of parabolic and hyperbolic equations.

Definition 2.15. *Let X be a Banach space. The **Bochner space***

$$L^p(0, T; X)$$

is the space of all strongly measurable functions $u : [0, T] \rightarrow X$ such that

$$\|u\|_{L^p(0,T;X)} := \left(\int_0^T \|u(t)\|_X^p \right)^{1/p} < \infty \quad \text{for } 1 \leq p < \infty,$$

and

$$\|u\|_{L^\infty(0,T;X)} := \operatorname{ess\,sup}_{0 \leq t \leq T} \|u(t)\|_X < \infty.$$

Definition 2.16. Let X denote a Banach space. The space $C([0, T]; X)$ comprises all continuous functions $u : [0, T] \rightarrow X$ with

$$\|u\|_{C([0, T]; X)} := \max_{0 \leq t \leq T} \|u(t)\|_X < \infty.$$

Definition 2.17. Let $u \in L^1(0, T; X)$. The function $v \in L^1(0, T; X)$ is the weak derivative of u , written

$$u' = v,$$

provided

$$\int_0^T \phi'(t)u(t) dt = - \int_0^T \phi(t)v(t) dt$$

for all scalar test functions $\phi \in C_c^\infty(0, T)$.

Definition 2.18. (i) The Bochner space

$$W^{1,p}(0, T; X)$$

consists of all functions $u \in L^p(0, T; X)$ such that u' exists in the weak sense and belongs to $L^p(0, T; X)$. It is associated with the norm

$$\|u\|_{W^{1,p}(0, T; X)} := \begin{cases} \left(\int_0^T \|u(t)\|_X^p + \int_0^T \|u'(t)\|_X^p \right)^{1/p}, & 1 \leq p < \infty, \\ \text{ess sup}_{0 \leq t \leq T} (\|u(t)\|_X + \|u'(t)\|_X), & p = \infty. \end{cases}$$

(ii) If $p = 2$, we write $H^1(0, T; X) = W^{1,2}(0, T; X)$.

Theorem 2.19. Let $u \in L^2(0, T; H_0^1(\Omega))$, with $u' \in L^2(0, T; H^{-1}(\Omega))$. Then

$$u \in C([0, T]; L^2(\Omega))$$

after possibly being redefined on a set of measure zero.

2.2.3 Compactness Theorems

Definition 2.20. Assume that X and Y are two Banach spaces such that $X \subset Y$. The space X is **compactly embedded** in Y , written $X \Subset Y$, provided

1. If $u \in X$, then $\|u\|_Y \leq C\|u\|_X$ for some constant C .

2. If a sequence $\{u_l\}_{l=1}^\infty \subset X$ satisfy $\sup_l \|u_l\|_X < \infty$, then there exist a subsequence $\{u_j\}_{j=1}^\infty \subset \{u_l\}_{l=1}^\infty$ that converges in Y to some limit u :

$$\lim_{j \rightarrow \infty} \|u_j - u\|_Y = 0.$$

Theorem 2.21 (Weak Compactness). *Let X be a reflexive Banach space and $\{u_k\}_{k=1}^\infty$ is a bounded sequence in X . Then, there exists a subsequence $\{u_{k_j}\}_{j=1}^\infty \subset \{u_k\}_{k=1}^\infty$ and $u \in X$ such that $u_{k_j} \rightharpoonup u$. This means that*

$$\int_{\Omega} u_{k_j} \phi \, d\mathbf{x} \rightarrow \int_{\Omega} u \phi \, d\mathbf{x},$$

for all test functions $\phi \in X^*$.

Theorem 2.22 (Rellich-Kondrachov Compactness Theorem). *Let Ω be a bounded open subset of \mathbb{R}^n and the boundary $\partial\Omega$ be C^1 . For $1 \leq p < n$, it holds*

$$W^{1,p}(\Omega) \Subset L^q(\Omega), \quad \text{for each } 1 \leq q < p^*,$$

where $p^* = \frac{np}{n-p}$.

Theorem 2.23 (Poincaré's Inequality). *Assume that Ω is a bounded, connected, open subset of \mathbb{R}^n and the boundary $\partial\Omega$ is C^1 . Assume also that $1 \leq p \leq \infty$. Then, there exists a constant C that depends only on n, p , and Ω , such that*

$$\|u - (u)_{\Omega}\|_{L^p(\Omega)} \leq C \|Du\|_{L^p(\Omega)}$$

for each $u \in W^{1,p}(\Omega)$, where $(u)_{\Omega} = \oint_{\Omega} u \, d\mathbf{x}$ = average of u over Ω .

2.2.4 Inequalities

We present here a set of elementary inequalities without proofs.

1. Cauchy's Inequality:

$$ab \leq \frac{a^2}{2} + \frac{b^2}{2}, \quad \forall a, b \in \mathbb{R}. \quad (2.18)$$

2. Cauchy's Inequality with ϵ :

$$ab \leq \epsilon a^2 + \frac{b^2}{4\epsilon}, \quad \forall a, b > 0, \epsilon > 0. \quad (2.19)$$

3. **Hölder's Inequality:** Let $1 \leq p, q \leq \infty$ with $\frac{1}{p} + \frac{1}{q} = 1$. If $u \in L^p(\Omega)$ and $v \in L^q(\Omega)$, then we have

$$\int_{\Omega} |uv| \, dx \leq \|u\|_{L^p(\Omega)} \|v\|_{L^q(\Omega)}. \quad (2.20)$$

4. **Gronwall's Inequality (Integral form):** Let $h = h(t)$ be a nonnegative, summable function on $[0, T]$. Assume also that, for almost every t , h satisfies the inequality

$$h(t) \leq C_1 \int_0^T h(s) \, ds + C_2,$$

for constants $C_1, C_2 > 0$. Then

$$h(t) \leq C_2(1 + C_1 t^{C_1 t}). \quad (2.21)$$

for almost all $t \in [0, T]$. Moreover, if

$$h(t) \leq C_1 \int_0^T h(s) \, ds,$$

for almost every $0 \leq t \leq T$, then

$$h(t) = 0, \quad \text{almost everywhere.} \quad (2.22)$$

5. **Jensen's Inequality:** Assume that $f : \mathbb{R}^m \rightarrow \mathbb{R}$ is convex and $\Omega \subset \mathbb{R}^n$ is open and bounded. Let $u : \Omega \rightarrow \mathbb{R}^m$ be summable. Then

$$f\left(\frac{1}{|\Omega|} \int_{\Omega} u \, d\mathbf{x}\right) \leq \frac{1}{|\Omega|} \int_{\Omega} f(u) \, d\mathbf{x}.$$

Chapter 3

The Vertical Equilibrium Model

This chapter studies the process of fluid displacement by another less viscous fluid in a saturated porous medium. The medium is assumed to be flat such that the thickness is much smaller than the horizontal directions. Such a process is crucial for many hydrogeological, petroleum, and environmental applications. Examples are enhanced oil recovery and carbon dioxide CO₂ sequestration in saline aquifers. It is described using the two-phase flow model introduced in Chapter 2. The complexity of the model and the large volume of saturated porous media in the subsurface lead to high computational complexity. Therefore, different approaches have been proposed to reduce the computational complexity based on the geometry of such flat media [13, 28, 29, 39, 43, 53].

We consider a model reduction approach proposed by Yortsos [53] that utilizes the medium's geometry to reduce the complexity of the two-phase flow model by decreasing the number of its unknowns. We call this model the **vertical equilibrium model** (VE-model). Another important feature of this model is its ability to describe the vertical dynamics of the flow, which has a great impact on well-estimating the spreading speed of the displacing fluid.

The aim of this chapter is demonstrating the numerical advantages of the VE-model over other classical and recent models that describe fluid flows in flat porous media. This chapter has the following structure: in Section 3.1, we discuss simulation difficulties of displacement processes, like the complexity of the two-phase flow model, size of the domain, and heterogeneity. Then, we introduce the assumption of vertical equilibrium, which is usually adopted in flat domain. After that, we summarize different approaches that utilize the vertical equilibrium assumption for reducing computational complexities. In Section 3.2, we present a set of classical and recently proposed models used to describe fluid flows in saturated flat porous media. These models include the two-phase flow model, a vertically aver-

aged two-phase flow model, and a multiscale model proposed by [31]. In Section 3.3, we present the VE-model proposed by Yortsos [53]. Section 3.4 provides a finite-volume scheme of the VE-model that is mass conservative and stable. Based on this scheme, we build a comparison study to show the numerical advantages of the VE-model over the models presented in Section 3.2. In addition, we prove that the multiscale model [31], in a vertical cross-section of a three dimensional domain, is equivalent to the VE-model [53]. Section 3.5 discusses the issue of reduced regularity of the VE-model. Finally, Section 3.6 summarizes the chapter.

3.1 Problem Description and Related Work

The two-phase flow model introduced in Chapter 2 is a coupled system of nonlinear differential equations with two unknowns, which we choose here to be saturation and pressure for one of the flowing fluids. For this model, different discretization techniques based on an implicit pressure and explicit saturation (IMPES) treatment have been developed [35]. Applying these techniques in saturated domains, which are very large with high heterogeneity, might be of high computational complexity. Consequently, many approaches that reduce the complexity of the two-phase flow model have been suggested. These approaches utilize the flat geometry of these domains, in which the horizontal directions are much larger than the vertical thickness. In such domains, fluids segregate relatively fast such that the vertical dynamics of the fluids is negligible. This means that the pressure of each fluid is essentially hydrostatic and could have the form [31]

$$p_\alpha(x, y, z, t) = \hat{p}_\alpha(x, y, t) + \rho_\alpha g z. \quad (3.1)$$

Here, \hat{p} is defined to be the reference pressure at the bottom of the domain, ρ_α is the density of the phase $\alpha \in \{i, d\}$, and g is the gravitational acceleration. This assumption on the pressure is called the **vertical equilibrium assumption**. It is not only applicable to flat domains, but also to domains with very high vertical permeability, where vertical forces, like gravity, capillary, and viscous forces, equilibrate very fast and lead to negligible vertical flows.

The vertical equilibrium assumption has been utilized by many researchers to integrate the three-dimensional two-phase flow model over the vertical coordinate. This reduces the spatial dimensionality of the model from three to two, and consequently reduces the computational complexity. For example, we refer to [39] in the field of petroleum studies and to [5] in the field of hydrogeology, where the assumption is well-known under the name of Dupuit's assumption. Recently, this

approach has received attention in the field of CO₂ sequestration in saline aquifers [13, 28, 29, 43].

Vertically integrated models have tendency to overestimate the horizontal spreading speed of the flow, mainly in domains where the vertical equilibrium assumption is not fully satisfied [16]. Examples of such domains are heterogeneous porous media with low permeability in the vertical direction, media with relatively large thickness, and the case when flowing fluids have a small difference in their densities. In such situations, the vertical equilibrium assumption is not fully valid since the time required for a complete fluid segregation is not small compared to the complete displacement time [16, 31].

There are recent approaches that modify the vertical integration approach by including fluid dynamics in the vertical direction. For example, a multiscale model that relaxes the vertical equilibrium assumption is proposed by Guo *et al.* in [31]. The model consists of a coarse scale vertically integrated equation for the vertically integrated pressure in the horizontal plane and a set of fine scale one-dimensional equations for saturation in the vertical direction. The two equations are coupled via a function that reconstructs the coarse scale pressure along the vertical coordinate.

Another approach for multilayered flat domains is proposed by Qin and Hasanizadeh [45]. In this approach, the dynamics in each layer is described by a macroscale thickness-integrated mass balance equation and the exchange between adjacent layers is taken into account using a number of exchange terms.

In this chapter, we focus on an approach that reduces the complexity of the two-phase flow model by decreasing the number of its unknowns. It was derived by Yortsos in [53], motivated by the numerical results in [14, 52, 55]. By applying asymptotic analysis to a dimensionless two-phase flow model, Yortsos derived a reduced model with the advantage that saturation of the injected fluid is the only unknown. We call this model the vertical equilibrium model (VE-model).

The VE-model has many numerical advantages. For example, its computational complexity is significantly reduced in comparison with the two-phase flow model. Moreover, it provides better estimations on the spreading speed than vertically integrated models, because it describes the vertical dynamics in the domain.

3.2 Background

We study displacement processes of incompressible fluids through nondeformable, saturated flat domains. Figure 3.1 shows a vertical cross-section of a flat domain saturated with a resident fluid and a less viscous invading fluid injected to the

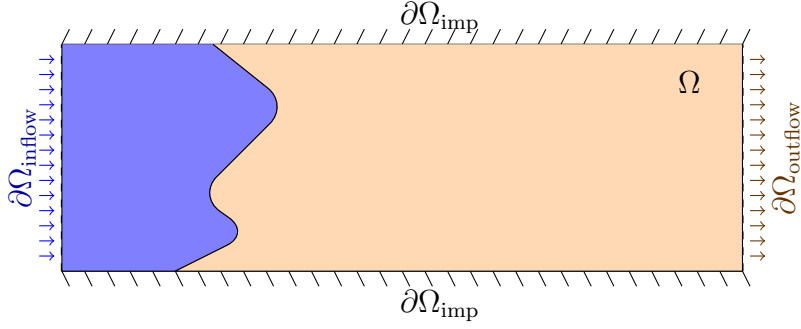


Figure 3.1: An illustration of the displacement process in a vertical-cross section Ω_v of a three-dimensional domain Ω .

domain at the left boundary with a constant injection speed $q > 0$. The injected fluid displaces the resident fluid from the medium due to its less viscosity.

In this section, we recall the main governing equations of the two-phase flow model in a three-dimensional domain. Then, we present a two-dimensional vertically integrated model that neglects the vertical dynamics in the domain. After that, we describe a multiscale model proposed by Guo *et al.* [31]. The goal of presenting these models is to compare them later with the VE-model [53] presented in Section 3.3.

3.2.1 The Two-Phase Flow Model

In a fully saturated domain $\Omega \subset \mathbb{R}^3$, the two-phase flow model is a combination of the continuity equation, Darcy's law, and incompressibility relation,

$$\begin{aligned} \phi \partial_t S_\alpha + \nabla \cdot \mathbf{v}_\alpha &= 0, \\ \mathbf{v}_\alpha &= -\lambda_\alpha \mathbf{K} (\nabla p_\alpha - \rho_\alpha g \mathbf{e}_3), \\ \nabla \cdot \mathbf{v} &= 0, \end{aligned} \tag{3.2}$$

respectively, in $\Omega \times (0, T)$, for both invading $\alpha = i$ and defending $\alpha = d$ fluids. The unknowns in this model are phase saturation $S_\alpha = S_\alpha(x, y, z, t) \in [0, 1]$ and phase pressure $p_\alpha = p_\alpha(x, y, z, t) \in \mathbb{R}^+$ for one of the flowing phases. The total velocity $\mathbf{v} = \mathbf{v}(x, y, z, t) \in \mathbb{R}^3$, for $(x, y, z, t) \in \Omega \times (0, T)$, is the sum of the phases velocity $\mathbf{v} = \mathbf{v}_i + \mathbf{v}_d$. It consists of two horizontal u, v , and one vertical w components. The intrinsic permeability tensor $\mathbf{K} = \mathbf{K}(x, y, z)$ is given, ϕ is the medium's porosity, ρ_α is phase density, g is the gravitational acceleration, and $\mathbf{e}_3 = (0, 0, 1)^T$. Phase mobility $\lambda_\alpha : [0, 1] \rightarrow (0, \infty)$ is given by $\lambda_\alpha(S_\alpha) := \frac{k_{r\alpha}(S_\alpha)}{\mu_\alpha}$, where $k_{r\alpha}$ is phase relative permeability and the constant $\mu_\alpha > 0$ is phase viscosity.

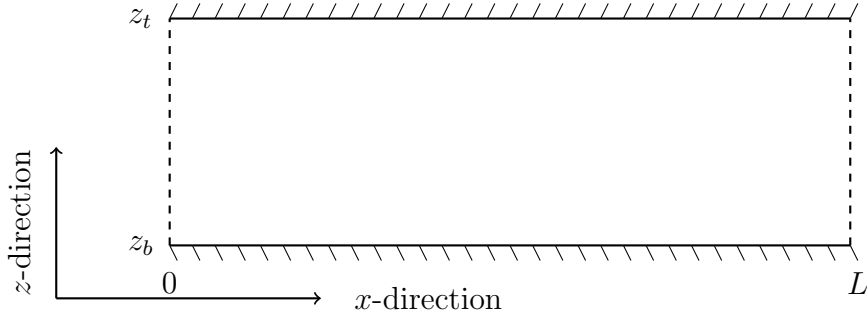


Figure 3.2: A vertical-cross section of a 3D domain with bottom $(0, L) \times \{z_b\}$ and top $(0, L) \times \{z_t\}$.

The two-phase flow model is associated with initial and boundary conditions that fit to the displacement process. Initially, the spatial domain $\Omega \subset \mathbb{R}^3$ is fully saturated with a resident fluid S_d . The boundary $\partial\Omega$, as illustrated in Figure 3.1, is decomposed into an inflow boundary $\partial\Omega_{\text{inflow}}$, an outflow boundary $\partial\Omega_{\text{outflow}}$ and an impermeable boundary $\partial\Omega_{\text{imp}}$. The initial and boundary conditions are summarized for the saturation of the invading fluid $S := S_i$ and the total velocity \mathbf{v} as follows

$$\begin{aligned}
 S &= S_0, & \text{in } \Omega, \\
 S &= S_{\text{inflow}}, & \text{on } \partial\Omega_{\text{inflow}} \times [0, T], \\
 \mathbf{n} \cdot \mathbf{v} &= 0, & \text{on } \partial\Omega_{\text{imp}} \times [0, T],
 \end{aligned} \tag{3.3}$$

where \mathbf{n} is the outer normal vector at the boundary $\partial\Omega_{\text{imp}}$.

3.2.2 The Vertically Integrated Model (VI-Model)

In the following, we present a vertically integrated model of the two-phase flow model (3.2), see for example [28, 29, 31]. Integrating the two-phase flow model (3.2) along the vertical coordinate from the bottom z_b to the top z_t (Figure 3.2) yields

$$\begin{aligned}
 \int_{z_b}^{z_t} (\phi \partial_t S_\alpha + \nabla \cdot \mathbf{v}_\alpha) dz &= 0, \\
 \int_{z_b}^{z_t} \mathbf{v}_\alpha dz &= - \int_{z_b}^{z_t} \lambda_\alpha \mathbf{K} (\nabla p_\alpha - \rho_\alpha g \mathbf{e}_3) dz, \\
 \int_{z_b}^{z_t} \nabla \cdot \mathbf{v} dz &= 0.
 \end{aligned} \tag{3.4}$$

Now, we define the vertically averaged variables

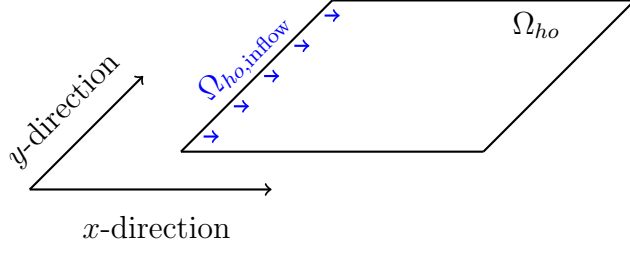


Figure 3.3: A horizontal cross section Ω_{ho} of a three-dimensional domain Ω .

$$\begin{aligned}
\Phi(x, y) &= \int_{z_b}^{z_t} \phi(x, y, z) dz, & \hat{\mathbf{v}}_{ho,\alpha} &= \int_{z_b}^{z_t} \mathbf{v}_{ho,\alpha} dz, \\
\hat{S}_\alpha(x, y, t) &= \frac{1}{\Phi(x, y)} \int_{z_b}^{z_t} \phi(x, y, z) S_\alpha(x, y, z, t) dz, & & (3.5) \\
\hat{\mathbf{K}}(x, y) &= \int_{z_b}^{z_t} \mathbf{K}(x, y, z) dz, & \hat{\lambda}_\alpha &= \hat{\mathbf{K}}^{-1} \int_{z_b}^{z_t} \mathbf{K} \lambda_\alpha dz,
\end{aligned}$$

where $\mathbf{v}_{ho,\alpha} = (u_\alpha, v_\alpha)^T$ is the velocity vector in the horizontal x and y directions, respectively. Using the vertical equilibrium assumption, the phase pressure is hydrostatic and therefore satisfies equation (3.1). Substituting equation (3.1) and (3.5) into (3.4) produces

$$\begin{aligned}
\Phi \partial_t \hat{S}_\alpha + \nabla_{ho} \cdot \hat{\mathbf{v}}_{ho,\alpha} &= 0, \\
\hat{\mathbf{v}}_{ho,\alpha} &= -\hat{\lambda}_\alpha \hat{\mathbf{K}} \nabla_{ho} \hat{p}_\alpha, & (3.6) \\
\nabla_h \cdot \hat{\mathbf{v}}_{ho} &= 0.
\end{aligned}$$

in $\Omega_{ho} \times (0, T)$ where Ω_{ho} is a horizontal cross-section of the three dimensional domain Ω , see Figure 3.3, with vertically averaged properties like porosity and permeability. We call this model the **vertically integrated model** (VI-model). In this model, $\hat{\mathbf{v}}_{ho} = \hat{\mathbf{v}}_{ho,i} + \hat{\mathbf{v}}_{ho,d}$ is the averaged total velocity in the horizontal directions and $\nabla_{ho} = (\partial_x, \partial_y)^T$ is the gradient operator in the horizontal x - and y -directions. This model has a reduced dimensionality due to the vertical averaging. However, it still has two unknowns which are the averaged saturation $\hat{S}_\alpha = \hat{S}_\alpha(x, y, t) \in [0, 1]$ and the averaged pressure $\hat{p}_\alpha = \hat{p}_\alpha(x, y, t) \in \mathbb{R}$, for one of the fluid phases $\alpha \in \{i, d\}$.

The initial and boundary conditions in (3.3) are also vertically averaged for the VI-model and given as

$$\begin{aligned}
\hat{S} &= \hat{S}_0, & \text{in } \Omega_{ho}, \\
\hat{S} &= \hat{S}_{inflow}, & \text{in } \partial\Omega_{ho,inflow} \times [0, T],
\end{aligned} \tag{3.7}$$

where $\partial\Omega_{ho,\text{inflow}}$ is the inflow boundary of the horizontal cross-section Ω_{ho} , as illustrated in Figure 3.3.

3.2.3 The Multiscale Model

The multiscale model is proposed by Guo *et al.* [31] to describe CO₂ storage whenever the vertical equilibrium assumption is not fully applicable. The model relaxes the vertical equilibrium assumption, but maintains much of the computational efficiencies of the VI-model.

The multiscale model consists of two scales: a coarse scale which is a horizontal cross-section Ω_{ho} of the three-dimensional domain Ω , with vertically averaged properties like porosity and permeability, and a fine scale which is a series of one-dimensional vertical columns across the formation (Figure 3.4). The governing equations for this model are of two types: the two-dimensional equations for the vertically averaged pressure \hat{p}_i in the VI-model (3.6), and the two-phase flow model (3.2) rearranged to focus on the vertical dynamics. These two type of equations are connected using a reconstruction equation that reconstructs the vertically averaged (coarse-scale) pressure to describe the vertical dynamics in the medium. In the following, we present the multiscale model under the assumption of zero source terms and complete incompressibility of the medium and the fluids.

Substituting the second equation in (3.6) into the third equation in (3.6) yields the coarse-scale model for the vertically averaged phases pressure \hat{p}_α , $\alpha \in \{i, d\}$

$$\nabla_h \cdot \hat{\mathbf{K}}(\hat{\lambda}_i \nabla_{ho} \hat{p}_i + \hat{\lambda}_d \nabla_{ho} \hat{p}_d) = 0. \quad (3.8)$$

Using the closure relations $\hat{p}_c = \hat{p}_d - \hat{p}_i$ and $\hat{p}_c = \hat{p}_c(\hat{S}_i)$, equation (3.8) is reformulated such that the coarse-scale pressure \hat{p}_i of the invading phase is the unknown

$$\nabla_{ho} \cdot \hat{\mathbf{K}}(\hat{\lambda}_{tot}(\hat{S}) \nabla_{ho} \hat{p}_i + \hat{\lambda}_d(\hat{S}) \nabla_{ho} \hat{p}_c(\hat{S})) = 0, \quad \text{in } \Omega_{ho} \times (0, T), \quad (3.9)$$

where \hat{S} is the averaged saturation of the invading fluid. The vertically averaged pressure \hat{p}_d of the defending phase is then evaluated using $\hat{p}_d = \hat{p}_c(\hat{S}) + \hat{p}_i$.

The fine scale model is the two-phase flow model (3.2), reformulated to focus on the dynamics in the vertical direction

$$\begin{aligned} \phi \partial_t S_\alpha + \partial_z w_\alpha &= -\nabla_{ho} \cdot \mathbf{v}_{ho,\alpha}, \\ \mathbf{v}_{ho,\alpha} &= -\lambda_\alpha \mathbf{K}_{ho} \nabla_{ho} p_\alpha, \\ \partial_z w &= -\nabla_{ho} \cdot \mathbf{v}_{ho}, \end{aligned} \quad \text{in } \Omega \times (0, T), \quad (3.10)$$

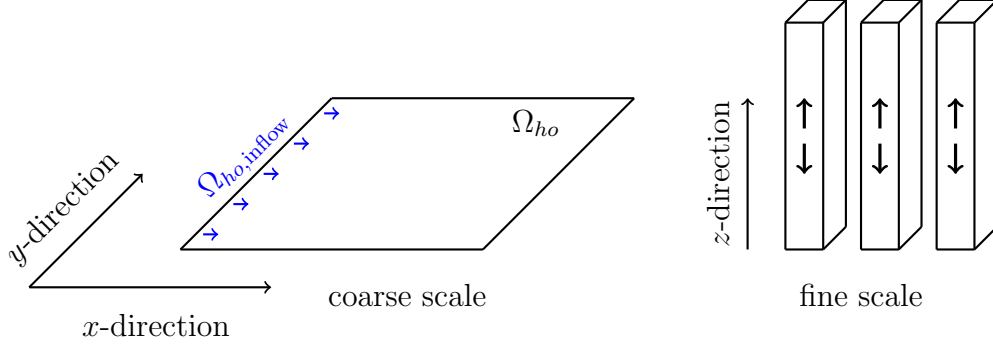


Figure 3.4: An illustration of the two scales in the multiscale model: the coarse-scale is the horizontal xy -plane while the fine-scale is a series of one-dimensional vertical domains. The arrows refer to the flow direction in the corresponding domains.

where $\Omega \subset \mathbb{R}^3$ is represented as a series of one dimensional vertical subdomains (Figure 3.4). Here, w_α is the phase velocity in the vertical direction and $\mathbf{v}_{ho,\alpha}$ is the phase velocity in the horizontal directions.

The coarse- and fine-scale models are connected using an equation that reconstructs the vertically averaged pressures \hat{p}_i, \hat{p}_d into fine-scale pressures p_i, p_d that account for vertical pressure changes

$$p_\alpha(x, y, z, t) = \hat{p}_\alpha(x, y, t) + \pi_\alpha(x, y, z, t). \quad (3.11)$$

According to [31], a preferred choice of π_α , that is simple to compute and represents the natural forces in the medium, is given as

$$\begin{aligned} \pi_i(\cdot, \cdot, z, \cdot) &= - \int_{z_b}^z \left((S_i \rho_i + S_d \rho_d) g + S_i \frac{\partial p_c(S_d)}{\partial z} \right) dz, \\ \pi_d(\cdot, \cdot, z, \cdot) &= - \int_{z_b}^z \left((S_i \rho_i + S_d \rho_d) g - S_i \frac{\partial p_c(S_d)}{\partial z} \right) dz, \end{aligned} \quad (3.12)$$

for any $z \in (z_b, z_t)$. Substituting the reconstructed pressures $p_\alpha, \alpha \in \{i, d\}$ into the second equation in (3.10) yields horizontal velocities $\mathbf{v}_{ho,\alpha}$. Summing these velocities for both phases yields the total velocity \mathbf{v}_{ho} in the horizontal directions. Then, substituting \mathbf{v}_{ho} into the third equation in (3.10) (incompressibility equation) yields the total velocity in the vertical direction w . Using the fractional flow formulation of Darcy's law (2.15), the vertical velocity of the invading phase is given as

$$w_i = f_i(S_i)w + \bar{\lambda}(S_i)K_3(\partial_z p_c(S_i) + (\rho_i - \rho_d)g). \quad (3.13)$$

As the fine-scale velocity $\mathbf{v}_i = (u_i, v_i, w_i)^T$ of the invading fluid is now known, the mass conservation equation in (3.10) provides saturation of the invading fluid in the whole domain.

The multiscale model is summarized for the invading phase $\alpha = i$ as follows:

$$\begin{aligned}
-\nabla_{ho} \cdot \hat{\mathbf{K}}(\lambda_{tot}(\hat{S})\nabla_{ho}\hat{p}_i) &= \nabla_h \cdot \hat{\mathbf{K}}(\hat{\lambda}_d(\hat{S})\nabla_{ho}\hat{p}_c(\hat{S})), \\
p_i(x, y, z, t) &= \hat{p}_i(x, y, t) + \pi_i(x, y, z, t), \\
\mathbf{v}_{ho,i} &= -\lambda_i \mathbf{K}_{ho} \nabla p_i, \\
\partial_z w &= -\nabla_{ho} \cdot \mathbf{v}_{ho}, \\
w_i &= f(S)w + \bar{\lambda}(S)K_3(\partial_z p_c(S) + (\rho_i - \rho_d)g), \\
\phi \partial_t S + \nabla \cdot \mathbf{v}_i &= 0,
\end{aligned} \tag{3.14}$$

The first equation in (3.14) holds in $\Omega_{ho} \times (0, T)$, while the other equations hold in $\Omega \times (0, T)$, where $\Omega \subset \mathbb{R}^3$. The unknowns in this model are the vertically averaged pressure $\hat{p}_i = \hat{p}_i(x, y, t) \in \mathbb{R}^+$ of the invading phase, the horizontal and vertical velocity component $\mathbf{v}_{ho,i} = \mathbf{v}_{ho,i}(x, y, z, t) \in \mathbb{R}$, $w_i = w_i(x, y, z, t) \in \mathbb{R}$ of the invading phase, respectively, and the saturation $S = S(x, y, z, t) \in [0, 1]$ of the invading fluid.

This model is associated with the following initial and boundary conditions

$$\begin{aligned}
\hat{S} &= \hat{S}_0, & \text{in } \Omega_{ho}, \\
\hat{S} &= \hat{S}_{inflow}, & \text{in } \partial\Omega_{ho,inflow} \times [0, T], \\
S &= S_0, & \text{in } \Omega, \\
S &= S_{inflow}, & \text{in } \partial\Omega_{inflow} \times [0, T], \\
\mathbf{n} \cdot \mathbf{v} &= 0, & \text{in } \partial\Omega_{imp} \times [0, T].
\end{aligned} \tag{3.15}$$

3.3 The Vertical Equilibrium Model (VE-Model)

In this section, we present the vertical equilibrium model proposed by Yortsos [53]. It is derived from the two-phase flow model (3.2) in a vertical cross-section $\Omega_v = (0, L) \times (0, H)$ of a three-dimensional flat domain $\Omega \subset \mathbb{R}^3$, such that the horizontal coordinate is parallel to the injection direction (Figure 3.5). Initially, the rectangular domain $\Omega_v = (0, L) \times (0, H)$ is fully saturated with a resident fluid S_d . As illustrated in Figure 3.5, the domain boundary $\partial\Omega_v$ is decomposed into an inflow boundary $\partial\Omega_{v,inflow}$, an outflow boundary $\partial\Omega_{v,outflow}$ and an impermeable boundary $\partial\Omega_{v,imp}$,

$$\partial\Omega_{v,inflow} := \{0\} \times (0, H), \quad \partial\Omega_{v,outflow} := \{L\} \times (0, H), \quad \partial\Omega_{v,imp} := (0, L) \times \{0, H\},$$

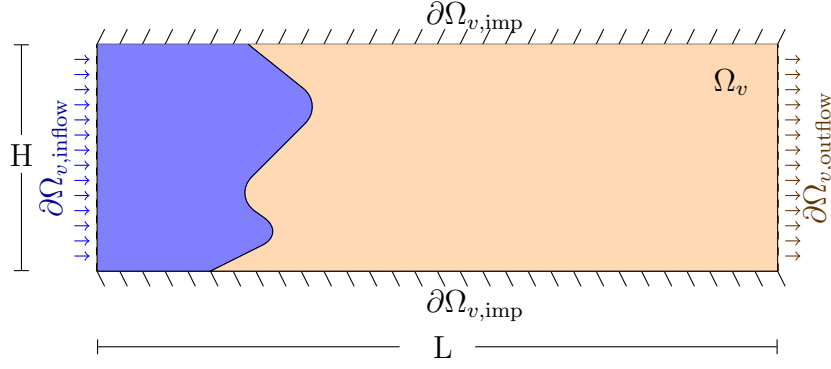


Figure 3.5: An illustration of the displacement process in a vertical-cross section of a domain Ω .

respectively. The initial and boundary conditions are now summarized as follows

$$\begin{aligned}
 S &= S_0, & \text{in } \Omega_v, \\
 S &= S_{\text{inflow}}, & \text{in } \partial\Omega_{v,\text{inflow}} \times [0, T], \\
 \mathbf{n} \cdot \mathbf{v} &= 0, & \text{in } \partial\Omega_{v,\text{imp}} \times [0, T],
 \end{aligned} \tag{3.16}$$

where \mathbf{n} is the outer normal vector at the boundary $\partial\Omega_{v,\text{imp}}$. We present the derivation of the VE-model under the assumption of negligible gravity and capillary forces. However, Yortsos [53] gives an extension of the model that includes the effects of these two forces. The derivation of the VE-model consists of two main steps. In the first step, the variables of the two-phase flow model are rescaled into dimensionless ones. This leads to a dimensionless two-phase flow model that explicitly accounts for the geometrical parameter $\gamma := \frac{H}{L}$. In the second step, asymptotic analysis with respect to γ is applied to the dimensionless two-phase flow model. This leads to the result that the vertical change of global pressure is of order $\mathcal{O}(\gamma)$. This result, the incompressibility of the velocity field, and the assumption of impermeable upper and lower boundaries allow reformulating the velocity in Darcy's equation as a nonlinear nonlocal operator of saturation alone. The first and the second steps are illustrated in Sections 3.3.1 and 3.3.2, respectively.

3.3.1 Dimensionless Two-Phase Flow Model

The first step for deriving the vertical equilibrium model is rescaling the two-phase flow model (3.2) using the dimensionless variables,

$$\begin{aligned}
 \bar{x} &= \frac{x}{L}, & \bar{z} &= \frac{z}{H}, & \bar{t} &= \frac{t}{L/q}, & \kappa_j &= \frac{K_j}{k_j} \\
 \bar{u}_\alpha &= \frac{u_\alpha}{q}, & \bar{w}_\alpha &= \frac{w_\alpha}{q}, & \bar{p}_\alpha &= \frac{p_\alpha}{Lq\mu_n/k_1},
 \end{aligned} \tag{3.17}$$

for $j \in \{1, 3\}$ and $\alpha \in \{i, d\}$. Here, $q > 0$ is the inflow speed at the inflow boundary $\partial\Omega_{\text{inflow}}$ and k_j is the mean value of the corresponding permeability function K_j . Applying the chain rule on the two-phase flow model (3.2) then using (3.17) yield a dimensionless two-phase flow model

$$\begin{aligned}\phi\partial_{\bar{t}}S_\alpha + \partial_{\bar{x}}(\bar{u}_\alpha) + \frac{1}{\gamma}\partial_{\bar{z}}(\bar{w}_\alpha) &= 0, \\ \partial_{\bar{x}}(\bar{u}) + \frac{1}{\gamma}\partial_{\bar{z}}(\bar{w}) &= 0, \\ \bar{u}_\alpha &= -\bar{\lambda}_\alpha(S_\alpha)\kappa_1\partial_{\bar{x}}\bar{p}_\alpha, \\ \frac{\gamma}{\beta}\bar{w}_\alpha &= -\bar{\lambda}_\alpha(S_\alpha)\kappa_2\partial_{\bar{z}}\bar{p}_\alpha,\end{aligned}\tag{3.18}$$

in the dimensionless domain $\bar{\Omega}_v \times (0, \bar{T})$, where $\bar{\Omega}_v = (0, 1)^2$, for both invading and defending phases $\alpha \in \{i, d\}$. Here, $\bar{\lambda}_\alpha = \mu_d\lambda_\alpha$ is the dimensionless mobility of the phase α ,

$$\gamma := \frac{H}{L}, \quad \text{and} \quad \beta := \frac{k_3}{k_1}.$$

Using Assumption 2.4(1), we have $\beta = 1$. Omitting the bar-sign from the dimensionless variables, system (3.18) is written as

$$\begin{aligned}\phi\partial_t S_\alpha + \partial_x u_\alpha + \frac{1}{\gamma}\partial_z w_\alpha &= 0, \\ \partial_x u + \frac{1}{\gamma}\partial_z w &= 0, \\ u_\alpha &= -\lambda_\alpha(S_\alpha)\kappa\partial_x p_\alpha, \\ \gamma w_\alpha &= -\lambda_\alpha(S_\alpha)\kappa\partial_z p_\alpha,\end{aligned}\tag{3.19}$$

in $\Omega_v \times (0, T)$ with $\kappa := \kappa_1 = \kappa_3$. The initial and boundary conditions are defined in (3.16) with the dimensionless boundaries

$$\partial\Omega_{v,\text{inflow}} = \{0\} \times (0, 1), \quad \partial\Omega_{v,\text{outflow}} = \{1\} \times (0, 1), \quad \text{and} \quad \Omega_{v,\text{imp}} = (0, 1) \times \{0, 1\}.$$

In the following, system (3.19) is reformulated in the fractional flow formulation. The assumption of negligible capillary pressure implies $p_i = p_d =: p$. Thus, for the horizontal velocity u_α , $\alpha \in \{i, d\}$, the third equation in (3.19) gives

$$\frac{u_i}{\lambda_i\kappa} = \frac{u - u_i}{(\lambda_{\text{tot}} - \lambda_i)\kappa},$$

where $u = u_i + u_d$ and $\lambda_{\text{tot}} = \lambda_i + \lambda_d$. Using the positivity of the permeability κ then reordering the terms, we have

$$u_i = f(S_i)u, \quad (3.20)$$

where $f(S_i) = \frac{\lambda_i(S_i)}{\lambda_{tot}(S_i)}$ is the fractional flow function of the invading phase $\alpha = i$. Analogously, the dimensionless vertical velocity component satisfies

$$w_i = f(S_i)w, \quad (3.21)$$

where $w = w_i + w_d$. Substituting equation (3.20) and (3.21) into (3.19) produces a dimensionless two-phase flow model in fractional flow formulation. Using the notation $S := S_i$ then associating the variables S , p , u , and w with the geometrical parameter γ , we obtain

$$\begin{aligned} \phi \partial_t S^\gamma + \partial_x(f(S^\gamma)u^\gamma) + \frac{1}{\gamma} \partial_z(f(S^\gamma)w^\gamma) &= 0, \\ \partial_x(u^\gamma) + \frac{1}{\gamma} \partial_z(w^\gamma) &= 0, \\ u^\gamma &= -\lambda_{tot}(S^\gamma)\kappa \partial_x p^\gamma, \\ \gamma w^\gamma &= -\lambda_{tot}(S^\gamma)\kappa \partial_z p^\gamma, \end{aligned} \quad (3.22)$$

in $\Omega_v \times (0, T)$. In the next subsection, asymptotic analysis as $\gamma \rightarrow 0$, is applied to system (3.22), which finally reduces into the VE-model with the unknown $S := \lim_{\gamma \rightarrow 0} S^\gamma$.

3.3.2 Asymptotic Analysis

The second step for deriving the vertical equilibrium model is applying asymptotic analysis, with respect to the small parameter γ , to the dimensionless two-phase flow model (3.22). For the analysis, we assume that for each $\gamma > 0$ there exists a solution $(S^\gamma, p^\gamma, u^\gamma, w^\gamma)$, with the asymptotic expansions

$$\begin{aligned} Z^\gamma &= Z_0 + \gamma Z_1 + \mathcal{O}(\gamma^2), \quad \text{for } Z^\gamma \in \{S^\gamma, p^\gamma, u^\gamma\}, \\ w^\gamma &= \gamma w_1 + \mathcal{O}(\gamma^2). \end{aligned} \quad (3.23)$$

Note that the second equation in (3.23) implies a small vertical velocity w^γ , which is a consequence of the vertical equilibrium assumption. Using Assumption 2.4(2) and 2.4(3), we have the Taylor expansions

$$\begin{aligned} \lambda_{tot}(S^\gamma) &= \lambda_{tot}(S_0) + \lambda'_{tot}(S_0)(\gamma S_1) + \mathcal{O}(\gamma^2), \\ f(S^\gamma) &= f(S_0) + f'(S_0)(\gamma S_1) + \mathcal{O}(\gamma^2), \end{aligned} \quad (3.24)$$

respectively. The second equation in (3.22) (dimensionless incompressibility) allows writing the first equation in (3.22) (dimensionless continuity equation) in a nonconservative form. Substituting the expansions (3.23) and (3.24) into (3.22), then considering terms of order $\mathcal{O}(1)$ in each equation leads to

$$\begin{aligned}\phi\partial_t S_0 + u_0\partial_x f(S_0) + w_1\partial_z f(S_0) &= \mathcal{O}(\gamma), \\ \partial_x u_0 + \partial_z w_1 &= \mathcal{O}(\gamma), \\ -\lambda_{tot}(S_0)\kappa\partial_x p_0 &= u_0, \\ -\lambda_{tot}(S_0)\kappa\partial_z p_0 &= \mathcal{O}(\gamma).\end{aligned}\tag{3.25}$$

Due to the positivity of the total mobility λ_{tot} and the permeability κ , the last equation in (3.25) simplifies to

$$\partial_z p_0 = \mathcal{O}(\gamma).\tag{3.26}$$

Thus, as $\gamma \rightarrow 0$, the global pressure p_0 is independent of the z -coordinate

$$p_0 = p_0(x, t).\tag{3.27}$$

In the following, result (3.27) is used to reformulate the velocity $\mathbf{v} = (u, w)^T$ in terms of saturation only. Integrating the second equation in (3.25) along the vertical direction from 0 to 1, then using impermeability of the top and the bottom parts $\partial\Omega_{\text{imp}}$ of the domain Ω yield

$$\partial_x \int_0^1 u_0 dz = - \int_0^1 \partial_z w_1(x, z, t) dz = 0,\tag{3.28}$$

as $\gamma \rightarrow 0$. Thus, we have

$$\int_0^1 u_0 dz = h,\tag{3.29}$$

for some function $h = h(t)$. Integrating the third equation in (3.25) along the vertical direction from 0 to 1, then using equation (3.29) give

$$- \int_0^1 \lambda_{tot}(S_0(x, z, t))\kappa(x, z)\partial_x p_0(x, t) dz = h(t).$$

Since p_0 is independent of the vertical coordinate z , we obtain that

$$\partial_x p_0(x, t) = - \frac{h(t)}{\int_0^1 \lambda_{tot}(S_0(x, z, t))\kappa(x, z) dz}.\tag{3.30}$$

Substituting (3.30) into the third equation in (3.25) gives a pressure independent formula for the horizontal velocity component u_0 ,

$$u_0[x, z, t; S_0(x, z, t)] = \frac{h(t)\lambda_{tot}(S_0(x, z, t))\kappa(x, z)}{\int_0^1 \lambda_{tot}(S_0(x, r, t))\kappa(x, r) dr}, \quad (3.31)$$

for all $(x, z) \in \Omega_v$ and $t \in (0, T)$. This pressure independent formula is substituted in the second equation in (3.25) to produce a pressure independent formula for the vertical velocity component w_1 ,

$$w_1[x, z, t; S_0(x, z, t)] = -h(t)\partial_x \frac{\int_0^z \lambda_{tot}(S_0(x, r, t))\kappa(x, r) dr}{\int_0^1 \lambda_{tot}(S_0(x, r, t))\kappa(x, r) dr}, \quad (3.32)$$

for all $(x, z) \in \Omega_v$ and $t \in (0, T)$. Rescaling the time using $t \mapsto \bar{t} = \int_0^t h(r)dr + h(0)t$, then omitting the subscripts $\{0, 1\}$ and the bar-signs, the **vertical equilibrium model (VE-model)** is given as,

$$\begin{aligned} \phi \partial_t S + \partial_x (u[\cdot, \cdot; S] f(S)) + \partial_z (w[\cdot, \cdot; S] f(S)) &= 0, \\ u[\cdot, \cdot; S] &= \frac{\lambda_{tot}(S)\kappa}{\int_0^1 \lambda_{tot}(S(\cdot, r, \cdot))\kappa(\cdot, r) dr}, \\ w[\cdot, z; S(\cdot, z, \cdot)] &= -\partial_x \frac{\int_0^z \lambda_{tot}(S(\cdot, r, \cdot))\kappa(\cdot, r) dr}{\int_0^1 \lambda_{tot}(S(\cdot, r, \cdot))\kappa(\cdot, r) dr}, \end{aligned} \quad (3.33)$$

for all $z \in (0, 1)$ in $(0, 1)^2 \times (0, T)$. The unknown in the model is saturation $S = S(x, z, t) \in [0, 1]$ only.

Remark 3.1. *As mentioned in Section 3.1, the vertical equilibrium assumption is also valid in domains with very high vertical permeability κ_3 . Therefore, the derivation of the vertical equilibrium model is also valid if the parameters γ, β satisfies $\gamma = \mathcal{O}(1)$ and $\beta \gg 1$, see [53].*

3.4 Models Comparison

This section is the main contribution of this chapter, where we show the numerical validation and computational efficiency of the VE-model (3.33), based on comparisons with the three models presented in Section 3.2. In addition to this, we prove that the multiscale model (3.14), in a vertical cross-section of a three dimensional domain, is equivalent to the VE-model.

This section has the following structure: Section 3.4.1 establishes a finite-volume scheme to the VE-model that is locally mass conservative and stable.

Section 3.4.2 compares the VE-model to the dimensionless two-phase flow model. Then, the VE-model and the VI-model are compared in Section 3.4.3. Finally, Section 3.4.4 investigates the relation between the VE-model and the multiscale model.

3.4.1 Finite-Volume Scheme

For the numerical comparisons in the following subsections, we establish an upwind explicit finite-volume scheme to the VE-model (3.33), [37]. Then, we show that the scheme is stable whenever the time step size satisfies a given CFL-condition.

We consider a Cartesian grid of the dimensionless spatial domain $\Omega_v = (0, 1)^2$

$$\mathcal{T} = \left\{ T_{i,j} = [x_{i-\frac{1}{2}}, x_{i+\frac{1}{2}}) \times [z_{j-\frac{1}{2}}, z_{j+\frac{1}{2}}) \mid (i, j) \in \mathcal{I}_x \times \mathcal{I}_z \subset \mathbb{N} \times \mathbb{N} \right\},$$

with the set of midpoints $\{(x_i, z_j) \mid (i, j) \in \mathcal{I}_x \times \mathcal{I}_z\}$. This grid is admissible as it satisfies the following properties

- $\Omega_v = (0, 1)^2 = \cup_{(i,j) \in \mathcal{I}_x \times \mathcal{I}_z} T_{i,j}$.
- For any $(i, j) \neq (l, k)$, it holds that $T_{i,j} \cap T_{l,k} = \emptyset$, a common point, or a common edge of both cells.

The set of edges of the cell $T_{i,j}$ is denoted by $\{E_l \mid l \in \theta_{i,j}\}$ where

$$\theta_{i,j} := \left\{ \left(i - \frac{1}{2}, j \right), \left(i + \frac{1}{2}, j \right), \left(i, j - \frac{1}{2} \right), \left(i, j + \frac{1}{2} \right) \right\}.$$

The set of neighbor cells of $T_{i,j}$ is defined as $\{T_{(i,j)_l} \mid l \in \theta_{i,j}\}$, where $T_{(i,j)_l}$ is the neighbor cell to $T_{i,j}$ with the common edge E_l . Let N_x and N_z be the number of cells in the horizontal and vertical directions, respectively. Then, the size of the cell is $|T_{i,j}| = \Delta x \Delta z$, where $\Delta x := \frac{1}{N_x}$ and $\Delta z := \frac{1}{N_z}$. For the initial condition $S_0 \in [0, 1]$, we define the cell-averaged values

$$S_{i,j}^0 = \frac{1}{|T_{i,j}|} \int_{T_{i,j}} S_0(x, z) dx dz, \quad (i, j) \in \mathcal{I}_x \times \mathcal{I}_z. \quad (3.34)$$

Given a positive integer N , the time interval $[0, T]$ is discretized into a set of disjoint subintervals $[t^n, t^{n+1})$, $n \in \{0, 1, 2, \dots, N\}$, each of length $\Delta t > 0$ such that $t^0 = 0$ and $t^N = T$. Then, a finite-volume scheme of the VE-model (3.33) is given

in the following equation

$$\frac{S_{i,j}^{n+1} - S_{i,j}^n}{\Delta t} + \frac{1}{\Delta x \Delta z} \sum_{l \in \theta_{i,j}} \mathcal{F}_l(\bar{S}_{i,j}^n, S_{i,j}^n, S_{(i,j)l}^n) = 0, \quad (3.35)$$

where the numerical flux function $\mathcal{F}_l(\bar{S}_{i,j}^n, S_{i,j}^n, S_{(i,j)l}^n)$ is defined by

$$\mathcal{F}_l(\bar{S}_{i,j}^n, S_{i,j}^n, S_{(i,j)l}^n) := |E_l| \left(\max\{\mathbf{n}_l \cdot \mathbf{v}_l[\bar{S}_{i,j}^n], 0\} f(S_{i,j}^n) + \min\{\mathbf{n}_l \cdot \mathbf{v}_l[\bar{S}_{i,j}^n], 0\} f(S_{(i,j)l}^n) \right), \quad (3.36)$$

\mathbf{n}_l is the outer normal to the edge E_l of the cell $T_{i,j}$, $|E_l|$ is the length of the edge E_l , and $\bar{S}_{i,j}^n := \{S_{r,m} \mid r \in \{i-1, i, i+1\}, m \in \mathcal{I}_z\}$. The discrete velocity $\mathbf{v}_l^n[\bar{S}_{i,j}^n] = (u_l^n[\bar{S}_{i,j}^n], w_l^n[\bar{S}_{i,j}^n])^T$ is defined as

$$u_{i+\frac{1}{2},j}^n = \frac{1}{2} \left(\frac{\lambda_{tot}(S_{i+1,j}^n) \kappa_{i+1,j}}{\Delta z \sum_{m=1}^{N_z} \lambda_{tot}(S_{i+1,m}^n) \kappa_{i+1,m}} + \frac{\lambda_{tot}(S_{i,j}^n) \kappa_{i,j}}{\Delta z \sum_{m=1}^{N_z} \lambda_{tot}(S_{i,m}^n) \kappa_{i,m}} \right) \quad \text{at } E_{i+\frac{1}{2},j},$$

$$w_{i,j+\frac{1}{2}}^n = -\frac{\Delta z}{\Delta x} \sum_{m=1}^j \left(u_{i+\frac{1}{2},m}^n - u_{i-\frac{1}{2},m}^n \right) \quad \text{at } E_{i,j+\frac{1}{2}}. \quad (3.37)$$

Using the quadratic relative permeabilities (2.3), the fractional flow function f and the total mobility λ_{tot} are given as

$$f(S) = \frac{MS^2}{MS^2 + (1-S)^2}, \quad \lambda_{tot}(S) = MS^2 + (1-S)^2, \quad (3.38)$$

respectively, where $M := \frac{\mu_d}{\mu_i}$ is the viscosity ratio of the defending phase to the invading phase.

It is straightforward to prove that the finite-volume scheme satisfies the following two properties:

Lemma 3.2. (*Mass-Conservation*) *If the numerical flux function is defined as in (3.36), then the finite-volume scheme (3.35) is mass conservative. This means if $E_l = E_{l'}$ such that $l \in \theta_{i,j}$ and $l' \in \theta_{(i,j)l}$, then for all $P_{i,j} \in [0, 1]$ it holds that*

$$\mathcal{F}_l(\bar{P}_{i,j}, P_{i,j}, P_{(i,j)l}) = -\mathcal{F}_{l'}(\bar{P}_{(i,j)l}, P_{(i,j)l}, P_{i,j}). \quad (3.39)$$

Lemma 3.3. (*Incompressibility*) *If the discrete velocity $\mathbf{v}_l^n[\bar{S}_{i,j}^n] = (u_l^n[\bar{S}_{i,j}^n], w_l^n[\bar{S}_{i,j}^n])^T$, $l \in \theta_{i,j}$, is defined as in (3.37), then $\sum_{l \in \theta_{i,j}} \mathbf{n}_l \cdot \mathbf{v}_l^n[\bar{S}_{i,j}^n] = 0$.*

Now, we prove the stability of the scheme.

Lemma 3.4. (*L[∞]-Estimate*) *Let Assumption 2.4 be satisfied with $0 \leq f' \leq L$, for a constant $L > 0$. Assume also that the initial condition satisfies $S_0 \in [0, 1]$, and the CFL-condition,*

$$\Delta t \leq \frac{\Delta x \Delta z}{L \left(2\Delta z \max_{i,j} \left| u_{i+\frac{1}{2},j}^n \right| + 2\Delta x \max_{i,j} \left| w_{i,j+\frac{1}{2}}^n \right| \right)}, \quad (3.40)$$

holds. Then, we have

$$S_{i,j}^n \in [0, 1], \quad \forall (i, j) \in \mathcal{I}_x \times \mathcal{I}_z, n \in \{0, 1, \dots, N\}.$$

Proof. Using the incompressibility property in Lemma 3.3, we have

$$\sum_{l \in \theta_{i,j}} \mathcal{F}_l(\bar{S}_{i,j}^n, S_{i,j}^n, S_{(i,j)_l}^n) = 0.$$

Thus, the finite-volume scheme (3.35) can be written as

$$\begin{aligned} S_{i,j}^{n+1} &= S_{i,j}^n - \frac{\Delta t}{\Delta x \Delta z} \sum_{l \in \theta_{i,j}} \mathcal{F}_l(\bar{S}_{i,j}^n, S_{i,j}^n, S_{(i,j)_l}^n) + \frac{\Delta t}{\Delta x \Delta z} \sum_{l \in \theta_{i,j}} \mathcal{F}_l(\bar{S}_{i,j}^n, S_{i,j}^n, S_{i,j}^n), \\ &= S_{i,j}^n + \frac{\Delta t}{\Delta x \Delta z} \sum_{l \in \theta_{i,j}} C_l(\bar{S}_{i,j}^n, S_{i,j}^n, S_{(i,j)_l}^n) (S_{(i,j)_l}^n - S_{i,j}^n), \end{aligned}$$

where the coefficient $C_l(\bar{S}_{i,j}^n, S_{i,j}^n, S_{(i,j)_l}^n)$ is defined as

$$C_l(\bar{S}_{i,j}^n, S_{i,j}^n, S_{(i,j)_l}^n) := \frac{\mathcal{F}_l(\bar{S}_{i,j}^n, S_{i,j}^n, S_{(i,j)_l}^n) - \mathcal{F}_l(\bar{S}_{i,j}^n, S_{i,j}^n, S_{i,j}^n)}{S_{(i,j)_l}^n - S_{i,j}^n}.$$

The numerical flux (3.36) and the monotonicity of the fractional flux function imply

$$C_l(\bar{S}_{i,j}^n, S_{i,j}^n, S_{(i,j)_l}^n) = \frac{|E_l| \min \{ \mathbf{n}_l \cdot \mathbf{v}_l[\bar{S}_{i,j}^n], 0 \} \left(f(S_{i,j}^n) - f(S_{(i,j)_l}^n) \right)}{S_{(i,j)_l}^n - S_{i,j}^n} \geq 0. \quad (3.41)$$

Thus, we have

$$S_{i,j}^{n+1} = a_{i,j}^n S_{i,j}^n + \sum_{l \in \theta_{i,j}} b_{(i,j)_l}^n S_{(i,j)_l}^n,$$

where

$$a_{i,j}^n = 1 - \frac{\Delta t}{\Delta x \Delta z} \sum_{l \in \theta_{i,j}} C_l(\bar{S}_{i,j}^n, S_{i,j}^n, S_{(i,j)l}^n),$$

$$b_{(i,j)l}^n = \frac{\Delta t}{\Delta x \Delta z} C_l(\bar{S}_{i,j}^n, S_{i,j}^n, S_{(i,j)l}^n).$$

The CFL-condition (3.40) and the definition of C_l in inequality (3.41) imply that

$$a_{i,j}^n, b_{(i,j)l}^n \geq 0 \quad \text{and} \quad a_{i,j}^n + \sum_{l \in \theta_{i,j}} b_{(i,j)l}^n = 1.$$

Hence, we obtain that

$$\max_{i,j} |S_{i,j}^{n+1}| \leq \max_{i,j} |S_{i,j}^n| \leq \cdots \leq \max_{i,j} |S_{i,j}^0|.$$

Then, using the assumption that $S_0 \in [0, 1]$, we get the required estimate. \square

Lemma 3.4 shows the stability of the finite-volume scheme whenever the time step Δt satisfies the CFL-condition (3.40). However, this condition depends on the discrete velocity component $w_{i,j+\frac{1}{2}}^n$, which can be arbitrarily large for small enough Δx . This implies that the Δt might also be arbitrarily small for a small enough Δx . Therefore, we show in Lemma 3.5 that for any $\Delta x > 0$ there exist constants $c > 0$ and $\Delta t > 0$ such that $\Delta t > c$ and satisfies the CFL-condition (3.40).

Lemma 3.5. *Let Assumption 2.4 be satisfied and the velocity components u and w are discretized as in (3.37). Then, there exists a constant $C > 0$ such that*

$$0 < \left| u_{i+\frac{1}{2},j}^n \right| \leq C, \quad \text{and} \quad \left| w_{i,j+\frac{1}{2}}^n \right| \leq \frac{2C}{\Delta x}.$$

Moreover, for any $\Delta x > 0$ and $\Delta z \in (0, 1]$ the time step Δt , defined as

$$\Delta t = \frac{\Delta z \Delta x}{8LC}, \tag{3.42}$$

is strictly positive and fulfills the CFL-condition (3.40).

Proof. Using equation (3.37) and Assumption 2.4(1) and 2.4(2), we obtain

$$\left| u_{i+\frac{1}{2},j}^n \right| \leq \frac{\max_{p \in [0,1]} (\lambda_{tot}(P)) \max_{(i,j) \in \mathcal{I}_x \times \mathcal{I}_z} \kappa_{i+1,j}}{\min_{p \in [0,1]} (\lambda_{tot}(P)) \min_{(i,j) \in \mathcal{I}_x \times \mathcal{I}_z} \kappa_{i+1,j}} =: C. \tag{3.43}$$

Using (3.37) and the upper bound in (3.43), we also have

$$\begin{aligned} \left| w_{i,j+\frac{1}{2}}^n \right| &\leq \frac{\Delta z}{\Delta x} \sum_{m=1}^j \left(u_{i+\frac{1}{2},m}^n + u_{i-\frac{1}{2},m}^n \right), \\ &\leq \frac{2C}{\Delta x}. \end{aligned} \quad (3.44)$$

Using (3.43) and (3.44), we have

$$\begin{aligned} \frac{\Delta x \Delta z}{L \left(2\Delta z \max_{i,j} \left| u_{i+\frac{1}{2},j}^n \right| + 2\Delta x \max_{i,j} \left| w_{i,j+\frac{1}{2}}^n \right| \right)} &\geq \frac{\Delta x \Delta z}{L (2\Delta z C + 4C)} \\ &\geq \frac{\Delta x \Delta z}{L6C}. \end{aligned}$$

Hence, setting $\Delta t := \frac{\Delta x \Delta z}{L6C}$ completes the proof. \square

3.4.2 VE-Model vs. Two-Phase Flow Model

This section demonstrates the validity and computational efficiency of the VE-model (3.33). For this, we design several numerical examples comparing the VE-model with the two-phase flow model (3.2). We assume constant porosity $\phi = 1$, constant horizontal permeability $\kappa = 1$, and we use the dimensionless two-phase flow model (3.22),

$$\begin{aligned} \partial_t S^\gamma + \partial_x (f(S^\gamma) u^\gamma) + \frac{1}{\gamma} \partial_z (f(S^\gamma) w^\gamma) &= 0, \\ \partial_x (u^\gamma) + \frac{1}{\gamma} \partial_z (w^\gamma) &= 0, \\ u^\gamma &= -\lambda_{tot}(S^\gamma) \partial_x p^\gamma, \\ \gamma w^\gamma &= -\lambda_{tot}(S^\gamma) \partial_z p^\gamma, \end{aligned} \quad (3.45)$$

in $(0, 1)^2 \times (0, T)$. We also consider the initial condition $S_0 = 0$ and a time-constant inflow condition

$$S_{v,\text{inflow}}(z) = \begin{cases} 0 & : z \leq \frac{2}{5} \text{ and } z > \frac{3}{5}, \\ 0.9 & : \frac{2}{5} < z \leq \frac{3}{5}. \end{cases}$$

The end time $T = 0.3$ is chosen such that $S = 0$ on the outflow boundary $\partial\Omega_{v,\text{outflow}}$. We also consider the viscosity ratio $M = \mu_d/\mu_i = 5$.

Example 1: We consider the two-phase flow model in five domains $\Omega_{v,L} = (0, L) \times (0, 1)$, $L \in \{1, 4, 8, 16, 32\}$ and show that the corresponding numerical solutions converge to that of the VE-model as the parameter $\gamma = \frac{1}{L}$ tends to zero.

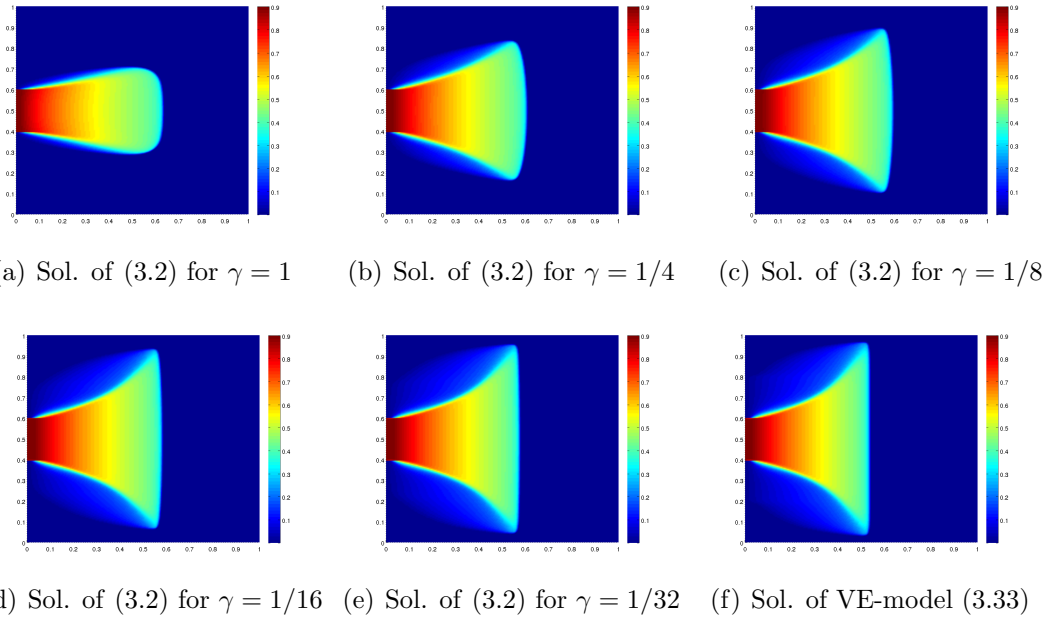


Figure 3.6: A comparison of the two-phase model (3.2), in domains with a decreasing parameter $\gamma \in \{1, \frac{1}{4}, \frac{1}{8}, \frac{1}{16}, \frac{1}{32}\}$, to the VE-model (3.33), for $M = 5$, and $T = 0.3$.

Figures (3.6(a) - 3.6(e)) present the numerical solutions of the dimensionless two-phase flow model (3.45) using the IMPES-method (implicit pressure - explicit saturation) [35] with pressure $p = 1$ at the inflow boundary and $p = 0$ at the outflow boundary. In this method, the elliptic equation for pressure (3.45(b)), (3.45(c)), and (3.45(d)) is implicitly solved in each time step to produce discrete velocity values that are used then to solve the saturation equation (3.45(a)) explicitly. Figure (3.6(f)) present the numerical solution of the VE-model (3.33) using the upwind explicit finite-volume scheme (3.35)-(3.37). The numerical solutions in Figure 3.6 correspond to a uniform Cartesian grid of 200×200 elements in the domain $(0, 1)^2$.

Figure 3.6 shows that numerical solutions of the two-phase flow model (3.2) converge to the corresponding numerical solution of the VE-model, as the domain parameter $\gamma = (1/L)$ tends to 0. Also, the spreading speed of the invading front is captured well by the VE-model.

Example 2: We consider the dimensionless two-phase flow model with the geometrical parameter $\gamma = 1/60$. The domain $(0, 1)^2$ is discretized into a uniform Cartesian grid with equal numbers of vertical N_z and horizontal N_x cells.

Table 3.1 presents the CPU-time required by the two models using equal numbers of horizontal and vertical cells. It shows that the computational time of the VE-model is almost 6 times faster than that of the two-phase flow model (3.2).

This is a consequence of the two-dimensional elliptic equation for pressure, which requires solving a linear system of equations.

Grid size $N_x \times N_z$	100×100	200×200	400×400
VE-model	0.94 s	10 s	124.51 s
two-phase model	6.4 s	64.5 s	722.79 s

Table 3.1: CPU-time of VE-model compared to two-phase flow model using Cartesian grids with number of elements $N_x \times N_z$ such that $N_x = N_z$, $\gamma = 1/60$, $T = 0.3$ and $M = 5$.

Example 3: This example also compares the CPU-time of the VE-model to that of the dimensionless two-phase flow model when the number of horizontal cells is a multiple of the vertical cells, $N_x = iN_z$, $i = 2, 4, 8, 16$. This scenario is more natural than that in Example 2, as horizontal dimensions in saturated media are significantly larger than the thickness.

Table 3.2 presents the CPU-time required by the two models using different numbers of horizontal and vertical cells. It shows that the VE-model is 10 times faster than the two-phase flow models when $N_x = 2 \times N_z$. However, the speed increases to 18 times when $N_x = 16 \times N_z$. This example demonstrates that most of the computational complexity of the VE-model results from the vertically integrated terms in the velocity, which is limited here. On the contrary, the computational complexity of the two-phase flow model increases as the dimensions of the linear system, corresponding to the elliptic equation of pressure, enlarge.

Grid size $N_x \times N_z$	200×100	400×100	800×100	1600×100
VE-model	2.5 s	9 s	25 s	109 s
two-phase model	25.98 s	106.76 s	458.87 s	1971 s

Table 3.2: CPU-time of the VE-model vs. the two-phase flow model using $N_x \times N_z$ elements, such that $N_x = iN_z$, $i \in \{2, 4, 8, 16\}$, $\gamma = 1/60$, $T = 0.3$ and $M = 5$.

3.4.3 VE-Model vs. VI-Model

In a vertical cross-section of $\Omega \subset \mathbb{R}^3$, the VI-model (3.6) reduces to the one-dimensional equation, in the fractional flow formulation,

$$\begin{aligned}
\Phi \partial_t \hat{S} + \partial_x (\hat{u} f(\hat{S})) &= 0, \\
\hat{u}_i &= -\hat{\lambda}_i \hat{\mathbf{K}} \partial_x \hat{p}, \\
\partial_x \hat{u} &= 0.
\end{aligned} \tag{3.46}$$

The third equation in (3.46) implies that the horizontal velocity \hat{u} is independent of the x -coordinate. Hence, there exists a function of time $h = h(t)$ such that $\hat{u} = h$. Rescaling the time using $t \mapsto \bar{t} = \int_0^t h(r)dr + h(0)t$, then omitting hat-signs, equation (3.46) reduces to

$$\partial_t S + \partial_x f(S) = 0, \quad \text{in } (0, 1) \times (0, T), \quad (3.47)$$

We establish a comparison between the one-dimensional VI-model (3.47) and the two-dimensional VE-model (3.33) such that the domain $\Omega_v = (0, 1) \times (0, 1)$ consists of a set of adjacent horizontal layers as in Figure 3.7. This reduces the two-dimensional VE-model into a coupled system of one-dimensional equations, each of them describes the dynamics in the corresponding layer and takes into account the mass-vertical exchange between adjacent layers. In such a situation, the number of vertical cells N_z in the finite-volume scheme (3.35) equals the number of layers in the domain.

It is easy to check that the VI-model (3.47) corresponds to a one layer scenario $N_z = 1$ of the VE-model. Therefore, the comparison of the VE-model (3.33) with the VI-model (3.47) is based on varying the number of layers in the domain: $N_z = 1$ (the VI-model), $N_z = 2$, and $N_z = 5$. The VE-model with $N_z = 100$ is used as a reference for accuracy.

It is clear that the computational complexity of the VE-model with $N_z = 1$ (the VI-model) is the lowest, and increases by increasing the number of layers. However, the following examples show that decreasing the number of layers to $N_z = 1$ has a strong impact on overestimating the spreading speed of the invading fluid.

The models comparison is based on three examples with different setups. In the first example, we assume that the permeability κ and the inflow saturation S_{inflow} are independent of the vertical coordinate z . In the second example, S_{inflow} is independent of z , but the permeability κ changes along the vertical axis. In the third example, κ is z -independent and S_{inflow} is located only at the lower part of the inflow boundary. In all examples, we assume a viscosity ratio $M = 2$, $N_x = 1000$ cells, and the end time $T = 0.3$.

Example 1: We consider a homogeneous two-dimensional medium with intrinsic permeability $\kappa = 1$ such that the saturation of invading fluid is constant along the entire inflow boundary

$$S_{\text{inflow}} = 1, \quad \text{on } \partial\Omega_{\text{inflow}} := \{0\} \times (0, 1). \quad (3.48)$$

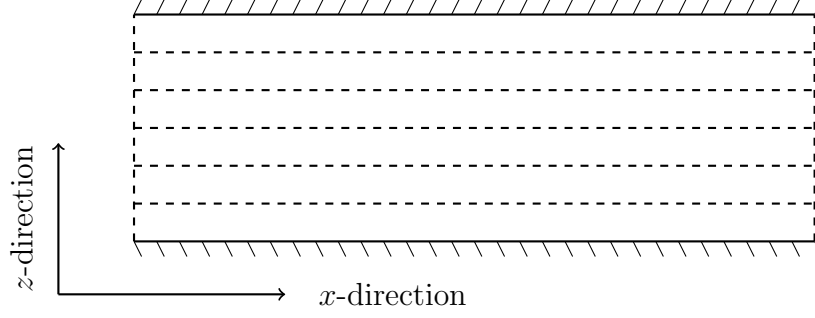


Figure 3.7: A vertical-cross section of a 3D domain consisting of 6 thin layers.

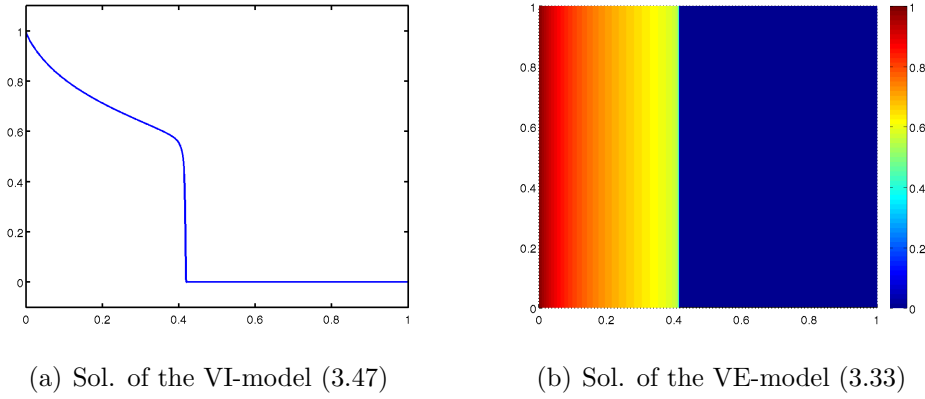


Figure 3.8: A comparison of the VI-model (3.47) to the VE-model (3.33) using $S_{\text{inflow}} = 1$, $\kappa = 1$, $M = 2$, $T = 0.3$, $\Delta x = 0.001$, and $\Delta z = 0.01$.

In this case, it is easy to check that the VE-model (3.33) simplifies into the VI-model (3.47) and therefore we neglect the cases with $N = 2$ or $N = 5$ layers. Figure 3.8 shows that the spreading speed and the saturation distribution of the invading fluid using the VI-model coincide with those of the VE-model.

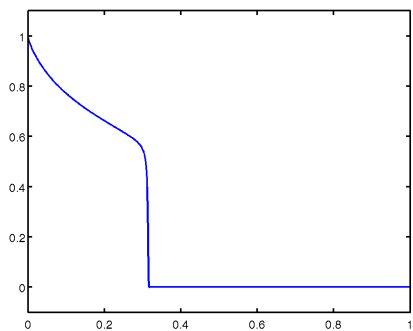
Example 2: We assume constant saturation along the inflow boundary as defined in equation (3.48), but the domain consists of two parts with different permeabilities

$$\kappa = \begin{cases} 1 & : \text{in } \Omega_{\text{upper}} := (0, 1) \times (0.5, 1), \\ 0.5 & : \text{in } \Omega_{\text{lower}} := (0, 1) \times (0, 0.5). \end{cases} \quad (3.49)$$

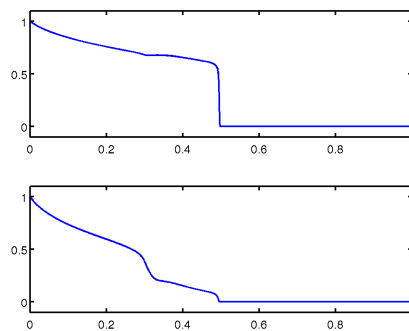
This condition is approximated according to the number of layers in the domain

$$\kappa_j = \frac{1}{\Delta z} \int_{(j-1)\Delta z}^{j\Delta z} \kappa(z) dz. \quad (3.50)$$

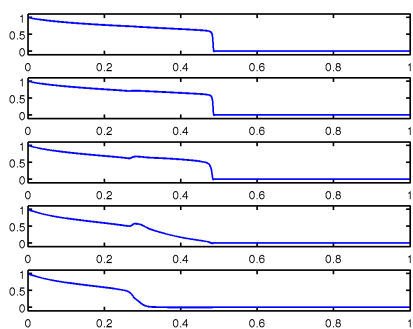
Figure 3.9 shows the effect of assuming different permeabilities in the horizontal layers of the medium on the accuracy of the two models. Figure 3.9(a) presents



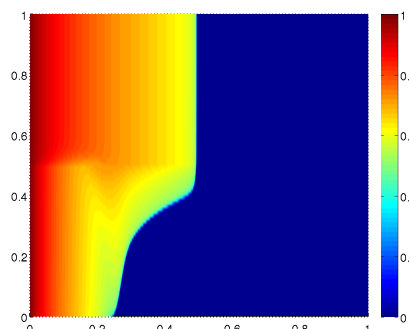
(a) VI model (3.47)



(b) VE-model (3.33) with $N = 2$



(c) VE-model (3.33) with $N = 5$

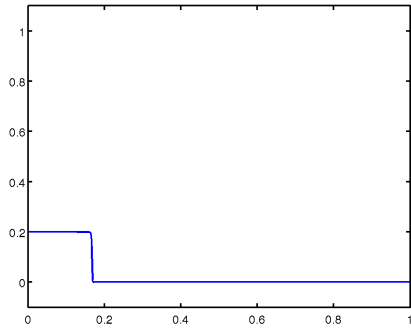


(d) VE-model (3.33) with $N = 100$

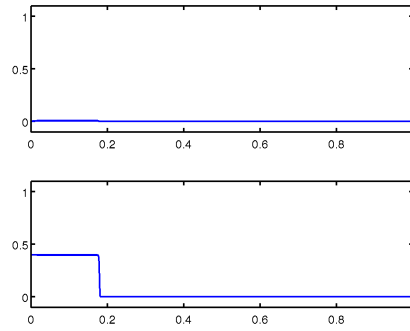
Figure 3.9: A comparison of the VI-model (3.47) to the VE-model (3.33) for κ as in (3.49), $S_{\text{inflow}} = 1$, $\mu_i = 1$, $\mu_d = 2$, $T = 0.3$, and $\Delta x = 0.001$.

the numerical solution of the VI-model (3.47) with averaged permeability $\kappa = 0.75$. In Figure 3.9(b), the domain consists of two layers: the lower layer has low permeability $\kappa_1 = 0.5$ and upper layer has high permeability $\kappa_3 = 1$. The numerical solution in both layers corresponds to the finite-volume scheme (3.35) with $\Delta z = 0.5$. In Figure 3.9(c), the domain consists of five layers. The averaged permeabilities in the layers are given as: $\kappa_1 = 0.5$, $\kappa_3 = 0.5$, $\kappa_3 = 0.75$, $\kappa_4 = 1$ and $\kappa_5 = 1$, respectively from bottom to top. The numerical solution in the layers corresponds to the finite-volume scheme (3.35) with $\Delta z = 0.2$. Figure 3.9(d) represents the numerical solution of the VE-model (3.33) using vertical step size $\Delta z = 0.01$. This numerical solution is considered as a reference for accuracy.

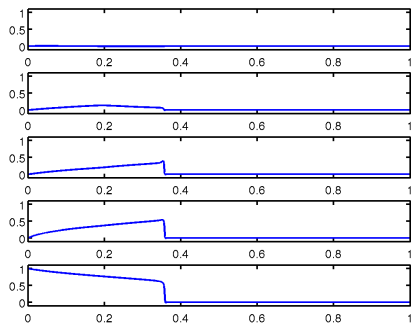
Figure 3.9 shows that the spreading speed of the invading fluid is overestimated by the VI-model (3.47), compared to the reference solution in Figure 3.9(d). On the contrary, the VE-model gives better estimations using two layers $N_z = 2$. Further, it well-estimates the spreading speed and the saturation distribution of the invading fluid using five layers $N_z = 5$.



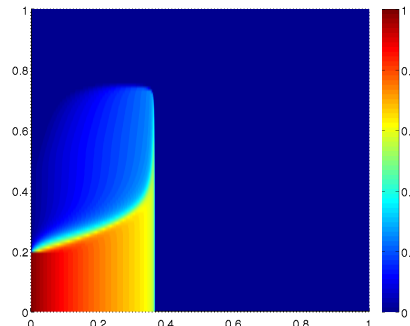
(a) VI-model (3.47)



(b) VE-model (3.33) with $N = 2$



(c) VE-model (3.33) with $N = 5$



(d) VE-model (3.33) with $N = 100$

Figure 3.10: A comparison of the VI-model (3.47) with the VE-model (3.33) for S_{inflow} as in (3.51), $\kappa = 1$, $\mu_i = 1$, $\mu_d = 2$, $T = 0.3$, and $\Delta x = 0.001$.

Example 3: We consider a homogeneous domain with permeability $\kappa = 1$ such that the invading fluid is injected only at the lower part of the inflow boundary

$$S_{\text{inflow}}(z) = \begin{cases} 1 & : 0 \leq z \leq 0.2, \\ 0 & : 0.2 \leq z \leq 1. \end{cases} \quad (3.51)$$

This condition is approximated according to the number of layers N_z in the domain

$$S_{\text{inflow},j} = \frac{1}{\Delta z} \int_{(j-1)\Delta z}^{j\Delta z} S_{\text{inflow}}(z) dz. \quad (3.52)$$

Figure 3.10 shows the effect of varying the injection position of the invading fluid on the accuracy of the VE-model and the VI-model. In Figure 3.10(a), the numerical solution of the VI-model (3.47) with averaged inflow $S_{\text{inflow}} = 0.2$ is presented. Figure 3.10(b) provides the numerical solution of the VE-model with $N_z = 2$ such that $S_{\text{inflow},1} = 0.4$ in the lower layer and $S_{\text{inflow},2} = 0$ in the upper

one. The numerical solution of the VE-model with $N_z = 5$ is presented in Figure 3.10(c) with $S_{\text{inflow},1} = 1$, $S_{\text{inflow},2} = 0$, $S_{\text{inflow},3} = 0$, $S_{\text{inflow},4} = 0$ and $S_{\text{inflow},5} = 0$ from bottom to top. Finally, the numerical solution of the VE-model (3.33) with $\Delta z = 0.01$ is presented in Figure 3.10(d) as a reference for accuracy.

This example emphasizes the weakness of the VI-model (3.47) whenever the injection position depends on the z -coordinate of the domain. In contrast to Example 2, the two-layers case $N_z = 2$ in the VE-model is not sufficient to give a good estimation of the spreading speed. However, spreading speed and fluids distribution in the five layers case $N_z = 5$ are well-estimated in comparison to the reference solution in Figure 3.10(d).

3.4.4 VE-Model vs. Multiscale Model

This section studies the relation between the VE-model (3.33) and the multiscale model (3.14). First, we consider the dimensionless multiscale model with negligible capillary pressure in a vertical cross-section of $\Omega \subset \mathbb{R}^3$ and show that including gravity force in the pressure reconstruction function corresponds to strong gravity effects in domains with small parameter γ . This leads to a fast fluid segregation and consequently the vertical equilibrium assumption is fully satisfied, which contradicts the goal of proposing the multiscale model. After that, we prove the equivalence between the VE-model and the multiscale model in the case of negligible gravity and capillary forces. Finally, we provide a numerical example that shows the numerical efficiency of the VE-model over the multiscale model. It is based on the finite volume scheme in Section 3.4.1 for the VE-model and a multiscale-IMPES algorithm proposed in [31] for the multiscale model.

Gravity-Segregated Flows in the Multiscale Model

We consider the multiscale model (3.14) in a vertical cross-section $\Omega_v = (0, L) \times (0, H)$ of a three-dimensional domain with negligible capillary forces using the dimensionless variables in (3.17). After omitting the bar-signs, we have

$$\begin{aligned}
-\partial_x (\hat{\lambda}_{tot}(S) \hat{\kappa} \partial_x \hat{p}) &= 0, \\
p(x, z, t) &= \hat{p}(x, t) + \pi(x, z, t), \\
u &= -\lambda_{tot}(S) \kappa \partial_x p, \\
\frac{1}{\gamma} \partial_z w &= -\partial_x u, \\
w_i &= f(S)w + \frac{gk(\rho_i - \rho_d)}{\gamma^2 q^3 \mu_d} \kappa f(S) \lambda_d(S), \\
\phi \partial_t S + \partial_x (uf(S)) + \frac{1}{\gamma} \partial_z (w_i) &= 0.
\end{aligned} \tag{3.53}$$

The first equation in this model holds in $(0, 1) \times (0, T)$, where $(0, 1)$ is the dimensionless coarse-scale horizontal domain. The other equations hold in $\Omega_v \times (0, T)$, where $\Omega_v = (0, 1)^2$. The dimensionless reconstruction function is now given as

$$\pi(\cdot, z, \cdot) = -\frac{1}{\gamma q \mu_d} \int_0^z (S_i \rho_i + S_d \rho_d) g dr, \quad \text{for any } z \in (0, 1). \quad (3.54)$$

We claim here that in media with a small parameter γ , the reconstruction function (3.54) implies strong gravity effects in the medium such that the fluids in the domain segregate very fast and the vertical equilibrium assumption is valid. In this case, it is known that the VI-model is sufficient to describe to the displacement process in the medium.

To prove fluids segregation, we follow [53] and consider the fifth equation in (3.53)

$$w_i = f(S)w + \frac{gk(\rho_i - \rho_d)}{\gamma^2 q^3 \mu_d} \kappa f(S) \lambda_d(S). \quad (3.55)$$

With respect to the parameter γ , the term on the left side and the first term on the right side of equation (3.55) are of order $\mathcal{O}(1)$. However, the second term on the right side is of order $\mathcal{O}(\gamma^{-2})$, which diverges as $\gamma \rightarrow 0$. This leads to a contradiction unless the product $f \lambda_d$ satisfies

$$f(S) \lambda_d(S) = 0, \quad (3.56)$$

which implies either $\lambda_d(S) = 0$ or $f(S) = 0$. This means that the fluids segregate in the medium as they cannot flow simultaneously.

Another way to avoid the contradiction in equation (3.55) is to assume a small gravity effect by multiplying the gravity term in the second and the fifth equations in (3.53) by a small parameter $N_G = \mathcal{O}(\gamma^2)$. By doing this, the second term in (3.55) is of order $\mathcal{O}(1)$. However, the gravity term in the second equation in (3.53) is of order $\mathcal{O}(\gamma)$. Therefore, this term can be neglect in media with a small parameter γ .

Models Equivalence

Under the same conditions assumed to derive the VE-model, we prove now that the multiscale model is equivalent to the VE-model. Thus, we assume a vertical cross-section $\Omega_v = (0, L) \times (0, H)$ of a three dimensional domain such that the horizontal direction (x -direction) is parallel to the injection direction (Figure 3.5).

We also assume negligible gravity and capillary forces. Then, the multiscale model (3.14) using the dimensionless variables (3.17) reduces to

$$\begin{aligned}
-\partial_x(\hat{\lambda}_{tot}(\hat{S})\hat{\kappa}_1\partial_x\hat{p}) &= 0, \\
p(x, z, t) &= \hat{p}(x, t), \\
u &= -\lambda_{tot}\kappa_1\partial_x p, \\
\frac{1}{\gamma}\partial_z w &= -\partial_x u, \\
\phi\partial_t S + \partial_x(uf(S)) + \frac{1}{\gamma}\partial_z(wf(S)) &= 0.
\end{aligned} \tag{3.57}$$

The first equation in this model holds in $(0, 1) \times (0, T)$, where $(0, 1)$ is the dimensionless coarse-scale horizontal domain. The other equations in (3.57) hold in $\Omega \times (0, T)$, where $\Omega = (0, 1)^2$ is the dimensionless vertical cross-section of the three-dimensional domain. This model is associated with the initial and boundary conditions

$$\begin{aligned}
\hat{S} &= \hat{S}_0, & \text{in } \Omega_{ho} &= (0, 1), \\
\hat{S} &= \hat{S}_{inflow}, & \text{on } \partial\Omega_{ho, inflow} &\times [0, T], \\
S &= S_0, & \text{in } \Omega_v &= (0, 1)^2, \\
S &= S_{inflow}, & \text{on } \partial\Omega_{v, inflow} &\times [0, T], \\
\mathbf{n} \cdot \mathbf{v} &= 0, & \text{on } \partial\Omega_{v, imp} &\times [0, T].
\end{aligned} \tag{3.58}$$

Proposition 3.6. *Let $(S_m, u_m, w_m, \hat{p}_m)$ be a solution of the dimensionless multiscale model (3.57) with the initial and boundary conditions (3.58). Let (S_{ve}, u_{ve}, w_{ve}) be a solution of the VE-model (3.33) with the initial and boundary conditions (3.16). Then, we have $S_m = S_{ve}$, $u_m = u_{ve}$, $w_m = w_{ve}$, and we can define a function $p_{ve} = p_{ve}(S_{ve})$,*

$$\partial_x p_{ve} = \frac{1}{\int_0^1 \kappa_1(x, z)\lambda_{tot}(S_{ve}(x, z, t)) dz},$$

which satisfies $\hat{p}_m = p_{ve}$.

Proof. The proof starts with the vertically integrated horizontal velocity

$$\hat{u} = -\hat{\lambda}_{tot}\hat{\kappa}\partial_x\hat{p}, \tag{3.59}$$

which satisfies the first equation in multiscale model (3.57)

$$\partial_x\hat{u} = 0. \tag{3.60}$$

Integrating (3.60) over the x -direction from 0 to an arbitrary $x \in (0, 1)$ yields

$$\hat{u}(x, t) - h(t) = 0, \quad (3.61)$$

where $h(t) = \hat{u}(0, t)$ is the averaged horizontal velocity at the inflow boundary $\partial\Omega_{\text{inflow}}$. Substituting (3.61) into (3.59) and noting that the vertically-averaged quantities $\hat{\kappa}$ and $\hat{\lambda}_{\text{tot}}$ are defined as

$$\hat{\kappa}(x) = \int_0^1 \kappa(x, z) dz, \quad \hat{\lambda}_{\text{tot}} = \hat{\kappa}^{-1} \int_0^1 \kappa(x, z) \lambda_{\text{tot}}(S(x, z, t)) dz, \quad (3.62)$$

respectively, we obtain that

$$\partial_x \hat{p}(x, t) = \frac{h(t)}{\int_0^1 \kappa_1(x, z) \lambda_{\text{tot}}(S(x, z, t)) dz}. \quad (3.63)$$

Since the reconstructed fine-scale pressure is equivalent to the coarse-scale pressure $p = \hat{p}$, using the second equation in (3.57), we obtain that

$$\partial_x p(x, t) = \frac{h(t)}{\int_0^1 \kappa(x, z) \lambda_{\text{tot}}(S(x, z, t)) dz}. \quad (3.64)$$

Substituting equation (3.64) into the third equation in (3.57) yields the horizontal velocity u as an operator of saturation alone

$$u[x, z, t; S] = - \frac{h(t) \kappa(x, z) \lambda_{\text{tot}}(S(x, z, t))}{\int_0^1 \kappa(x, z) \lambda_{\text{tot}}(S(x, z, t)) dz}. \quad (3.65)$$

Substituting (3.65) into the fourth equation in the multiscale model (3.57) then integrating over the vertical coordinate from 0 to an arbitrary $z \in (0, 1)$ yields the vertical velocity as an operator of saturation alone

$$\begin{aligned} w[x, z, t; S] &= - \gamma \partial_x \int_0^z u[x, r, t; S] dr, \\ &= - \gamma h(t) \partial_x \frac{\int_0^z \kappa(x, r) \lambda_{\text{tot}}(S(x, r, t)) dr}{\int_0^1 \kappa(x, r) \lambda_{\text{tot}}(S(x, r, t)) dr}. \end{aligned} \quad (3.66)$$

We substitute equation (3.65) and (3.66) into the continuity equation in fractional flow formulation, rescale the time using $t \mapsto \bar{t} = \int_0^t h(r) dr + h(0)t$, and omit the

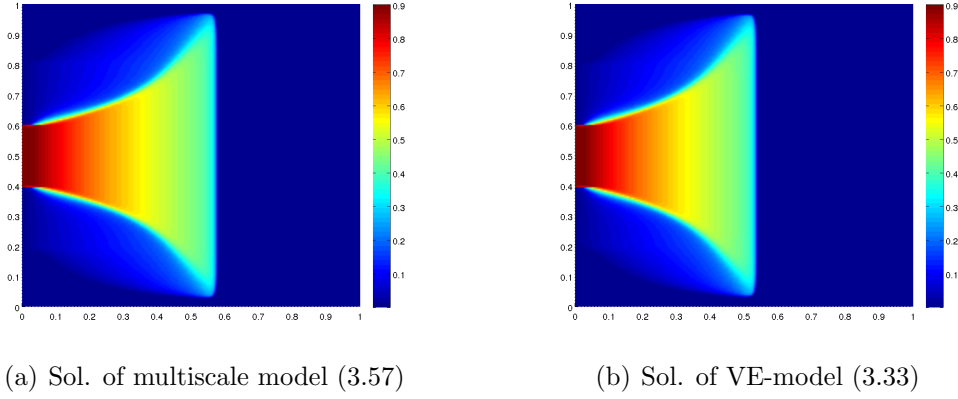


Figure 3.11: Numerical solution of the Multiscale model (3.57) and the numerical solution of the VE-model (3.33), for $\mu_i = 1$, $\mu_d = 5$, $T = 0.3$ and grid size (200×200) .

bar-sign. As a result, we obtain the VE-model

$$\begin{aligned} \partial_t S + \partial_x(u[\cdot, \cdot; S] f(S)) + \partial_z(w[\cdot, \cdot; S] f(S)) &= 0, \\ u[\cdot, \cdot; S] &= \frac{\lambda_{tot}(S)\kappa}{\int_0^1 \lambda_{tot}(S(\cdot, z, \cdot))\kappa(\cdot, z) dz}, \\ w[\cdot, z; S(\cdot, z, \cdot)] &= -\partial_x \frac{\int_0^z \lambda_{tot}(S(\cdot, r, \cdot))\kappa(\cdot, r) dr}{\int_0^1 \lambda_{tot}(S(\cdot, r, \cdot))\kappa(\cdot, r) dr}, \end{aligned}$$

for all $z \in (0, 1)$, in the dimensionless domain $(0, 1)^2 \times (0, T)$. This completes the proof. \square

Numerical Comparison

In spite of the equivalence between the multiscale model (3.57) and the VE-model, by Proposition 3.6, we show now that the models have different computational complexity. This is a result of the different numerical methods that fit to each model. For the VE-model, we use the finite-volume scheme, presented in Section 3.4.1, where the horizontal velocity u is evaluated as a nonlinear nonlocal operator of saturation. However, for the multiscale model, we use the multiscale algorithm proposed in [31]. This algorithm is based on the IMPES-method, in which the horizontal velocity u is evaluated by solving a one-dimensional elliptic equation for the vertically averaged pressure \hat{p} .

In the following, we present two examples that compare the two models. The first example shows the similarity of the numerical solutions for both models. The second example shows the computational efficiency of the VE-model over that of the multiscale model.

Grid size $N_x \times N_z$	100×100	200×100	400×100	800×100	1600×100
VE-model	1.08 s	2.58 s	9 s	25 s	109 s
multiscale model	0.91 s	2.97 s	12.32 s	64.85 s	413 s

Table 3.3: CPU-time of VE-model compared to the multiscale model using Cartesian grids with $N_x \times N_z$ elements, $T = 0.3$, and viscosity ratio $M = 5$.

Example 1: This example compares the numerical solutions for the VE-model with the multiscale model as presented in Figure 3.11. For the comparison, we use a Cartesian grid of size 200×200 , fluids viscosity $\mu_i = 1$, $\mu_d = 5$, and end time $T = 0.3$. Figure 3.11 shows a high similarity in the saturation distribution and spreading speed for both models.

Example 2: This example shows the reduced computational time of the VE-model over that of the multiscale model. Table 3.3 summarizes the CPU-time required by the two models using Cartesian grids with $N_z = 100$ vertical cells and $N_x = iN_z$, $i \in \{1, 2, 4, 8, 16\}$, horizontal cells. The table shows a notable reduction in the computational time of the VE-model over the multiscale model, mainly when the discretization in the horizontal direction is finer than in the vertical direction. This results from solving the elliptic equation of the vertically averaged pressure in the multiscale model, which consumes most of the CPU-time.

3.5 Reduced Regularity of the VE-Model

The VE-model is a nonlinear transport equation of saturation,

$$\partial_t S + \partial_x (f(S) u[x, z; S]) - \partial_z \left(f(S) \partial_x \int_0^z u[x, q; S] dq \right) = 0,$$

where shocks might develop in the saturation profile S , even for smooth initial conditions. Since the nonlinear operator $\int_0^z u[x, q; S] dq$ has a similar regularity, in the horizontal direction, to that of saturation $S \in L^\infty(\Omega \times (0, T))$, the vertical velocity $w = -\partial_x \int_0^z u[x, q; S] dq$ is expected to blow up at shocks, as illustrated in 3.12. Thus, the product $-f(S) \partial_x \int_0^z [x, q; S] dq$ is nonconservative as the x -partial derivative cannot be moved to test functions. Therefore, weak solutions in the distributional sense cannot be defined for the VE-model.

The problem of nonconservative products in hyperbolic equations appears in many applications, like the multilayer shallow water systems [44]. In the theory introduced by Dal Maso, LeFloch and Murat [20], weak solutions for such equations are defined using a family of Lipschitz continuous paths satisfying some regularity

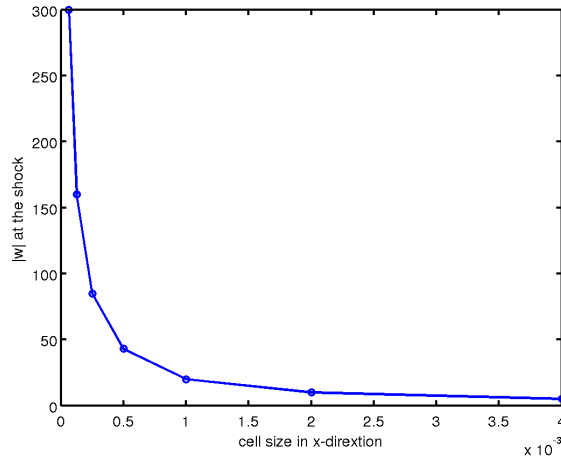


Figure 3.12: Numerical behavior of the absolute value of the vertical velocity w in the VE-model at a shock as the spatial step size $\Delta x \rightarrow 0$

and compatibility conditions. As weak solutions depend on the chosen family of paths, the difficulty in this theory is the necessity to choose, a priori, the family of paths that lead to the physically relevant weak solution.

3.6 Conclusion

This chapter studied the displacement processes of incompressible fluids in saturated flat porous media, where thickness is significantly smaller than the horizontal directions. We presented different models that describe fluid dynamics in such media, including the two-phase flow model, the VI-model, the multiscale model, and the VE-model.

We established a finite-volume scheme for the VE-model that is mass-conservative and stable. Then, we performed several tests that demonstrate the numerical efficiency of the VE-model in comparison with the above mentioned models. We concluded that

1. Numerical solutions of the two-phase flow model in domains with a decreasing geometrical parameter $\gamma = \frac{\text{width}}{\text{length}}$ converge to that of the VE-model. Moreover, the VE-model well captures the spreading speed of the invading fluid. Furthermore, the computational time of the VE-model is much reduced over that of the two-phase flow model, mainly when the number of vertical cells in the discretized domain is smaller than the number horizontal cells.
2. The VE-model provides better estimations on saturation distribution and spreading speed than the VI-model.

3. The computational complexity of the VE-model using the finite-volume scheme in Section 3.4.1 is reduced over that of the multiscale model using the multiscale algorithm in [31].

In addition, we showed that including the gravity force in the reconstruction function of the multiscale model is unnecessary. Furthermore, we proved the equivalence between the VE-model and the multiscale algorithm in a vertical cross-section of three dimensional reservoir. Finally, we investigated regularity of the VE-model and concluded that weak solutions in the distributional sense cannot be defined.

Chapter 4

The Brinkman Vertical Equilibrium Model

In this chapter, we propose a model that describes displacement processes of incompressible fluids in thin media where Darcy's law can be replaced by Brinkman's equation, like macroscopically heterogeneous media and media with high porosity. The proposed model is a higher-order extension of the VE-model that maintains much of its numerical advantages, analyzed in Chapter 3. We derive the model applying formal asymptotic analysis to the dimensionless two-phase flow model, in which Brinkman's equations replace Darcy's law. This leads to a third-order pseudo-parabolic equation of saturation alone, which we call the **Brinkman VE-model**.

On one hand, the Brinkman VE-model maintains much of the computational efficiency of the VE-model. This is a consequence of the saturation-dependent velocity components in both horizontal and vertical directions. On the other hand, the higher order terms in the Brinkman VE-model allow describing the phenomenon of saturation overshoots. These terms provide also a dissipative effect to the model such that weak solutions in the distributional sense can be defined, which will be further investigated in Chapter 5.

This chapter is structured as follows: Section 4.1 introduces the two-phase flow model with Brinkman's equations replacing Darcy's law, then comments on the domain's validity of this model. In Section 4.2, we derive the Brinkman VE-model. In Section 4.3, we design several numerical examples that show the numerical advantages of the Brinkman VE-model over the Brinkman two-phase flow model and the VE-model. Finally, Section 4.4 summarizes the chapter.

4.1 Brinkman Two-Phase Flow Model

Brinkman's equations describe the flow of incompressible fluids through a porous medium with high porosity [10]. These equations are a regularization of Darcy's law and are given as

$$\begin{pmatrix} -\mu_e \Delta u_\alpha + u_\alpha \\ -\mu_e \Delta w_\alpha + w_\alpha \end{pmatrix} = -\frac{k_{r\alpha}}{\mu_\alpha} \mathbf{K}(\nabla p_\alpha - \rho_\alpha \mathbf{g}). \quad (4.1)$$

The terms u_α and w_α are the horizontal and vertical components of the velocity \mathbf{v}_α for the phase $\alpha \in \{i, d\}$, respectively. The parameter $\mu_e > 0$ is the effective viscosity that depends on the geometry of the porous medium. The second-order terms Δu_α , Δw_α on the left side of (4.1) correspond to components of the divergence of the stress tensor $\nabla \cdot \nabla \mathbf{v}_\alpha$.

The validity of Brinkman's equation in porous media has been investigated by many researchers, see [3, 4] and the references therein. In media with high porosity, it is generally admitted that the effective viscosity μ_e is close to the dynamical viscosity. However, if the medium is macroscopically nonhomogeneous, the effective viscosity is very small $\mu_e \ll 1$, such that the second order term in (4.1) is considered as a corrector of Darcy's law [4].

In porous media with almost unidirectional fluid flows, Brinkman's equations can be derived by averaging the Navier-Stokes equations over a representative averaging volume. In [47], the authors describe a free flow at a porous surface by assuming that the porous medium has a Cantor-Taylor brush structure. This structure is constructed by dividing one of the horizontal coordinates of the medium into three equal parts. After removing the middle part, the process is repeated several times on the remaining two parts. This structure insures an unidirectional flow through the porous medium and reduces the number of assumptions required to solve the closure problem. Then, by averaging the Navier-Stokes equations over a representative elementary volume, they derive a modified Brinkman model of three equations. The first equation is a Stokes-like equation and describes the free flow of the incompressible fluids above the surface. The second equation describes the flow in the transition area between the free flow and the flow in the porous medium. The third equation is a Brinkman-like equation and describes the unidirectional flow in the porous medium. The third equation is also valid for almost unidirectional flows [47]. Now, We define the vector \mathbf{V}_α such that

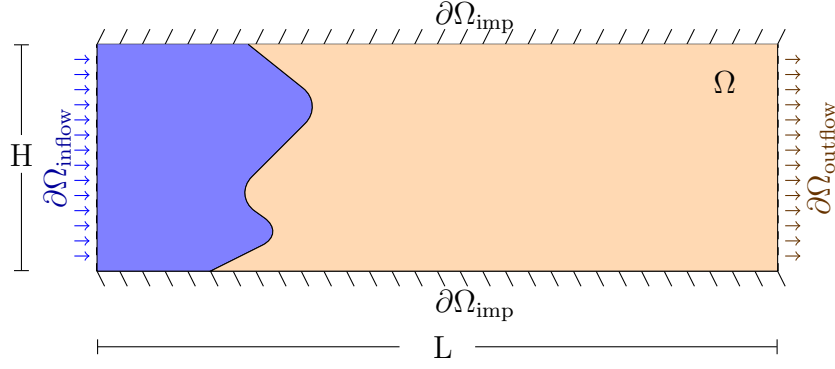


Figure 4.1: Displacement process in a vertical-cross section of the domain Ω .

$$\mathbf{V}_\alpha = \begin{pmatrix} U_\alpha \\ W_\alpha \end{pmatrix} := \begin{pmatrix} -\mu_e \Delta u_\alpha + u_\alpha \\ -\mu_e \Delta w_\alpha + w_\alpha \end{pmatrix} \quad (4.2)$$

for each phase $\alpha \in \{i, d\}$. For incompressible fluids flowing in a non-deformable porous medium with the assumption of negligible gravity force, the two-phase flow model with Brinkman's equations is a combination of the continuity equation, Brinkman's equations, and two incompressibility equations,

$$\begin{aligned} \phi \partial_t S_\alpha + \nabla \cdot \mathbf{v}_\alpha &= 0, \\ \mathbf{V}_\alpha &= -\frac{k_{r\alpha}}{\mu_\alpha} \mathbf{K} \nabla p_\alpha, \\ \nabla \cdot \mathbf{v} &= 0, \\ \nabla \cdot \mathbf{V} &= 0, \end{aligned} \quad (4.3)$$

respectively, for both invading and defending fluids $\alpha \in \{i, d\}$ in the spatial domain $\Omega := (0, L) \times (0, H)$ with $H \ll L$. Here, $\mathbf{v}_\alpha = (u_\alpha, w_\alpha)$ is phase velocity, \mathbf{K} is permeability tensor, and p_α is phase pressure. The third equation in (4.3) is the first incompressibility relation for the total velocity $\mathbf{v} = \mathbf{v}_i + \mathbf{v}_d$. It results from summing the continuity equation for the phases $\alpha \in \{i, d\}$ with the closure relation $S_i + S_d = 1$. The fourth equation in (4.3) is the second incompressibility relation for $\mathbf{V} = \mathbf{V}_i + \mathbf{V}_d$. It results from applying the divergence operator ($\nabla \cdot$) on \mathbf{V} , then using the first incompressibility equation

$$\begin{aligned} \nabla \cdot \mathbf{V} &= \nabla \cdot \begin{pmatrix} U \\ W \end{pmatrix} = -\mu_e \nabla \cdot \begin{pmatrix} \Delta u \\ \Delta w \end{pmatrix} + \nabla \cdot \begin{pmatrix} u \\ w \end{pmatrix}, \\ &= -\mu_e \Delta(\nabla \cdot \mathbf{v}) + \nabla \cdot \mathbf{v}, \\ &= 0. \end{aligned} \quad (4.4)$$

Assuming non-negligible capillary pressure $p_c = p_d - p_i$, the van-Genuchten model [51] provides the closure relation

$$p_c = p_c(S_i), \quad (4.5)$$

where we assumed here that the invading fluid is the wetting phase and the defending phase is the nonwetting phase.

Model (4.3) has to be completed with appropriate initial and boundary conditions that fit to the displacement process. Initially, the rectangular domain $\Omega = (0, L) \times (0, H)$ is assumed to be fully saturated with a resident fluid S_d . The domain's boundary $\partial\Omega$ is classified into an inflow boundary $\partial\Omega_{\text{inflow}}$, outflow boundary $\partial\Omega_{\text{outflow}}$, and impermeable top and bottom boundaries $\partial\Omega_{\text{imp}}$ (Figure 4.1) with

$$\partial\Omega_{\text{inflow}} := \{0\} \times (0, H), \quad \partial\Omega_{\text{outflow}} := \{L\} \times (0, H), \quad \partial\Omega_{\text{imp}} := (0, L) \times \{0, H\},$$

respectively. The initial and boundary conditions are similar to those in Section 3.3 with an extra periodic condition on the Laplacian of the vertical velocity Δw at the impermeable boundary $\partial_{\text{imp}}\Omega$,

$$\begin{aligned} S &= S_0, & \text{in } \Omega, \\ S &= S_{\text{inflow}}, & \text{on } \partial\Omega_{\text{inflow}} \times [0, T], \\ \mathbf{n} \cdot \mathbf{v} &= 0, & \text{on } \partial\Omega_{\text{imp}} \times [0, T], \\ \Delta w(x, 0, t) &= \Delta w(x, 1, t), & \text{for all } x \in [0, L], t \in [0, T], \end{aligned} \quad (4.6)$$

where \mathbf{n} is the outer normal vector at the boundary $\partial\Omega_{\text{imp}}$. Note that the last condition in (4.6) is not physical, however, it is necessary for the asymptotic analysis in Section 4.2.2.

4.2 The Brinkman VE-Model

In this section, we derive the Brinkman VE-model that describes displacement processes of incompressible fluids in a vertical cross-section $\Omega = (0, L) \times (0, H)$ of a thin porous medium. The domain is assumed to be fully saturated with a resident fluid, called defending phase $\alpha = d$, displaced by an injected fluid, called invading phase $\alpha = i$. Following [53], we rescale the variables in the Brinkman two-phase flow model (4.3) and obtain a dimensionless model depending on the geometrical parameter $\gamma = \frac{H}{L}$. Then, we apply asymptotic analysis to the dimensionless model

as $\gamma \rightarrow 0$. Finally, the Brinkman two-phase flow model reduces to the Brinkman VE-model that turns out to be a third-order pseudo-parabolic equation, in which the horizontal and vertical velocity components depend nonlocally on the unknown saturation.

4.2.1 Dimensionless Model

The first in deriving the Brinkman VE-model is rescaling the Brinkman two-phase flow model (4.3) using dimensionless variables, which leads to a dimensionless model associated with the small parameter γ . The dimensionless variables are

$$\begin{aligned} \bar{x} &= \frac{x}{L}, & \bar{z} &= \frac{z}{H}, & \bar{t} &= \frac{t}{L/q}, & \kappa_j &= \frac{K_j}{k_j}, \\ \bar{u}_\alpha &= \frac{u_\alpha}{q}, & \bar{w}_\alpha &= \frac{w_\alpha}{q}, & \bar{p}_\alpha &= \frac{p_\alpha}{Lq\mu_d/k_1}, & \bar{p}_c &= \frac{p_c}{\sqrt{k_1}}, \end{aligned} \quad (4.7)$$

for $j \in \{1, 3\}$ and $\alpha \in \{i, d\}$. Here, $q > 0$ is the inflow speed at the inflow boundary $\partial\Omega_{\text{inflow}}$ and k_j is the mean value of the permeability function K_j , defined as $k_j := \frac{1}{|\Omega|} \int_{\Omega} K_j(x, z) dx dz$. Using the relation $p_d - p_i = p_c$, we have

$$\begin{aligned} (\bar{p}_d - \bar{p}_i) \left(\frac{Lq\mu_d}{\kappa_1} \right) &= \sqrt{\kappa_1} \bar{p}_c, \\ \bar{p}_d - \bar{p}_i &= \epsilon_1 \bar{p}_c, \end{aligned} \quad (4.8)$$

where

$$\epsilon_1 := \frac{\kappa_1 \sqrt{\kappa_1}}{Lq\mu_d}. \quad (4.9)$$

Applying the chain rule on (4.2) gives

$$\begin{aligned} U_\alpha &= q \left(\bar{u}_\alpha - \mu_e \left(\frac{1}{L^2} \partial_{\bar{x}\bar{x}}(\bar{u}_\alpha) + \frac{1}{H^2} \partial_{\bar{z}\bar{z}}(\bar{u}_\alpha) \right) \right), \\ W_\alpha &= q \left(\bar{w}_\alpha - \mu_e \left(\frac{1}{L^2} \partial_{\bar{x}\bar{x}}(\bar{w}_\alpha) + \frac{1}{H^2} \partial_{\bar{z}\bar{z}}(\bar{w}_\alpha) \right) \right). \end{aligned}$$

We define the parameters

$$\beta_1 := \frac{\mu_e}{L^2}, \quad \beta_2 := \frac{\mu_e}{H^2}, \quad (4.10)$$

and the dimensionless components

$$\bar{U}_\alpha := \frac{U_\alpha}{q}, \quad \bar{W}_\alpha := \frac{W_\alpha}{q}. \quad (4.11)$$

Then, we get

$$\begin{aligned}\bar{U}_\alpha &= \bar{u}_\alpha - \beta_1 \partial_{\bar{x}\bar{x}}(\bar{u}_\alpha) - \beta_2 \partial_{\bar{z}\bar{z}}(\bar{u}_\alpha), \\ \bar{W}_\alpha &= \bar{w}_\alpha - \beta_1 \partial_{\bar{x}\bar{x}}(\bar{w}_\alpha) - \beta_2 \partial_{\bar{z}\bar{z}}(\bar{w}_\alpha).\end{aligned}\tag{4.12}$$

Applying the chain rule on equation (4.3), then using equation (4.7) and (4.11) yields the dimensionless model

$$\begin{aligned}\partial_t S_\alpha + \partial_{\bar{x}}(\bar{u}_\alpha) + (1/\gamma) \partial_{\bar{z}}(\bar{w}_\alpha) &= 0, \\ \bar{U}_\alpha &= -\lambda_\alpha \kappa_1 \partial_{\bar{x}} \bar{p}_\alpha, \\ (\gamma/\sigma) \bar{W}_\alpha &= -\lambda_\alpha \kappa_3 \partial_{\bar{z}} \bar{p}_\alpha, \\ \partial_{\bar{x}}(\bar{u}) + (1/\gamma) \partial_{\bar{z}}(\bar{w}) &= 0, \\ \partial_{\bar{x}}(\bar{U}) + (1/\gamma) \partial_{\bar{z}}(\bar{W}) &= 0,\end{aligned}\tag{4.13}$$

in $\bar{\Omega}_T := (0, 1)^2 \times \bar{T}$ for both invading and defending phases $\alpha \in \{i, d\}$, where $\lambda_\alpha = \frac{\mu_d k_{r\alpha}}{\mu_\alpha}$ is the dimensionless mobility of the phase α and

$$\gamma := \frac{H}{L} \quad \text{and} \quad \sigma := \frac{k_3}{k_1}.\tag{4.14}$$

Omitting the over-line from the dimensionless variables yields

$$\begin{aligned}\partial_t S_\alpha + \partial_x u_\alpha + (1/\gamma) \partial_z w_\alpha &= 0, \\ U_\alpha &= -\lambda_\alpha (S_\alpha) \kappa_1 \partial_x p_\alpha, \\ (\gamma/\sigma) W_\alpha &= -\lambda_\alpha (S_\alpha) \kappa_3 \partial_z p_\alpha, \\ \partial_x u + (1/\gamma) \partial_z w &= 0, \\ \partial_x U + (1/\gamma) \partial_z W &= 0,\end{aligned}\tag{4.15}$$

for both invading and defending phases $\alpha \in \{i, d\}$. The initial and boundary conditions are defined in (4.6) for the dimensionless boundaries

$$\partial\Omega_{\text{inflow}} = \{0\} \times (0, 1), \quad \partial\Omega_{\text{outflow}} = \{1\} \times (0, 1) \quad \text{and} \quad \Omega_{\text{imp}} = (0, 1) \times \{0, 1\}.$$

In the following, we reformulate system (4.15) in the fractional flow formulation. Substituting the second equation in (4.15) into equation (4.8) gives

$$\partial_x p_d - \partial_x p_i = -\frac{U - U_i}{(\lambda_{\text{tot}} - \lambda_i) \kappa_1} + \frac{U_i}{\lambda_i \kappa_1} = \epsilon_1 \partial_x p_c,$$

where $U = U_i + U_d$, $\lambda_{tot} = \lambda_i + \lambda_d$, and ϵ_1 is defined in (4.9). Reordering the terms yields

$$U_i = f(S_i)U + \epsilon_1 \kappa_1 \bar{\lambda}(S_i) \partial_x p_c, \quad (4.16)$$

where $f(S_i) = \frac{\lambda_i(S_i)}{\lambda_{tot}(S_i)}$ is the fractional flow function and $\bar{\lambda}(S_i) = \frac{\lambda_i(S_i) \lambda_d(S_i)}{\lambda_{tot}(S_i)}$ is the diffusion function of the invading phase $\alpha = i$. Analogously, substituting the third equation in (4.15) into equation (4.8) gives

$$\gamma W_i = \gamma f(S_i)W + \sigma \epsilon_1 \kappa_3 \bar{\lambda}(S_i) \partial_z p_c, \quad (4.17)$$

where $W := W_i + W_d$. Applying the operator $1 - \beta_1 \partial_{xx} - \beta_2 \partial_{zz}$ to the dimensionless continuity equation in (4.15), for the invading phase $\alpha = i$, then using (4.12) yields

$$\partial_t S_i - \beta_1 \partial_{xxt} S_i - \beta_2 \partial_{zzt} S_i + \partial_x U_i + \frac{1}{\gamma} \partial_z W_i = 0. \quad (4.18)$$

Using equation (4.16) and (4.17), we can write equation (4.18) in the fractional flow formulation for the invading fluid $\alpha = i$ with $S := S_i$ and $p := p_i$,

$$\begin{aligned} \partial_t S - \beta_1 \partial_{xxt} S - \beta_2 \partial_{zzt} S + \partial_x (f(S)U) + \frac{1}{\gamma} \partial_z (f(S)W) \\ + \epsilon_1 \partial_x (\kappa_1 \bar{\lambda}(S) \partial_x p_c) + \epsilon_2 \partial_z (\kappa_3 \bar{\lambda}(S) \partial_z p_c) = 0, \end{aligned}$$

where U and W satisfy

$$\begin{aligned} U &= -\lambda_{tot}(S) \kappa_1 \partial_x p - \epsilon_1 \kappa_1 \lambda_d(S) \partial_x p_c(S), \\ \gamma W &= -\lambda_{tot}(S) \kappa_3 \partial_z p - \sigma \epsilon_1 \kappa_3 \lambda_d(S) \partial_z p_c(S), \end{aligned}$$

and

$$\epsilon_2 := \frac{L \kappa_1 \sqrt{\kappa_1}}{H^2 q \mu_d}. \quad (4.19)$$

This dimensionless model is now summarized such that the unknown variables S , p , U , and W are associated with the geometrical parameter γ ,

$$\begin{aligned} \partial_t S^\gamma - \beta_1 \partial_{xxt} S^\gamma - \beta_2 \partial_{zzt} S^\gamma + \partial_x (f(S^\gamma)U^\gamma) + \frac{1}{\gamma} \partial_z (f(S^\gamma)W^\gamma) \\ + \epsilon_1 \partial_x (\kappa_1 \bar{\lambda}(S^\gamma) \partial_x p_c(S^\gamma)) + \epsilon_2 \partial_z (\kappa_3 \bar{\lambda}(S^\gamma) \partial_z p_c(S^\gamma)) = 0, \\ U^\gamma &= -\lambda_{tot}(S^\gamma) \kappa_1 \partial_x p^\gamma - \epsilon_1 \kappa_1 \lambda_d \partial_x p_c(S^\gamma), \\ \gamma W^\gamma &= -\lambda_{tot}(S^\gamma) \kappa_3 \partial_z p^\gamma - \sigma \epsilon_1 \kappa_3 \lambda_d \partial_z p_c(S^\gamma), \\ \partial_x U^\gamma + \frac{1}{\gamma} \partial_z W^\gamma &= 0. \end{aligned} \quad (4.20)$$

In the next subsection, asymptotic analysis, as $\gamma \rightarrow 0$, is applied to system (4.20), which finally leads to the Brinkman VE-model with the unknown $S = \lim_{\gamma \rightarrow 0} S^\gamma$.

4.2.2 Asymptotic Analysis

In this section, we apply asymptotic analysis, with respect to the small parameter γ , to the dimensionless model (4.20). The existence of a weak solution $(S^\gamma, p^\gamma, U^\gamma, W^\gamma)$ of the system (4.20) with appropriate initial and boundary conditions is established in [15]. We assume in this section that each component in $(S^\gamma, p^\gamma, U^\gamma, W^\gamma)$ has enough regularity to define the asymptotic expansions,

$$\begin{aligned} Z^\gamma &= Z_0 + \gamma Z_1 + \mathcal{O}(\gamma^2), \quad \text{for } Z^\gamma \in \{S^\gamma, p^\gamma, U^\gamma\}, \\ W^\gamma &= \gamma W_1 + \mathcal{O}(\gamma^2). \end{aligned} \tag{4.21}$$

Note that the second equation in (4.21) is a consequence of the assumption that the vertical velocity in flat domains is small.

Using the asymptotic expansion of S^γ in (4.21) and Assumption 2.4, we have the Taylor expansions

$$G(S^\gamma) = G(S_0) + G'(S_0)(\gamma S_1) + \mathcal{O}(\gamma^2), \quad \text{for } G \in \{\lambda_{tot}, f, \bar{\lambda}, p_c, \lambda_d\}. \tag{4.22}$$

The first incompressibility relation in (4.20) allows writing the continuity equation in the nonconservative form. Moreover, Assumption 2.4(1) implies that σ , defined in (4.14), satisfies $\sigma = 1$ and, therefore, we set $\kappa = \kappa_1 = \kappa_3$. Substituting equation (4.21) and (4.22) into (4.20), then using the property $\epsilon_1 = \mathcal{O}(\gamma)$ in the third and fourth equations of (4.20), the terms of order $\mathcal{O}(1)$ satisfy

$$\begin{aligned} \partial_t S_0 - \beta_1 \partial_{xxt} S_0 - \beta_2 \partial_{zzt} S_0 + \partial_x (f(S_0) U_0) + \epsilon_1 \partial_x (\kappa \bar{\lambda}(S_0) \partial_x p_c(S_0)) \\ + \partial_z (f(S_0) W_1) + \epsilon_2 \partial_z (\kappa \bar{\lambda}(S_0) \partial_z p_c(S_0)) &= \mathcal{O}(\gamma), \\ U_0 &= -\lambda_{tot}(S_0) \kappa \partial_x p_0, \\ \lambda_{tot}(S_0) \kappa \partial_z p_0 &= \mathcal{O}(\gamma), \\ \partial_x U_0 + \partial_z W_1 &= \mathcal{O}(\gamma). \end{aligned} \tag{4.23}$$

Using the positivity of the total mobility λ_{tot} and the permeability κ , the third equation of (4.23) implies that p_0 is independent of the z -coordinate,

$$p_0 = p_0(x, t), \tag{4.24}$$

as $\gamma \rightarrow 0$. Integrating the last equation in (4.23) over the vertical direction from 0 to 1 then using the zero-Neumann boundary condition and the periodicity of Δw at the impermeable boundaries $\partial_{\text{imp}}\Omega$ in equation (4.6), we obtain

$$\partial_x \int_0^1 U_0 dz = - \int_0^1 \partial_z W_1 dz = - \int_0^1 \partial_z (w_1 - \mu_e \Delta w_1) dz = 0.$$

This yields

$$\int_0^1 U_0 dz = q(t), \quad (4.25)$$

for some positive function $q = q(t)$. Substituting the second equation in (4.23) into equation (4.25) yields

$$- \int_0^1 \lambda_{\text{tot}}(S_0) \kappa \partial_x p_0 dz = q(t).$$

Then, using equation (4.24), we have

$$\partial_x p_0(x, t) = - \frac{q(t)}{\int_0^1 \lambda_{\text{tot}}(S_0(x, z, t)) \kappa(x, z) dz}, \quad (4.26)$$

for all $x \in (0, 1)$ and $t \in (0, T)$. Substituting (4.26) into the second equation in (4.23), we obtain a nonlocal saturation-dependent formula for U_0 ,

$$U_0[x, z, t; S_0(x, z, t)] = \frac{q(t) \lambda_{\text{tot}}(S_0(x, z, t)) \kappa(x, z)}{\int_0^1 \lambda_{\text{tot}}(S_0(x, z, t)) \kappa(x, z) dz}, \quad (4.27)$$

for all $(x, z) \in (0, 1)^2$ and $t \in (0, T)$. Consequently, the incompressibility relation in (4.23) yields also a nonlocal saturation-dependent formula for W_1 ,

$$W_1[x, z, t; S_0(x, z, t)] = -\partial_x \int_0^z U_0[x, r, t; S_0(x, r, t)] dr, \quad (4.28)$$

for all $(x, z) \in (0, 1)^2$ and $t \in (0, T)$. Using equation (4.27) and (4.28), omitting the subscripts $\{0, 1\}$, rescaling the time using

$$t \mapsto \bar{t} = \int_0^t q(r) dr + q(0)t, \quad (4.29)$$

then omitting the bar-sign, system (4.23) reduces to a third-order pseudo-parabolic equation of saturation alone that accounts fluid dynamics in the vertical direction.

We call this equation the **Brinkman VE-model**,

$$\begin{aligned} \partial_t S + \partial_x (f(S)U[., .; S]) + \partial_z (f(S)W[., .; S]) - \epsilon_1 \partial_x (D(S)\partial_x S) \\ - \epsilon_2 \partial_z (D(S)\partial_z S) - \beta_1 \partial_{xxt} S - \beta_2 \partial_{zzt} S = 0, \end{aligned} \quad (4.30)$$

where

$$U[., .; S] = \frac{\lambda_{tot}(S)\kappa}{\int_0^1 \lambda_{tot}(S)\kappa dz}, \quad W[., z; S] = -\partial_x \int_0^z U(., r; S(., r, .)) dr, \quad (4.31)$$

for all $z \in (0, 1)$ and

$$D(S) = \frac{\kappa \bar{\lambda}(S) |p'_c(S)|}{q}. \quad (4.32)$$

Remark 4.1. *The definition of the parameters ϵ_1 , ϵ_2 , β_1 and β_2 yields that*

$$\begin{aligned} \epsilon_1 &= \mathcal{O}(\gamma), & \beta_1 &= \mathcal{O}(\gamma^2), \\ \epsilon_2 &= \mathcal{O}(\gamma^{-1}), & \beta_2 &= \mathcal{O}(1). \end{aligned}$$

This implies that the viscosity dissipative effect in the horizontal direction is much less than that in the vertical direction.

4.3 Numerical Results

This section displays the numerical advantages of the Brinkman VE-model (4.30), (4.31), and (4.32) over the dimensionless Brinkman two-phase flow model (4.20) and the VE-model (3.33). For the numerical examples, we consider a linear capillary pressure function $p_c(S) = -S$ and dimensionless quadratic mobility functions

$$\lambda_i(S) = MS^2, \quad \lambda_d(S) = (1 - S)^2,$$

where $M := \frac{\mu_d}{\mu_i}$ is the viscosity ratio of the defending phase to the invading phase. In the Brinkman VE-model (4.30), (4.31), and (4.32), we assume that $q = 1$ such that the diffusion coefficient D satisfies $D(S) = \kappa \bar{\lambda}(S)$. Since we are interested in traveling wave solutions, we set $\epsilon_1 = \epsilon_2 = \epsilon$ and $\beta_2 = \beta_1 = \tau \epsilon^2$, where $\epsilon = 10^{-3}$ and τ is a positive constant. Then, the Brinkman VE-model simplifies to

$$\begin{aligned} \partial_t S + \partial_x (f(S)U[., .; S]) + \partial_z (f(S)W[., .; S]) - \epsilon \nabla \cdot (D(S)\nabla S) \\ - \tau \epsilon^2 \Delta \partial_t S = 0. \end{aligned} \quad (4.33)$$

with

$$U[.,.; S] = \frac{\lambda_{tot}(S)\kappa}{\int_0^1 \lambda_{tot}(S)\kappa dz}, \quad W[., z; S] = -\partial_x \int_0^z U[., r; S(., r, .)] dr, \quad (4.34)$$

for all $z \in (0, 1)$ and

$$f(S) = \frac{MS^2}{MS^2 + (1 - S)^2}, \quad D(S) = \kappa \frac{MS^2(1 - S)^2}{MS^2 + (1 - S)^2}. \quad (4.35)$$

Dividing the medium $\Omega = (0, 1)^2$ into $N_z \in \mathbb{N}$ layers, each of width $\Delta z = \frac{1}{N_z}$, the Brinkman VE-model (4.33), (4.34), and (4.35) reduces into a coupled system of N_z equations. Applying Euler method to the time derivatives, then an upwind finite volume scheme [37] to the coupled system produces

$$\begin{aligned} & \frac{S_{i,j}^{n+1} - S_{i,j}^n}{\Delta t} + \frac{1}{\Delta x \Delta z} \sum_{l \in \theta_{i,j}} \mathcal{F}_l(\bar{S}_{i,j}^n, S_{i,j}^n, S_{(i,j)_l}^n) \\ &= \frac{\epsilon}{\Delta x^2} \left(D(S_{i+\frac{1}{2},j}^n) (S_{i+1,j}^n - S_{i,j}^n) - D(S_{i-\frac{1}{2},j}^n) (S_{i,j}^n - S_{i-1,j}^n) \right) \\ & \quad + \frac{\epsilon}{\Delta z^2} \left(D(S_{i,j+\frac{1}{2}}^n) (S_{i,j+1}^n - S_{i,j}^n) - D(S_{i,j-\frac{1}{2}}^n) (S_{i,j}^n - S_{i,j-1}^n) \right) \\ & \quad + \frac{\tau \epsilon^2}{\Delta x^2 \Delta t} \left((S_{i+1,j}^{n+1} - 2S_{i,j}^{n+1} + S_{i-1,j}^{n+1}) - (S_{i+1,j}^n - 2S_{i,j}^n + S_{i-1,j}^n) \right) \\ & \quad + \frac{\tau \epsilon^2}{\Delta z^2 \Delta t} \left((S_{i,j+1}^{n+1} - 2S_{i,j}^{n+1} + S_{i,j-1}^{n+1}) - (S_{i,j+1}^n - 2S_{i,j}^n + S_{i,j-1}^n) \right), \end{aligned} \quad (4.36)$$

where Δx and Δz are the spatial step sizes in the horizontal and the vertical directions, respectively. The numerical flux function $\mathcal{F}_l(\bar{S}_{i,j}^n, S_{i,j}^n, S_{(i,j)_l}^n)$ is given as

$$\begin{aligned} & \mathcal{F}_l(\bar{S}_{i,j}^n, S_{i,j}^n, S_{(i,j)_l}^n) \\ & := |E_l| \left(\max\{\mathbf{n}_l \cdot \mathbf{V}_l[\bar{S}_{i,j}^n], 0\} f(S_{i,j}^n) + \min\{\mathbf{n}_l \cdot \mathbf{V}_l[\bar{S}_{i,j}^n], 0\} f(S_{(i,j)_l}^n) \right), \end{aligned} \quad (4.37)$$

where \mathbf{n}_l is the outer normal to the edge E_l of the cell $T_{i,j}$, $|E_l|$ is the length of the edge E_l , and $\mathbf{V}_l^n = (U_l^n, W_l^n)^T$ is the discrete velocity vector with

$$\begin{aligned} U_{i+\frac{1}{2},j}^n &= \frac{1}{2} \left(\frac{\lambda_{tot}(S_{i+1,j}^n)\kappa_{i+1,j}}{\Delta z \sum_{m=1}^{N_z} \lambda_{tot}(S_{i+1,m}^n)\kappa_{i+1,m}} + \frac{\lambda_{tot}(S_{i,j}^n)\kappa_{i,j}}{\Delta z \sum_{m=1}^{N_z} \lambda_{tot}(S_{i,m}^n)\kappa_{i,m}} \right), \\ W_{i,j+\frac{1}{2}}^n &= -\frac{\Delta z}{\Delta x} \sum_{m=1}^j \left(U_{i+\frac{1}{2},j}^n - U_{i-\frac{1}{2},j}^n \right), \end{aligned} \quad (4.38)$$

at the edges $E_{i+\frac{1}{2},j}$ and $E_{i,j+\frac{1}{2}}$, respectively. The initial condition $S_j^0 \in H^1(\Omega)$ is defined in each layer j as follows

$$S_j^0(x) = \frac{S_{\text{inflow},j}(1-x)^2}{10^5 x^2 + (1-x)^2},$$

for a constant $S_{\text{inflow},j} \in [0, 1]$, $j = 1, \dots, N_z$ and $x \in (0, 1)$.

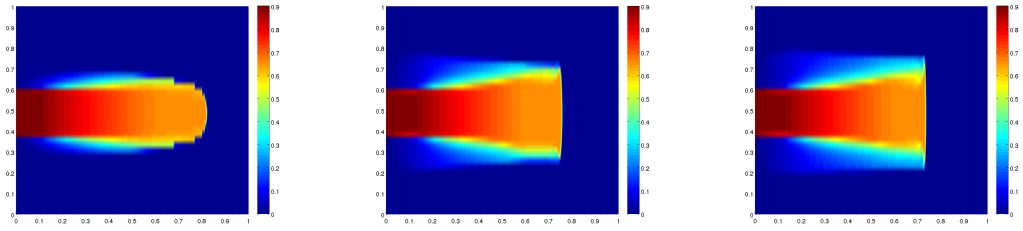
4.3.1 Brinkman VE-model vs. Brinkman Two-Phase Flow Model

This section investigates the validity and computational efficiency of the Brinkman VE-model (4.33), (4.34), and (4.35) by comparing it to the Brinkman two-phase flow model (4.3). For consistency with the Brinkman VE-model, we neglect capillary pressure in the second and third equation of the dimensionless Brinkman two-phase flow model (4.20). Then equation (4.20) reduces to

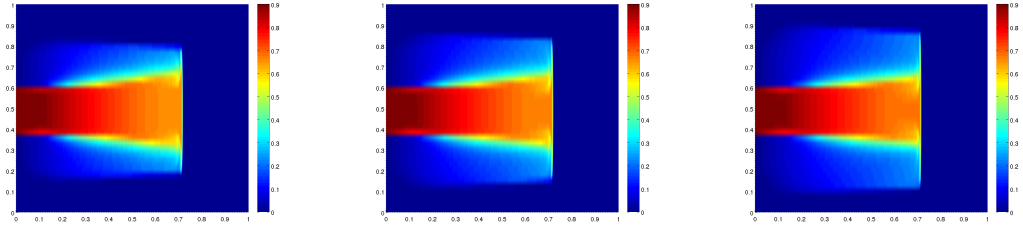
$$\begin{aligned} \partial_t S^\gamma - \tau \epsilon^2 \partial_{xxt} S^\gamma - \tau \epsilon^2 \partial_{zzt} S^\gamma + \partial_x (f(S^\gamma) U^\gamma) + \frac{1}{\gamma} \partial_z (f(S^\gamma) W^\gamma) \\ + \epsilon \partial_x (\kappa_1 \bar{\lambda}(S^\gamma) \partial_x p_c(S^\gamma)) + \epsilon \partial_z (\kappa_3 \bar{\lambda}(S^\gamma) \partial_z p_c(S^\gamma)) = 0, \\ U^\gamma = -\lambda_{\text{tot}}(S^\gamma) \kappa_1 \partial_x p^\gamma, \\ \gamma W^\gamma = -\lambda_{\text{tot}}(S^\gamma) \kappa_3 \partial_z p^\gamma, \\ \partial_x U^\gamma + \frac{1}{\gamma} \partial_z W^\gamma = 0, \end{aligned} \tag{4.39}$$

in the scaled domain $(0, 1)^2 \times (0, T)$, where $\gamma = \frac{1}{L}$ is the geometrical parameter of the domain. For solving this model, we use the IMPES-method [35] with pressure $p = 1$ at the inflow boundary and $p = 0$ on the outflow boundary.

In the following we present three examples that compare the Brinkman VE-model to the Brinkman two-phase flow model. The first example shows the convergence of numerical solutions for the dimensionless Brinkman two-phase flow model (4.39) to the corresponding solution of the Brinkman VE-model as the geometrical parameter $\gamma \rightarrow 0$. The second example shows the ability of the Brinkman two-phase flow model and the Brinkman VE-model to describe the phenomenon of saturation overshoots. It also shows the effect of decreasing the parameter γ on saturation overshoots. The third example investigates the effect of increasing the viscosity ratio M of the fluids on the accuracy of the Brinkman VE-model.



(a) Sol. of (4.39) for $\gamma = 1$ (b) Sol. of (4.39) for $\gamma = 1/16$ (c) Sol. of (4.39) for $\gamma = 1/32$



(d) Sol. of (4.39) for $\gamma = 1/64$ (e) Sol. of (4.39) for $\gamma = 1/128$ (f) Brinkman VE-model

Figure 4.2: A comparison of the dimensionless Brinkman two-phase model (4.39) with a decreasing parameter $\gamma \in \{1, \frac{1}{16}, \frac{1}{32}, \frac{1}{64}, \frac{1}{128}\}$ to the Brinkman VE-model (4.33), (4.34), and (4.35), for $N_x = 1000$, $N_z = 40$, $\tau = 1$, $M = 2$, and $T = 0.6$.

Example 1: In this example, we consider a viscosity ratio $M = 2$ of the flowing fluids and the inflow boundary condition

$$S_{\text{inflow}} = \begin{cases} 0 & : z \leq \frac{2}{5} \text{ and } z > \frac{3}{5}, \\ 0.9 & : \frac{2}{5} < z \leq \frac{3}{5}. \end{cases}$$

Figures (4.2(a) - 4.2(e)) present the numerical solutions of the dimensionless Brinkman two-phase flow model (4.39) using different geometrical parameters $\gamma \in \{1, \frac{1}{16}, \frac{1}{32}, \frac{1}{64}, \frac{1}{128}\}$, respectively. Figure 4.2(f) presents the numerical solution of the Brinkman VE-model (4.33), (4.34), and (4.35) using the numerical scheme (4.36), (4.37), and (4.38). The spatial domain $(0, 1)^2$ for both models is discretized into a uniform Cartesian grid with $N_x = 1000$ cells in the horizontal direction and $N_z = 40$ cells in the vertical and the end time is $T = 0.6$.

Figure 4.2 shows that numerical solutions of the dimensionless Brinkman two-phase flow model converge to the numerical solution of the Brinkman VE-model as the geometrical parameter $\gamma \rightarrow 0$. Moreover, the spreading speed of invading fluid using the Brinkman VE-model is captured very well.

For a better presentation of the convergence, we show in Figure 4.3 the numerical solution of both models in the middle layer only. The figure shows that saturation distribution and spreading speed of the dimensionless Brinkman two-

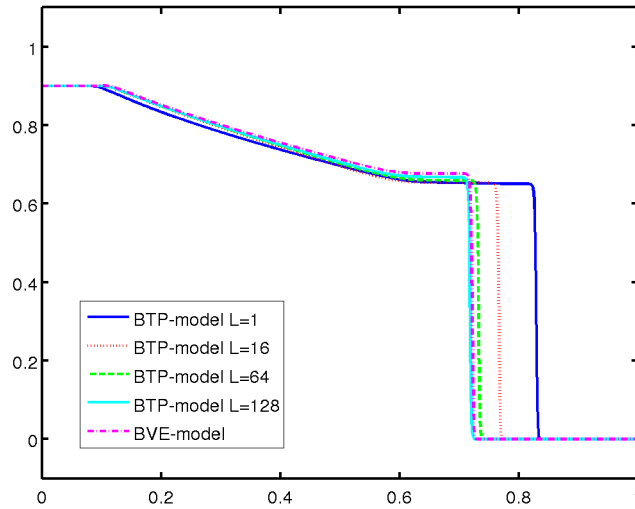


Figure 4.3: Saturation distribution in the middle layer using the dimensionless Brinkman two-phase model (BTP) (4.39) with a decreasing parameter $\gamma \in \{1, \frac{1}{16}, \frac{1}{64}, \frac{1}{128}\}$ and the Brinkman VE-model (BVE), for $\Delta x = 0.0005$, $\tau = 2$, $\mu_i = 1$, $\mu_d = 2$, and $T = 0.6$.

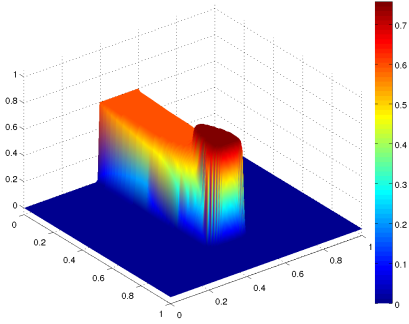
phase flow model, using $\gamma = 1/128$, almost coincide with those of the Brinkman VE-model.

Table 4.1 presents the CPU-time required by the Brinkman VE-model (4.33), (4.34), and (4.35) and the Brinkman two-phase flow model (4.39) using $\gamma = 100$. It is noticeable that for a small number of horizontal cells ($N_x = 100$), the computational time required by both models is similar. On the contrary, the Brinkman VE-model is almost 1.4 times faster than the Brinkman two-phase flow model when the numbers of horizontal cells is large ($N_x = 1000$). The extra time required by the Brinkman two-phase flow model is used to solve a linear system for pressure, which becomes larger by increasing the number of horizontal cells. However, using large numbers of horizontal cells is necessary to describe the phenomenon of saturation overshoots as illustrated in the following examples.

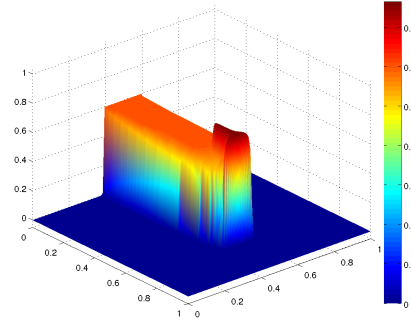
Example 2: In this example we consider the viscosity ratio $M = 2$ and the inflow boundary condition

$$S_{\text{inflow}} = \begin{cases} 0 & : z \leq \frac{2}{5} \text{ and } z > \frac{3}{5}, \\ 0.6 & : \frac{2}{5} < z \leq \frac{3}{5}. \end{cases}$$

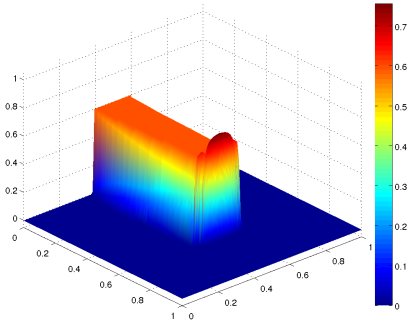
Figures (4.4(a) - 4.4(c)) present the numerical solutions of the dimensionless Brinkman two-phase flow model (4.39) using the geometrical parameters $\gamma \in \{1, \frac{1}{4}, \frac{1}{16}\}$, respectively. Finally, the numerical solution of the Brinkman



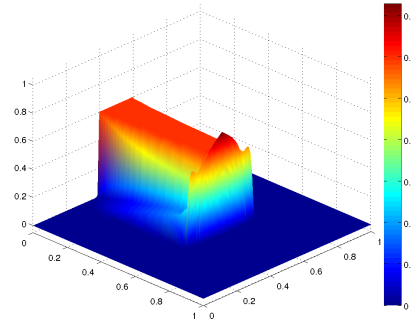
(a) Sol. of (4.39) for $\gamma = 1$



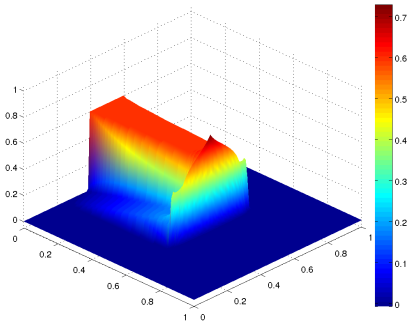
(b) Sol. of (4.39) for $\gamma = 1/4$



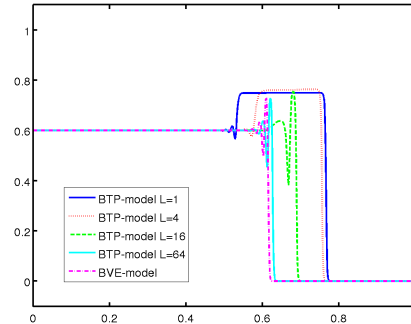
(c) Sol. of (4.39) for $\gamma = 1/16$



(d) Sol. of (4.39) for $\gamma = 1/64$



(e) Brinkman VE-model



(f) Sols. in the middle layer

Figure 4.4: A Comparison of the Brinkman two-phase model (4.39) with a decreasing parameter $\gamma \in \{1, \frac{1}{4}, \frac{1}{16}, \frac{1}{64}\}$ with the Brinkman VE-model using $N_x = 2000$, $N_z = 100$, $\tau = 2$, $M = 2$, and $T = 0.6$.

N_z	N_x	Model	CPU-Time
10	100	Brinkman VE-model	0.75 s
	100	Brinkman two-phase model	1.08 s
	1000	Brinkman VE-model	26.7 s
	1000	Brinkman two-phase model	39.4 s
40	100	Brinkman VE-model	3.34 s
	100	Brinkman two-phase model	4.33 s
	1000	Brinkman VE-model	187.3 s
	1000	Brinkman two-phase model	260 s
80	100	Brinkman VE-model	8.2 s
	100	Brinkman two-phase model	5.53 s
	1000	Brinkman VE-model	462.26 s
	1000	Brinkman two-phase model	678 s

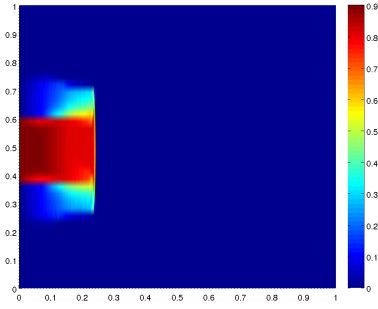
Table 4.1: Comparison of CPU time for the Brinkman VE-model and Brinkman two-phase flow model with $\gamma = 100$.

VE-model (4.33), (4.34), and (4.35) is presented in Figure 4.4(e). The spatial domain $(0, 1)^2$ for both models is discretized into a uniform Cartesian grid with $N_x = 2000$ cells in the horizontal direction and $N_z = 40$ cells in the vertical and the end time is $T = 0.6$.

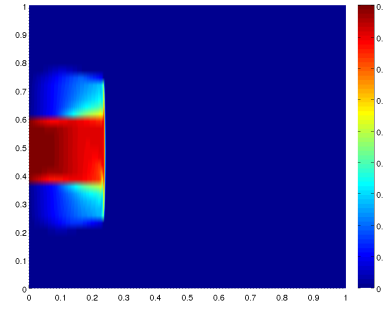
Figure 4.4 shows the ability of the two-phase flow model and the VE-model to describe the phenomenon of saturation overshoots when Darcy's equation is replaced by Brinkman's equations. In addition to this, the figure shows the effect of decreasing the geometrical parameter γ in the Brinkman two-phase flow model on reducing the saturation overshoots, which finally converges to the situation using the Brinkman VE-model. This is due to the fact that decreasing the parameter γ increases the vertical mass exchange at the wetting front such that saturation decreases to values that produce less overshoots.

For a better presentation of the convergence in Figure 4.4, we present in Figure 4.4(f) the saturation profile in the one-dimensional middle layer of the domain. Figure 4.4(f) shows the convergence of the saturation behavior and the spreading speed of the Brinkman two-phase flow model to those of the Brinkman VE-model. In addition to this, it shows the high reduction of saturation at the wetting front for both the Brinkman VE-model and the Brinkman two-phase flow model with $\gamma = 1/16$, under the effect of the high vertical exchange of mass. This explains the oscillating behavior of the solution at the interface, which corresponds to the case when $S_{\text{inflow}} \leq 0.5$ in the one dimensional model studied in [48, 49].

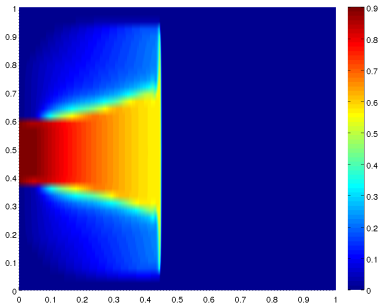
Example 3: In this example we study the effect of increasing the viscosity ratio $M \in \{1, 3, 5, 7, 9\}$ on the accuracy of the Brinkman VE-model. For this, we



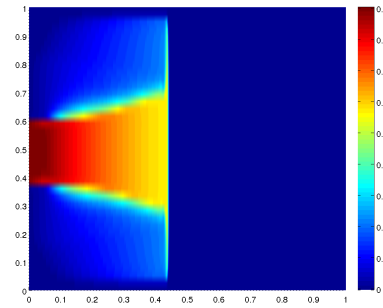
(a) Sol. of (4.39) for $M = 1$



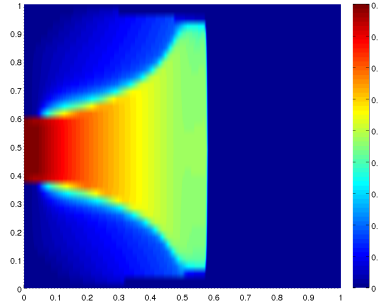
(b) Brinkman VE-model for $M = 1$



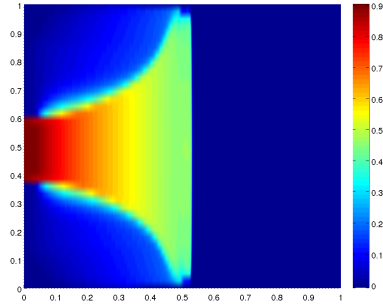
(c) Sol. of (4.39) for $M = 3$



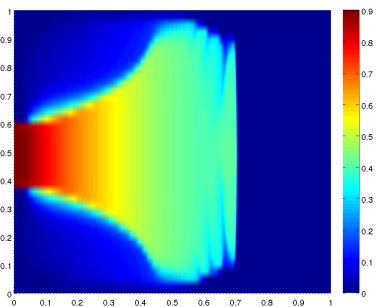
(d) Brinkman VE-model for $M = 3$



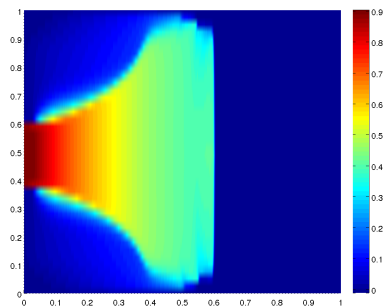
(e) Sol. of (4.39) for $M = 5$



(f) Brinkman VE-model for $M = 5$



(g) Sol. of (4.39) for $M = 7$



(h) Brinkman VE-model for $M = 7$

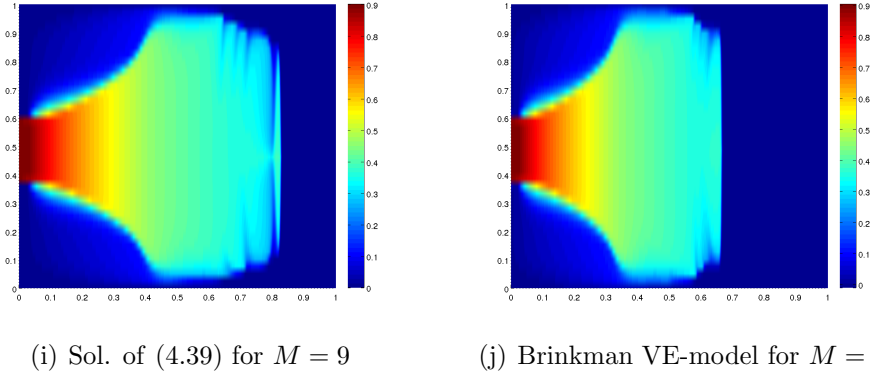


Figure 4.5: The Brinkman two-phase model (4.39) (left column) with $\gamma = 1/128$ and the Brinkman VE-model (4.33), (4.34), and (4.35) (right column) using different viscosity ratios $M \in \{1, 3, 5, 7, 9\}$, for $N_x = 1000$, $N_z = 40$, $\tau = 1$, and $T = 0.3$.

consider the inflow boundary condition

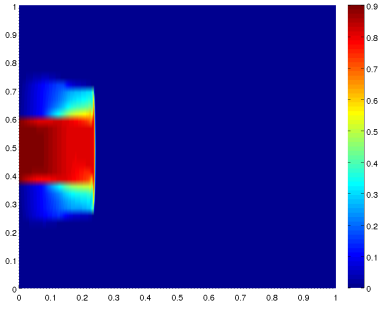
$$S_{\text{inflow}} = \begin{cases} 0 & : z \leq \frac{2}{5} \text{ and } z > \frac{3}{5}, \\ 0.9 & : \frac{2}{5} < z \leq \frac{3}{5}. \end{cases}$$

Figure 4.5(a), 4.5(c), 4.5(e), 4.5(g), and 4.5(i) present the numerical solutions of the dimensionless Brinkman two-phase flow model (4.39) using the geometrical parameter $\gamma = 1/128$ and the viscosity ratios $M \in \{1, 3, 5, 7, 9\}$, respectively. Figure 4.5(b), 4.5(d), 4.5(f), 4.5(h), 4.5(j) present the numerical solution of the Brinkman VE-model (4.33), (4.34), and (4.35) using the viscosity ratios $M \in \{1, 3, 5, 7, 9\}$, respectively. The spatial domain $(0, 1)^2$ for both models is discretized into a uniform Cartesian grid with $N_x = 1000$ cells in the horizontal direction and $N_z = 40$ cells in the vertical and the end time is $T = 0.3$.

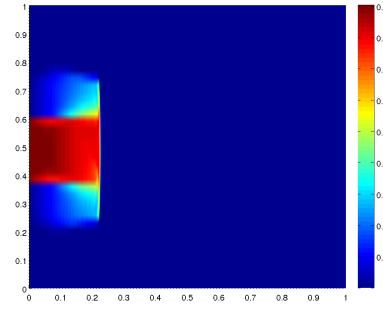
Figure 4.5 shows that numerical solutions of the dimensionless Brinkman two-phase flow model are very similar to the corresponding numerical solution of the Brinkman VE-model when the viscosity ratio is small, $M \in \{1, 3\}$. However, increasing the viscosity ratio to $M \in \{5, 7, 9\}$ has a bad effect on the convergence rate of the Brinkman two-phase flow model to the Brinkman VE-model and on the ability of the Brinkman VE-model to capture the spreading speed.

Figure 4.5 shows that the accuracy of the Brinkman VE-model is limited for small viscosity ratios $M \leq 3$. This is a consequence of rescaling the time variable t in (4.29) by the vertically averaged horizontal velocity q given as

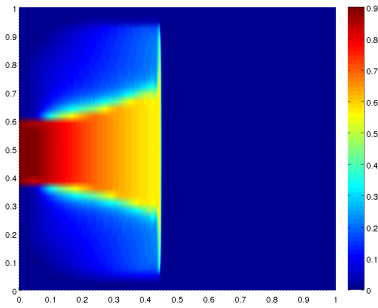
$$q(t) = - \int_0^1 \lambda_{\text{tot}}(S(0, z, t)) \kappa(0, z) \partial_x p(0, z, t) dz, \quad (4.40)$$



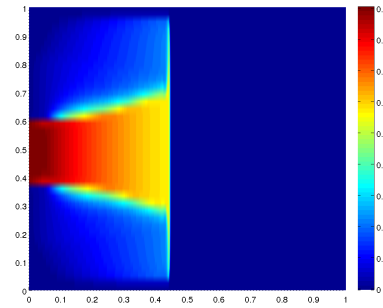
(a) Sol. of (4.39) for $M = 1$



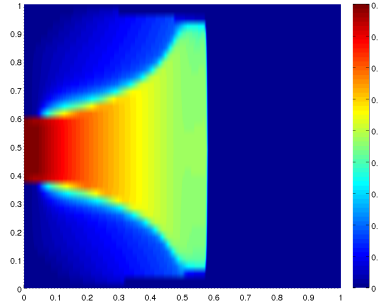
(b) Brinkman VE-model for $M = 1$



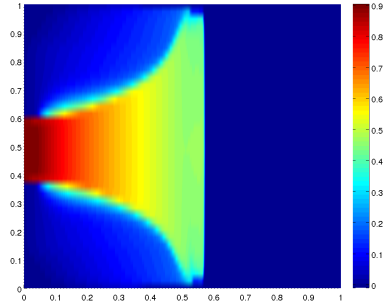
(c) Sol. of (4.39) for $M = 3$



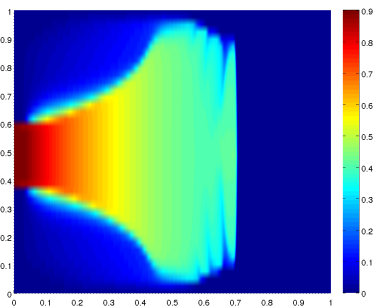
(d) Brinkman VE-model for $M = 3$



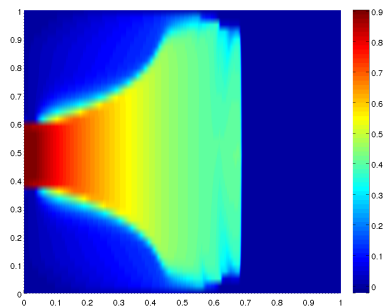
(e) Sol. of (4.39) for $M = 5$



(f) Brinkman VE-model for $M = 5$



(g) Sol. of (4.39) for $M = 7$



(h) Brinkman VE-model for $M = 7$

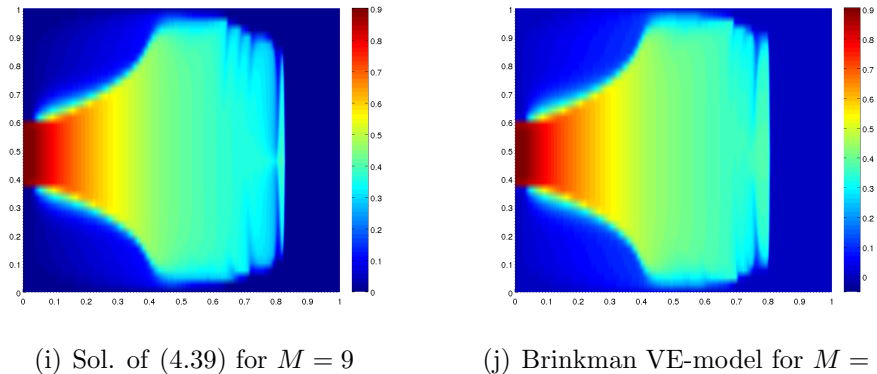


Figure 4.6: The Brinkman two-phase model (4.39) (left column) with $\gamma = 1/128$ and the non-rescaled Brinkman VE-model (4.27), (4.28), (4.33), and (4.35) (right column) using different viscosity ratios $M \in \{1, 3, 5, 7, 9\}$, for $N_x = 1000$, $N_z = 40$, $\tau = 1$, and $T = 0.3$.

$t \in [0, T]$ at the inflow boundary Ω_{inflow} . In Figure 4.6, we repeat the comparison from Figure 4.5 such that the numerical solutions for the Brinkman VE-model are considered before the rescaling step (4.29). However, evaluating the function q in (4.40) requires solving the elliptic equation

$$-\partial_x \int_0^1 \lambda_{\text{tot}}(S) \kappa \partial_x p \, dz = 0.$$

Hence, the computational complexity of the Brinkman VE-model increases, but remains less than that of the Brinkman two-phase flow model.

Figure 4.6(a), 4.6(c), 4.6(e), 4.6(g), and 4.6(i) present the numerical solutions of the dimensionless Brinkman two-phase flow model (4.39) using the geometrical parameter $\gamma = 1/128$ and the viscosity ratios $M \in \{1, 3, 5, 7, 9\}$, respectively. Figure 4.6(b), 4.6(d), 4.6(f), 4.6(h), 4.6(j) present the numerical solution of the Brinkman VE-model (4.27), (4.28), (4.33), and (4.35) using the viscosity ratios $M \in \{1, 3, 5, 7, 9\}$, respectively. Figure 4.6 shows that the spreading speed of the invading fluid is very well estimated using the Brinkman VE-model for all viscosity ratios $M \in \{1, 3, 5, 7, 9\}$. However, the convergence rate of the Brinkman two-phase flow model to the Brinkman VE-model using the viscosity ratios $M \in \{1, 3\}$ is better than that using $M \in \{5, 7, 9\}$.

4.3.2 Brinkman VE-model vs. VE-model

We give numerical examples that show the ability of the Brinkman VE-model (4.30), (4.31), and (4.32) to capture more physical properties than the VE-model

(3.33), namely, saturation overshoots and spreading speed for fluids with a small viscosity ratio M . Estimating spreading speed has been of special interest for many researchers as an indicator on the efficiency of oil recovery and the safety of CO₂ sequestration process. In [40, 41, 54], the authors develop different selection principles to find upper bounds on the speed of the mixing zone in the case of miscible displacement. Mathematically, the phenomenon of saturation overshoots is identified by undercompressive traveling wave solutions, which are known to be slower than classical compressive waves [8]. Yortsos and Salin [54] expect that sharp bounds on the spreading speed might be found using these waves.

The purpose of this section is to demonstrate the effect of the higher order terms in the Brinkman VE-model on the numerical solution. For this, we design a comparison of the Brinkman VE-model with the VE-model (3.33) based on two examples. In the first example the invading fluid is injected in the middle part of the inflow boundary, the domain is assumed to be homogeneous with permeability $\kappa = 1$, and the vertical dimension of the domain is discretized into $N_z = 40$ layers. In the second example, the invading fluid is injected along the inflow boundary and the domain consists of two main layers with different permeabilities. For a better comparison of the traveling wave solutions in this example, the vertical dimension of the domain is discretized into $N_z = 2$ layers.

Example 1: We consider a homogeneous domain with permeability $\kappa = 1$ such that the invading fluid is injected mainly into the middle part of the inflow boundary,

$$S_{\text{inflow}}(z) = \begin{cases} 0.1 & : z \leq \frac{1}{4} \text{ and } z > \frac{3}{4}, \\ 0.9 & : \frac{1}{4} < z \leq \frac{3}{4}. \end{cases}$$

The left part of Figure 4.7 corresponds to the VE-model and the right part corresponds to the Brinkman VE-model using a Cartesian grid with $N_x \times N_z = 2000 \times 40$, the parameters $M = 2$, $T = 0.6$, and $\tau = 2$.

Figure 4.7 shows that the Brinkman VE-model describes the phenomenon of saturation overshoots. Moreover, the spreading speed of the invading fluid $U \approx 1.27$ is smaller than that using the VE-model $u \approx 1.33$. Figure 4.8 shows the saturation profile in the one-dimensional middle layer of the domain, where the phenomenon of saturation overshoots and its effect on the spreading speed using the Brinkman VE-model are more visible.

Example 2: This example shows the effect of the vertical exchange of mass between adjacent layers in a flat medium on the phenomenon of saturation overshoots. For this, we assume constant saturation $S_{\text{inflow}} = 1$ along the inflow bound-

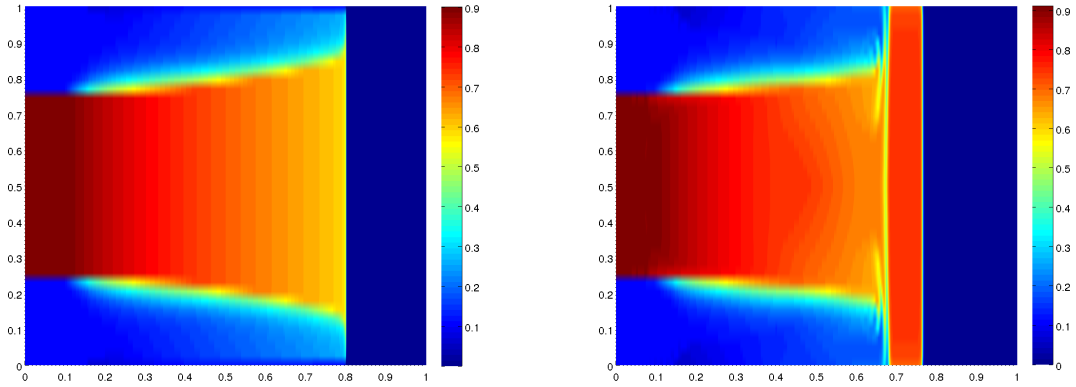


Figure 4.7: Numerical solution of the Brinkman VE-model (right) and of the VE-model (left), using $M = 2$, $\epsilon = 0.001$, $\tau = 2$, $N_x = 2000$, $N_z = 40$, and $T = 0.6$.

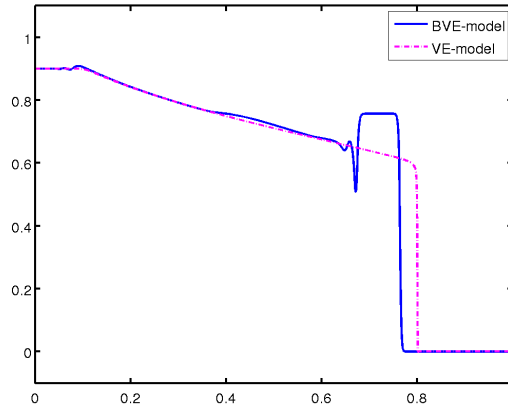


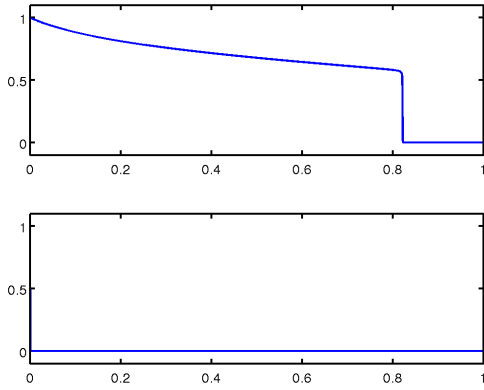
Figure 4.8: Numerical solution of the Brinkman VE-model and the VE-model in the middle layer, using $M = 2$, $\epsilon = 0.001$, $\tau = 2$, $N_x = 2000$, and $T = 0.6$.

ary and that the domain consists of two parts with different permeabilities

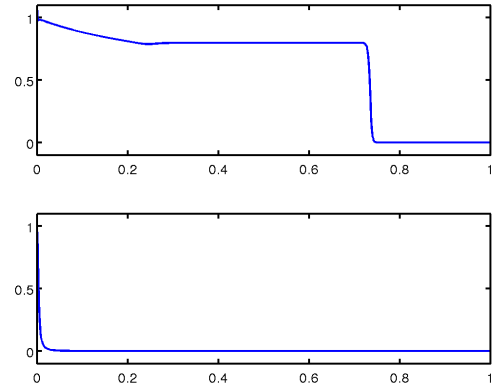
$$\kappa = \begin{cases} \kappa_1, & \text{in } \Omega_{\text{upper}} := (0, 1) \times (0.5, 1), \\ \kappa_3, & \text{in } \Omega_{\text{lower}} := (0, 1) \times (0, 0.5). \end{cases} \quad (4.41)$$

To keep the presentation simple, we assume that the domain consists of two main layers $N_z = 2$. Figure 4.9 shows a sequence of numerical solutions of the VE-model (left column) and the Brinkman VE-model (right column) with a fixed permeability $\kappa_1 = 1$ in the upper layer and changing permeability $\kappa_3 \in \{0, 0.2, 0.4, 0.6, 0.8, 1\}$ in the lower layer.

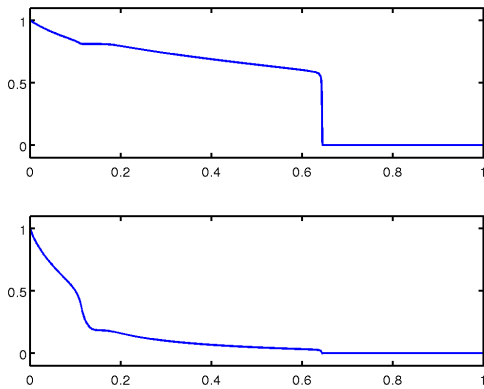
Figure 4.9(a), 4.9(c), 4.9(e), 4.9(g), 4.9(i), and 4.9(k) present saturation behavior of the invading fluid using the VE-model with the permeabilities $\kappa_1 = 1$ and $\kappa_3 = 0, 0.2, 0.4, 0.6, 0.8, 1$, respectively. In these figures saturation of the



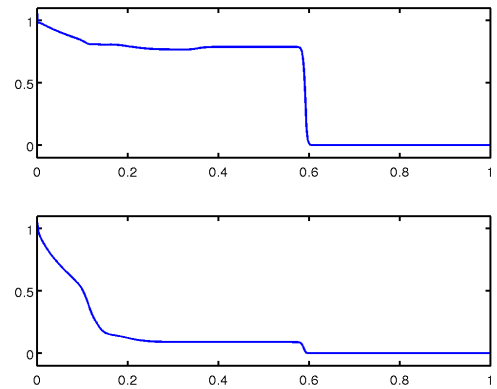
(a) VE-model: $\kappa_1 = 1, \kappa_3 = 0$



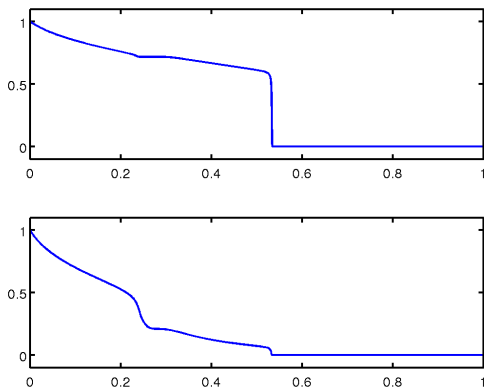
(b) Brinkman VE-model: $\kappa_1 = 1, \kappa_3 = 0$



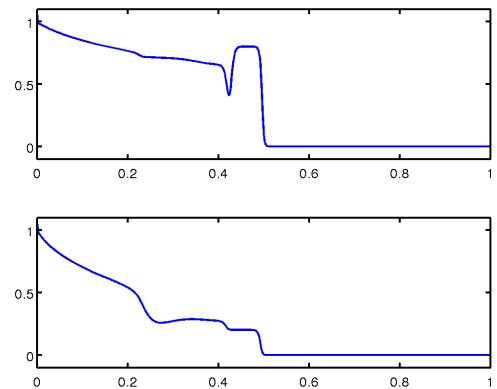
(c) VE-model: $\kappa_1 = 1, \kappa_3 = 0.2$



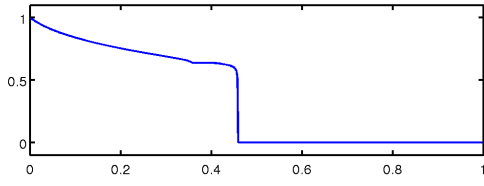
(d) Brinkman VE-model: $\kappa_1 = 1, \kappa_3 = 0.2$



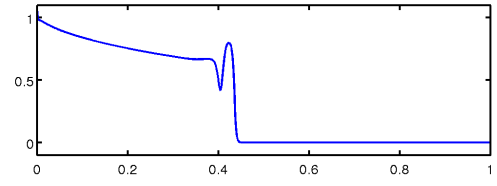
(e) VE-model: $\kappa_1 = 1, \kappa_3 = 0.4$



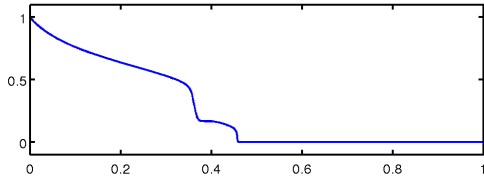
(f) Brinkman VE-model: $\kappa_1 = 1, \kappa_3 = 0.4$



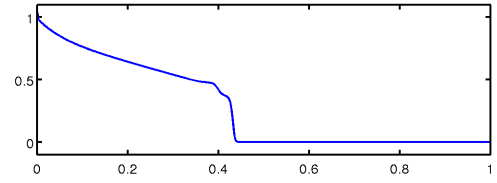
(g) VE-model: $\kappa_1 = 1, \kappa_3 = 0.6$



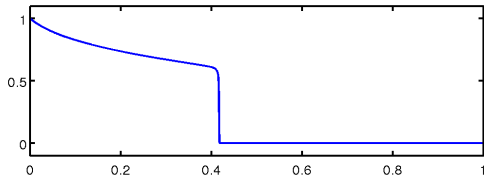
(h) Brinkman VE-model: $\kappa_1 = 1, \kappa_3 = 0.6$



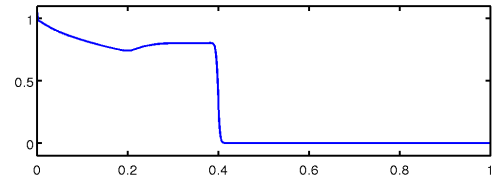
(i) VE-model: $\kappa_1 = 1, \kappa_3 = 0.8$



(j) Brinkman VE-model: $\kappa_1 = 1, \kappa_3 = 0.8$



(k) VE-model: $\kappa_1 = 1, \kappa_3 = 1$



(l) Brinkman VE-model: $\kappa_1 = 1, \kappa_3 = 1$

Figure 4.9: Numerical solutions of the VE-model (left) and the Brinkman VE-model (right) for different permeability ratios $\kappa_1 = 1, \kappa_3 = 0, 0.2, 0.4, 0.6, 0.8, 1$, $M = 2, \tau = 5, N_x = 2000$, and $T = 0.3$.

invading fluid decreases monotonically from the left state $S = 1$ to the right state $S = 0$ in a rarefaction wave followed by a compressive shock. Figure 4.9(b), 4.9(d), 4.9(f), 4.9(h), 4.9(j), and 4.9(l) present saturation behavior of the invading fluid using the Brinkman VE-model with the permeabilities $\kappa_1 = 1$ and $\kappa_3 = 0, 0.2, 0.4, 0.6, 0.8, 1$, respectively. In these figures saturation decays monotonically from the left state $S = 1$ to a plateau value $S^* < 1$ in a rarefaction wave then to the right state $S = 0$ in an undercompressive shock. This saturation behavior is expected according to the traveling wave analysis in [48, 49] as the vertical mixing between the two layers is very low. In Figure 4.9(f), 4.9(h), and 4.9(j) saturation profile is not monotone, which is a consequence of the higher amount of vertical flow from the upper layer to the lower. In these figures saturation rarefacts from the left state $S = 1$ to an intermediate state ($S_m < 1$), which is smaller than the plateau value S^* . This wave is then followed by an undercompressive shock to a higher value $S_u > S_m$ and then by a compressive shock to the left state $S = 0$. Figure 4.9 also shows that the spreading speed of the invading fluid using the Brinkman VE-model is smaller than that using the VE-model.

Figure 4.7 and 4.9 show the ability of the Brinkman VE-model and the VE-model to describe the vertical dynamics in the domain. However, the Brinkman VE-model is able to capture the phenomenon of saturation overshoots, in contrast to the VE-model and, consequently, it provides sharper estimates on the invasion speed. This ability is a consequence of the higher order terms in the model, which leads to a higher computational complexity compared to the VE-model.

4.4 Conclusion

We proposed the Brinkman VE-model to describe fluid flows in macroscopically heterogeneous flat media. The model is an extension of the VE-model and maintains much of its numerical advantages. We derived the model by applying asymptotic analysis to the dimensionless two-phase flow model with Brinkman's equations replacing Darcy's law. The Brinkman VE-model is a third-order pseudo-parabolic differential equation, in which the horizontal and vertical velocity components depend nonlocally on the unknown saturation.

The proposed model maintains much of the numerical efficiency of the VE-model and therefore has a reduced computational complexity over the two-phase flow with Brinkman's equations. In addition, it is able to describe more physical phenomena than the VE-model, such as saturation overshoots. To demonstrate

the model's advantages, we performed different numerical tests and concluded the following aspects:

1. Numerical solutions of the Brinkman two-phase flow model converge to the corresponding numerical solution of the Brinkman VE-model as the geometrical parameter $\gamma \rightarrow 0$.
2. The computational complexity of the Brinkman VE-model is much less than that of the Brinkman two-phase flow model.
3. The accuracy of the Brinkman VE-model is limited to low viscosity ratios ($M \leq 5$).
4. Including Brinkman's equation in the two-phase flow model and in the extended VE-model allows describing the phenomenon of saturation overshoots.
5. Decreasing the geometrical parameter $\gamma = \frac{\text{thickness}}{\text{length}}$ of a porous medium reduces the effect of saturation overshoot. This phenomenon can be explained as follows: decreasing the geometrical parameter γ in the Brinkman two-phase flow model increases the vertical velocity at the wetting front. Hence, the vertical exchange of mass increases, such that saturation decreases to values, at which saturation overshoots might be not expected to occur.

Chapter 5

Well-posedness of the Brinkman Vertical Equilibrium Model

We proposed in Chapter 4 the Brinkman VE-model to describe fluid flows in saturated flat porous media that are macroscopically heterogeneous. The proposed model is a third-order pseudo-parabolic differential equation of saturation alone that explicitly accounts for the vertical dynamics in the medium. The model has several numerical advantages over the Brinkman two-phase flow model and the VE-model. In addition to this, the higher order terms in the proposed model provide a dissipative effect, such that weak solutions in the distributional sense can be defined. Therefore, we investigate in this chapter the well-posedness of the Brinkman VE-model.

We consider the Brinkman VE-model (4.30), (4.31) and (4.32) under the assumptions $\kappa := 1$, $D(S) := 1$, and $\epsilon_1 = \epsilon_2 := 1$. We also set $\beta = \beta_1 = \beta_2$. Then, the model reduces to

$$\partial_t S + \partial_x (f(S)U[S]) + \partial_z (f(S)W[S]) - \Delta S - \beta \Delta \partial_t S = 0, \quad (5.1)$$

where

$$U[S] = \frac{\lambda_{tot}(S)}{\int_0^1 \lambda_{tot}(S) dz}, \quad W[S(\cdot, z, \cdot)] = -\partial_x \int_0^z U[S(\cdot, r, \cdot)] dr, \quad (5.2)$$

for all $z \in (0, 1)$ in the domain $\Omega \times (0, T)$. The definition of the velocity components U and W in (5.2) implies that the velocity $\mathbf{V} = (U, W)^T$ is incompressible

$$\nabla \cdot \mathbf{V} = 0. \quad (5.3)$$

The Brinkman VE-model (5.1), (5.2), and (5.3) is associated with the initial and boundary conditions

$$\begin{aligned} S(\cdot, \cdot, 0) &= S^0, & \text{in } \Omega, \\ S &= 0, & \text{on } \partial\Omega \times [0, T]. \end{aligned} \tag{5.4}$$

Remark 5.1. *Associating the Brinkman VE-model (5.1), (5.2), and (5.3) with Dirichlet boundary conditions is possible because the higher order terms in the model are linear. We choose a zero Dirichlet boundary condition in (5.4) to simplify the analysis. However, the analysis throughout the chapter can be extended to Dirichlet boundary conditions of the form $S = S_D$ on $\partial\Omega \times [0, T]$ such that S_D has appropriate regularity and satisfies $S_D = S^0$ on $\partial\Omega$ at time $t = 0$. In addition, this condition is still physically valid by assuming a larger domain with dry boundaries.*

Remark 5.2. *Proving the existence of a weak solution $S \in H^1(0, T; H^1(\Omega))$ for the Brinkman VE-model (5.1) and (5.2) with the initial and boundary condition (5.4) yields that $W[S] \in L^2(\Omega \times (0, T))$. With this information, we can solve the equation $W = w - \beta_2 \Delta w$ for the vertical velocity w from the previous chapter such that the zero Neumann condition on w and the periodicity condition on Δw in equation (4.6) are satisfied.*

The aim of this chapter is to prove existence and uniqueness of a weak solution for the Brinkman VE-model (5.1) and (5.2) in the bounded domain $\Omega_T := \Omega \times (0, T)$, where $\Omega = (0, 1)^2$. We do this in the following steps: in Section 5.1, we approximate the time derivatives in the model using the backward difference quotient then apply Galerkin's method to the resulting elliptic problem. After that, we prove the existence of a sequence of discrete solutions for the approximated problem. In Section 5.2, we show that the sequence of discrete solutions fulfills a set of a priori estimates. These estimates are used in Section 5.3 to conclude a strong convergence of the sequence in the space $L^2(\Omega_T)$. Then, we prove that the limit of the sequence is a weak solution of the Brinkman VE-model. Section 5.4 shows the boundedness of the weak solutions in the space $L^\infty(\Omega_T)$. After that, we prove in Section 5.5 the uniqueness of the weak solutions for the Brinkman VE-model when the fractional flow function and the horizontal velocity are linear. Finally, Section 5.6 summarizes the chapter.

5.1 Preliminaries and Assumptions

This chapter is concerned with finding weak solutions $S \in H^1(0, T; H^1(\Omega))$ for the Brinkman VE-model. Thus, it is not known a priori whether saturation is bounded ($S \in [0, 1]$) or not. Therefore, we extend in this chapter the domain of the fractional flow function f and the total mobility λ_{tot} from $[0, 1]$ to \mathbb{R} such that $f(S) = f(1)$ for all $S \in (1, \infty)$, $f(S) = f(0)$ for all $S \in (-\infty, 0)$, $\lambda_{tot}(S) = \lambda_{tot}(1)$ for all $S \in (1, \infty)$, and $\lambda_{tot}(S) = \lambda_{tot}(0)$ for all $S \in (-\infty, 0)$. Throughout this chapter, the following assumptions on the initial boundary value problem (5.1), (5.2), (5.3), and (5.4) hold.

Assumption 5.3. 1. *The spatial domain $\Omega \subset \mathbb{R}^2$ is open, connected, bounded with Lipschitz continuous boundary $\partial\Omega$ and $0 < T < \infty$.*

2. *The initial condition satisfies $S^0 \in H_0^1(\Omega)$.*

3. *The fractional flow function f is Lipschitz continuous, bounded, nonnegative and monotone increasing, such that there exist numbers $M, L > 0$ with $f \leq M$, $f' \leq L$.*

4. *The total mobility function λ_{tot} is Lipschitz continuous, bounded, strictly positive, such that there exist numbers $a, M, L > 0$ with $0 < a < \lambda_{tot} \leq M$ and $|\lambda'_{tot}| \leq L$.*

Note that the numbers $M, L > 0$ are chosen large enough such that Assumption 5.3(3) and 5.3(4) hold.

Definition 5.4. (*Weak Solution*) *A function $S \in H^1(0, T; H_0^1(\Omega))$ is called a weak solution of the Brinkman VE-model (5.1) and (5.2) with the initial and boundary conditions (5.4) whenever the following conditions hold,*

1. $U[S], W[S] \in L^2(\Omega_T)$ and

$$\begin{aligned} \int_0^T \int_{\Omega} (\partial_t S \phi - f(S)U[S]\partial_x \phi - f(S)W[S]\partial_z \phi + \nabla S \cdot \nabla \phi) dx dz dt \\ + \beta \int_0^T \int_{\Omega} \nabla \partial_t S \cdot \nabla \phi dx dz dt = 0, \end{aligned} \quad (5.5)$$

for all test functions $\phi \in L^2(0, T; H_0^1(\Omega))$.

2. *The weak incompressibility property*

$$\int_0^T \int_{\Omega} (U[S]\partial_x \phi + W[S]\partial_z \phi) dx dz dt = 0, \quad (5.6)$$

holds for all test functions $\phi \in L^2(0, T; H_0^1(\Omega))$.

3. $S(\cdot, \cdot, 0) = S^0$ almost everywhere.

Remark 5.5. Note that the integral $\int_0^z \lambda_{tot}(S(\cdot, r, \cdot)) dr$, $z \in (0, 1)$ in the definition of the velocity components U , W is an integral over a set of measure zero. However, it is well-defined in the trace sense as the Trace theorem 2.12 implies the existence of a bounded linear operator $T : H^1(\Omega) \rightarrow L^2(\{x\} \times (0, z))$, for almost all x and $z \in (0, 1)$, and a constant C such that

$$\|TS\|_{L^2(\{x\} \times (0, z))} \leq \|S\|_{H^1(\Omega)}.$$

Remark 5.6. If the velocity component W would be Lipschitz continuous with respect to S , then the well-posedness of the model (5.1), (5.2), (5.3), and (5.4) follows [26].

Lemma 5.7. If Assumption 5.3(4) holds, then the velocity components U and W satisfy the properties:

1. U is bounded, such that $\|U[Q]\|_{L^\infty(\Omega_T)} \leq \frac{M}{a}$ for any function $Q \in L^2(\Omega_T)$.

2. For any functions $Q_1, Q_2 \in L^2(\Omega_T)$, the horizontal velocity U satisfies

$$\|U[Q_1] - U[Q_2]\|_{L^2(\Omega_T)} \leq \frac{2ML}{a^2} \|Q_1 - Q_2\|_{L^2(\Omega_T)}.$$

3. For any function $Q \in L^2(0, T; H^1(\Omega))$, the component W satisfies the growth condition

$$\|W[Q]\|_{L^2(\Omega_T)} \leq \frac{2ML}{a^2} \|\partial_x Q\|_{L^2(\Omega_T)}.$$

Proof. 1. Using Assumption 5.3(4) we have

$$\|U[Q]\|_{L^\infty(\Omega_T)} = \left\| \frac{\lambda_{tot}(Q)}{\int_0^1 \lambda_{tot}(Q(\cdot, z, \cdot)) dz} \right\|_{L^\infty(\Omega_T)} \leq \frac{M}{a}.$$

2. Using the chain rule and the triangle inequality, we have

$$\begin{aligned}
& \|U[Q_1] - U[Q_2]\|_{L^2(\Omega_T)} \\
&= \left\| \frac{\lambda_{tot}(Q_1)}{\int_0^1 \lambda_{tot}(Q_1) dz} - \frac{\lambda_{tot}(Q_2)}{\int_0^1 \lambda_{tot}(Q_2) dz} \right\|_{L^2(\Omega_T)}, \\
&\leq \left\| \frac{\lambda_{tot}(Q_1) \int_0^1 (\lambda_{tot}(Q_2) - \lambda_{tot}(Q_1)) dz}{\int_0^1 \lambda_{tot}(Q_1) dz \int_0^1 \lambda_{tot}(Q_2) dz} \right\|_{L^2(\Omega_T)} \\
&\quad + \left\| \frac{\int_0^1 \lambda_{tot}(Q_1) dz (\lambda_{tot}(Q_2) - \lambda_{tot}(Q_1))}{\int_0^1 \lambda_{tot}(Q_1) dz \int_0^1 \lambda_{tot}(Q_2) dz} \right\|_{L^2(\Omega_T)}, \\
&\leq \frac{M}{a^2} \left\| \int_0^1 \lambda'_{tot}(Q)(Q_2 - Q_1) dz \right\|_{L^2(\Omega_T)} + \frac{ML}{a^2} \|Q_2 - Q_1\|_{L^2(\Omega_T)},
\end{aligned}$$

for some $Q \in L^2(\Omega_T)$. Note that the first term in the above inequality is constant in the vertical direction. Applying Jensen's inequality, then Fubini's inequality to this term yields

$$\|U[Q_1] - U[Q_2]\|_{L^2(\Omega_T)} \leq \frac{2ML}{a^2} \|Q_2 - Q_1\|_{L^2(\Omega_T)}.$$

3. Using the chain rule and the triangle inequality, we have for any $z \in (0, 1)$

$$\begin{aligned}
\|W[Q]\|_{L^2(\Omega_T)} &= \left\| -\partial_x \frac{\int_0^z \lambda_{tot}(Q(\cdot, r, \cdot)) dr}{\int_0^1 \lambda_{tot}(Q(\cdot, r, \cdot)) dr} \right\|_{L^2(\Omega_T)}, \\
&= \left\| \frac{\int_0^z \lambda'_{tot}(Q(\cdot, r, \cdot)) \partial_x Q(\cdot, r, \cdot) dr \int_0^1 \lambda_{tot}(Q(\cdot, r, \cdot)) dr}{\left(\int_0^1 \lambda_{tot}(Q(\cdot, r, \cdot)) dr\right)^2} \right\|_{L^2(\Omega_T)} \\
&\quad + \left\| \frac{\int_0^1 \lambda'_{tot}(Q(\cdot, r, \cdot)) \partial_x Q(\cdot, r, \cdot) dr \int_0^z \lambda_{tot}(Q(\cdot, r, \cdot)) dr}{\left(\int_0^1 \lambda_{tot}(Q(\cdot, r, \cdot)) dr\right)^2} \right\|_{L^2(\Omega_T)}, \\
&\leq \frac{ML}{a^2} \left(\left\| \int_0^z \partial_x Q(\cdot, r, \cdot) dr \right\|_{L^2(\Omega_T)} + \left\| \int_0^1 \partial_x Q(\cdot, r, \cdot) dr \right\|_{L^2(\Omega_T)} \right).
\end{aligned}$$

Applying Jensen's inequality, Fubini's inequality and the fact that $\|\partial_x Q\|_{L^2(\Omega_T)}$ is constant in the vertical direction yields

$$\|W[Q]\|_{L^2(\Omega_T)} \leq \frac{2ML}{a^2} \int_0^1 \|\partial_x Q\|_{L^2(\Omega_T)} dr \leq \frac{2ML}{a^2} \|\partial_x Q\|_{L^2(\Omega_T)},$$

□

For $N \in \mathbb{N}$, $\Delta t := T/N$, and any $t \in (0, T)$ we use the backward difference quotient $\frac{S(t) - S(t - \Delta t)}{\Delta t}$ to approximate the time derivative $\partial_t S$. Then, equation (5.1) is approximated by

$$\begin{aligned} \frac{S(t) - S(t - \Delta t)}{\Delta t} + \partial_x \left(f(S(t)) U[S(t)] \right) + \partial_z \left(f(S(t)) W[S(t)] \right) - \Delta S(t) \\ - \beta \frac{\Delta S(t) - \Delta S(t - \Delta t)}{\Delta t} = 0. \end{aligned} \quad (5.7)$$

Weak solutions of the approximated model (5.7) and (5.2) are expected to belong to the Hilbert space $V(\Omega) := H_0^1(\Omega)$, for almost all $t \in (0, T)$. Since $H_0^1(\Omega)$ is separable [1], it has a countable orthonormal basis

$$\{w_i\}_{i \in \mathbb{N}} \subset V(\Omega). \quad (5.8)$$

By applying Galerkin's method to (5.7), the solution space $V(\Omega)$ is projected into a finite dimensional space $V_m(\Omega)$ spanned by a finite number of the orthonormal functions w_i , $i = 1, \dots, m$. For positive integers m, N , we search a function

$$S_m^N(x, z, t) := \sum_{i=1}^m c_{mi}^N(t) w_i(x, z), \quad (5.9)$$

where the unknown coefficients $c_{m,i}^N \in L^\infty((0, T))$, $i = 1, \dots, m$, are chosen such that for almost all $t \in (0, T)$

$$\begin{aligned} \int_{\Omega} (S_m^N(t) - S_m^N(t - \Delta t)) w_i - \Delta t f(S_m^N(t)) (U[S_m^N(t)] \partial_x w_i + W[S_m^N(t)] \partial_z w_i) dx dz \\ + \int_{\Omega} (\Delta t \nabla S_m^N(t) + \beta \nabla (S_m^N(t) - S_m^N(t - \Delta t))) \cdot \nabla w_i dx dz = 0, \end{aligned} \quad (5.10)$$

holds for all $i = 1, \dots, m$, with

$$\begin{aligned} U[S_m^N(t)(x, z)] &= \frac{\lambda_{tot}(S_m^N(t)(x, z))}{\int_0^1 \lambda_{tot}(S_m^N(t)(x, r)) dr}, \\ W[S_m^N(t)(x, z)] &= -\partial_x \int_0^z U[S_m^N(t)(x, r)] dr, \end{aligned} \quad (5.11)$$

for almost all $t \in (0, T)$ and $(x, z) \in (0, 1)^2$. The function S_m^N is also required to satisfy the weak incompressibility relation

$$\int_{\Omega} \mathbf{V}[S_m^N] \cdot \nabla w_i dx dz = 0, \quad \text{for all } i = 1, \dots, m. \quad (5.12)$$

The initial data is chosen to be

$$S_m^N(t) = S_m^0, \quad \text{for } t \in (-\Delta t, 0], \quad (5.13)$$

where S_m^0 is the L^2 -projection of the initial data S^0 to the finite dimensional space $V_m(\Omega)$.

To prove the existence of a weak solution of the discrete problem (5.10), (5.11), and (5.12) we need the following technical lemma on the existence of zeros of a vector field [25].

Lemma 5.8. *(Zeros of a vector field, [25]) Let $r > 0$ and $\mathbf{v} : \mathbb{R}^n \rightarrow \mathbb{R}^n$ be a continuous vector field, which satisfies $\mathbf{v}(\mathbf{x}) \cdot \mathbf{x} \geq 0$ if $|\mathbf{x}| = r$. Then, there exists a point $\mathbf{x} \in B(0, r)$ such that $\mathbf{v}(\mathbf{x}) = \mathbf{0}$.*

Lemma 5.9. *For any $m, N \in \mathbb{N}$ and for almost all $t \in (0, T)$, if $S_m^N(t - \Delta t) \in V_m(\Omega)$ is known, then problem (5.10), (5.11), and (5.12) has a solution $S_m^N(t) \in V_m(\Omega)$ that satisfies*

$$\begin{aligned} & \int_{\Omega} (S_m^N(t) - S_m^N(t - \Delta t)) \phi \, dx \, dz - \Delta t \int_{\Omega} f(S_m^N) U[S_m^N] \partial_x \phi + f(S_m^N) W[S_m^N] \partial_z \phi \, dx \, dz \\ & + \int_{\Omega} [\Delta t \nabla S_m^N + \beta \nabla (S_m^N(t) - S_m^N(t - \Delta t))] \cdot \nabla \phi \, dx \, dz = 0, \end{aligned} \quad (5.14)$$

for all $\phi \in V_m(\Omega)$.

Proof. Before starting with the proof, we notify that $S_m^N(t - \Delta t)$ for $t \in (0, \Delta t]$ is well-defined by the choice of the initial condition (5.13). Now, we define the vector field $\mathbf{K} : \mathbb{R}^m \rightarrow \mathbb{R}^m$, $\mathbf{K} = (k_1, \dots, k_m)$, and $\mathbf{c}_m^N(t) = (c_{m,1}^N(t), \dots, c_{m,m}^N(t))$ of the unknown coefficients in equation (5.9) such that, for almost all $t \in (0, T)$,

$$\begin{aligned} k_i(\mathbf{c}_m^N(t)) & := \int_{\Omega} (S_m^N(t) - S_m^N(t - \Delta t)) w_i \, dx \, dz \\ & - \Delta t \int_{\Omega} f(S_m^N) U[S_m^N] \partial_x w_i + f(S_m^N) W[S_m^N] \partial_z w_i \, dx \, dz \\ & + \int_{\Omega} (\Delta t \nabla S_m^N + \beta \nabla (S_m^N(t) - S_m^N(t - \Delta t))) \cdot \nabla w_i \, dx \, dz, \end{aligned} \quad (5.15)$$

for all $i = 1, \dots, m$. The vector field \mathbf{K} is continuous by Assumption 5.3(3) and 5.3(4). Moreover, using equation (5.9), we have

$$\begin{aligned}
& \mathbf{K}(\mathbf{c}_m^N(t)) \cdot \mathbf{c}_m^N(t) \\
&= \int_{\Omega} (S_m^N(t) - S_m^N(t - \Delta t)) S_m^N(t) \, dx \, dz \\
&\quad - \Delta t \int_{\Omega} f(S_m^N) (U[S_m^N] \partial_x S_m^N + W[S_m^N] \partial_z S_m^N) \, dx \, dz, \\
&\quad + \int_{\Omega} (\Delta t \nabla S_m^N(t) + \beta \nabla (S_m^N(t) - S_m^N(t - \Delta t))) \cdot \nabla S_m^N(t) \, dx \, dz. \quad (5.16)
\end{aligned}$$

Let $F(S) := \int_0^S f(q) dq$, then the second term on the right side of (5.16) satisfies

$$\begin{aligned}
\int_{\Omega} f(S_m^N) (U[S_m^N] \partial_x S_m^N + W[S_m^N] \partial_z S_m^N) \, dx \, dz &= \int_{\Omega} f(S_m^N) \mathbf{V}[S_m^N] \cdot \nabla S_m^N \, dx \, dz, \\
&= \int_{\Omega} \mathbf{V}(S_m^N) \cdot \nabla F(S_m^N) \, dx \, dz,
\end{aligned}$$

where $\mathbf{V}[S_m^N] = (U[S_m^N], W[S_m^N])$. Using the assumption that S_m^N vanishes on the boundary $\partial\Omega$ by equation (5.4) and the property $F(0) = 0$, the weak incompressibility of $\mathbf{V}[S_m^N]$ in equation (5.12) also holds with $F(S_m^N) \in L^2(0, T; H_0^1(\Omega))$ replacing w_i . Thus, we have

$$\int_{\Omega} \mathbf{V}(S_m^N) \cdot \nabla F(S_m^N) \, dx \, dz = 0. \quad (5.17)$$

Substituting equations (5.17) into (5.16), then applying Cauchy's inequality yields

$$\begin{aligned}
\mathbf{K}(\mathbf{c}_m^N(t)) \cdot \mathbf{c}_m^N(t) &\geq \frac{1}{2} \|S_m^N\|_{L^2(\Omega)}^2 + \left(\frac{\beta}{2} + \Delta t\right) \|\nabla S_m^N\|_{L^2(\Omega)}^2 - \frac{1}{2} \|S_m^N(t - \Delta t)\|_{L^2(\Omega)}^2 \\
&\quad - \frac{\beta}{2} \|\nabla S_m^N(t - \Delta t)\|_{L^2(\Omega)}^2.
\end{aligned}$$

Equation (5.9) and the orthonormality of w_i , $i \in \{1, \dots, m\}$ yield

$$\begin{aligned}
\mathbf{K}(\mathbf{c}_m^N(t)) \cdot \mathbf{c}_m^N(t) &\geq \left(\frac{1}{2} + \frac{\beta}{2} + \Delta t\right) |\mathbf{c}_m^N|^2 - \frac{1}{2} \|S_m^N(t - \Delta t)\|_{L^2(\Omega)} \\
&\quad - \frac{\beta}{2} \|\nabla S_m^N(t - \Delta t)\|_{L^2(\Omega)}.
\end{aligned}$$

Note that $S_m^N(t - \Delta t) \in V_m(\Omega)$ is known. Set $r = |\mathbf{c}_m^N(t)|$, we conclude that $\mathbf{K}(\mathbf{c}_m^N(t)) \cdot \mathbf{c}_m^N(t) \geq 0$ provided that r is large enough. Thus, Lemma 5.8 ensures the existence of a vector $\mathbf{c}_m^N(t) \in \mathbb{R}^m$ with $\mathbf{K}(\mathbf{c}_m^N(t)) = \mathbf{0}$. Using equation (5.15) we

conclude the existence of an $S_m^N(t)$, defined as in (5.9), that satisfies the discrete problem (5.10), (5.11), and (5.12). \square

Remark 5.10. *The function S_m^N is defined for all $t \in (0, T)$ and is a step function in time. This results from the structure of equation (5.10), which implies that $S_m^N(t)$ for all $t \in [(n-1)\Delta t, n\Delta t)$ is determined inductively using the given data $S_m^N(t - \Delta t)$.*

5.2 A priori Estimates

So far, we proved the existence of a sequence $\{S_m^N\}_{m, N \in \mathbb{N}} \subset V_m(\Omega)$ of solutions for the discrete problem (5.10), (5.11), and (5.12). In the following, we show that this sequence satisfies a set of a priori estimates, which are essential to establish the convergence results in the next section.

Lemma 5.11. *The sequence of solutions $\{S_m^N\}_{N, m \in \mathbb{N}}$ for the discrete problem (5.10), (5.11), and (5.12) satisfies the estimate*

$$\begin{aligned} \operatorname{ess\,sup}_{t \in [0, T]} \left(\|S_m^N(t)\|_{L^2(\Omega)}^2 + \beta \|\nabla S_m^N(t)\|_{L^2(\Omega)}^2 \right) + \|\nabla S_m^N\|_{L^2(\Omega_T)}^2 \\ \leq \|S_m^0\|_{L^2(\Omega)}^2 + \beta \|\nabla S_m^0\|_{L^2(\Omega)}^2, \end{aligned}$$

for all $N, m \in \mathbb{N}$.

Proof. Multiplying equation (5.10) by $c_{m,i}^N$, summing for $i = 1, \dots, m$, and then integrating from 0 to an arbitrary time $\tau \in (0, T)$ yields

$$\begin{aligned} \frac{1}{\Delta t} \int_0^\tau \int_\Omega (S_m^N(t) - S_m^N(t - \Delta t)) S_m^N(t) \, dx \, dz \, dt - \int_0^\tau \int_\Omega \mathbf{V}[S_m^N] f(S_m^N) \cdot \nabla S_m^N \, dx \, dz \, dt \\ + \int_0^\tau \int_\Omega |\nabla S_m^N|^2 + \frac{\beta}{\Delta t} (\nabla S_m^N(t) - \nabla S_m^N(t - \Delta t)) \cdot \nabla S_m^N(t) \, dx \, dz \, dt = 0, \quad (5.18) \end{aligned}$$

where $\mathbf{V}[S_m^N] = (U[S_m^N], W[S_m^N])^T$. Using summation by parts, the first term on the left side of equation (5.18) satisfies

$$\begin{aligned} \frac{1}{\Delta t} \int_0^\tau \int_\Omega (S_m^N(t) - S_m^N(t - \Delta t)) S_m^N(t) \, dx \, dz \, dt = \frac{1}{2\Delta t} \int_{\tau - \Delta t}^\tau \int_\Omega (S_m^N(t))^2 \, dx \, dz \, dt \\ - \frac{1}{2\Delta t} \int_{-\Delta t}^0 \int_\Omega (S_m^N(t))^2 \, dx \, dz \, dt. \end{aligned}$$

Since S_m^N is a step function in time, the above equation simplifies to

$$\begin{aligned} \frac{1}{\Delta t} \int_0^\tau \int_\Omega (S_m^N(t) - S_m^N(t - \Delta t)) S_m^N(t) dx dz dt \\ = \frac{1}{2} \int_\Omega (S_m^N(\tau))^2 - (S_m^0)^2 dx dz. \end{aligned} \quad (5.19)$$

Similarly, we have

$$\begin{aligned} \int_0^\tau \int_\Omega \frac{\nabla S_m^N(t) - \nabla S_m^N(t - \Delta t)}{\Delta t} \cdot \nabla S_m^N(t) dx dz dt \\ = \frac{1}{2} \int_\Omega |\nabla S_m^N(\tau)|^2 - |\nabla S_m^0|^2 dx dz. \end{aligned} \quad (5.20)$$

Using the primitive $F(S) = \int_0^S f(q) dq$ and the weak incompressibility of the velocity (5.12), we obtain as in equation (5.17) that

$$\int_0^\tau \int_\Omega \mathbf{V}[S_m^N] f(S_m^N) \cdot \nabla S_m^N dx dz dt = \int_0^\tau \int_\Omega \mathbf{V}[S_m^N] \cdot \nabla F(S_m^N) dx dz dt = 0. \quad (5.21)$$

Since the time $\tau \in (0, T)$ is arbitrarily chosen, substituting equation (5.19), (5.20), and (5.21) into (5.18) yields

$$\begin{aligned} \operatorname{ess\,sup}_{\tau \in (0, T)} \|S_m^N(\tau)\|_{L^2(\Omega)} + \beta \sup_{\tau \in (0, T)} \|\nabla S_m^N(\tau)\|_{L^2(\Omega)} + 2 \int_0^T \|\nabla S_m^N\|_{L^2(\Omega)} dt \\ \leq \|S_m^0\|_{L^2(\Omega)}^2 + \beta \|\nabla S_m^0\|_{L^2(\Omega)}^2, \end{aligned}$$

for all $N, m \in \mathbb{N}$. □

In the following lemma, we prove an estimate on the approximated time derivatives $\frac{S_m^N(t) - S_m^N(t - \Delta t)}{\Delta t}$ and $\frac{\nabla S_m^N(t) - \nabla S_m^N(t - \Delta t)}{\Delta t}$, which depends on the small parameter $\beta > 0$.

Lemma 5.12. *There exists a constant $C \geq 0$ independent of $N, m \in \mathbb{N}$, such that for almost all $t \in (0, T)$,*

$$\|S_m^N(t) - S_m^N(t - \Delta t)\|_{L^2(\Omega_T)}^2 + \beta \|\nabla (S_m^N(t) - S_m^N(t - \Delta t))\|_{L^2(\Omega_T)}^2 \leq \frac{C}{\beta} (\Delta t)^2,$$

holds for all $N, m \in \mathbb{N}$.

Proof. Multiplying equation (5.10) by $(c_{m,i}^N(t) - c_{m,i}^N(t - \Delta t))$, summing for $i = 1, \dots, m$, then integrating from 0 to T yields

$$\begin{aligned} & \|S_m^N(t) - S_m^N(t - \Delta t)\|_{L^2(\Omega_T)}^2 + \beta \|\nabla(S_m^N(t) - S_m^N(t - \Delta t))\|_{L^2(\Omega_T)}^2 \\ &= \Delta t \int_0^T \int_{\Omega} \mathbf{V}[S_m^N] f(S_m^N) \cdot \nabla(S_m^N(t) - S_m^N(t - \Delta t)) \, dx \, dz \, dt \\ &\quad - \Delta t \int_0^T \int_{\Omega} \nabla S_m^N \cdot \nabla(S_m^N(t) - S_m^N(t - \Delta t)) \, dx \, dz \, dt. \end{aligned}$$

Applying Cauchy's inequality (2.19) (with $\epsilon = \beta/4$) to the right side of the above inequality yields

$$\begin{aligned} & \|S_m^N(t) - S_m^N(t - \Delta t)\|_{L^2(\Omega_T)}^2 + \beta \|\nabla(S_m^N(t) - S_m^N(t - \Delta t))\|_{L^2(\Omega_T)}^2 \\ &\leq \frac{\Delta t^2}{\beta} \|\mathbf{V}[S_m^N] f(S_m^N)\|_{L^2(\Omega_T)}^2 + \frac{\beta}{4} \|\nabla(S_m^N(t) - S_m^N(t - \Delta t))\|_{L^2(\Omega_T)}^2 \\ &\quad + \frac{(\Delta t)^2}{\beta} \|\nabla S_m^N\|_{L^2(\Omega_T)}^2 + \frac{\beta}{4} \|\nabla(S_m^N(t) - S_m^N(t - \Delta t))\|_{L^2(\Omega_T)}^2. \end{aligned}$$

The growth conditions in Lemma 5.7.3 and the apriori estimate in Lemma 5.11 give

$$\begin{aligned} & \|S_m^N(t) - S_m^N(t - \Delta t)\|_{L^2(\Omega_T)}^2 + \frac{\beta}{2} \|\nabla(S_m^N(t) - S_m^N(t - \Delta t))\|_{L^2(\Omega_T)}^2 \\ &\leq \frac{(\Delta t)^2}{\beta} \left(\frac{M^4 |\Omega| T}{a^2} + \left(\frac{4M^4 L^2}{a^2} + 1 \right) \|\nabla S_m^N\|_{L^2(\Omega_T)}^2 \right), \\ &\leq \frac{(\Delta t)^2}{\beta} \left(\frac{M^4 |\Omega| T}{a^2} + \left(\frac{4M^4 L^2}{a^2} + 1 \right) \left(\|S_m^0\|_{L^2(\Omega_T)}^2 + \nabla \|S_m^0\|_{L^2(\Omega_T)}^2 \right) \right), \\ &\leq C \frac{(\Delta t)^2}{\beta}, \end{aligned}$$

where $C = \left(\frac{M^4 |\Omega| T}{a^2} + \left(\frac{4M^4 L^2}{a^2} + 1 \right) \left(\|S_m^0\|_{L^2(\Omega_T)}^2 + \nabla \|S_m^0\|_{L^2(\Omega_T)}^2 \right) \right)$. This completes the proof. \square

5.3 Convergence Analysis

In this section, we state and prove the first main theorem in this chapter, which provides the existence of a weak solution of the Brinkman VE-model (5.1) and (5.2) associated with the initial and boundary conditions (5.4).

Theorem 5.13. *Let Assumption 5.3 be satisfied. Then, there exists a weak solution of the Brinkman VE-model (5.1), (5.2), and (5.4) satisfying Definition 5.4.*

Proof. The uniform estimates in Lemma 5.11 imply the existence of a weakly convergent subsequence of $\{S_m^N\}_{m,N \in \mathbb{N}}$, denoted in the same way, and a function $S \in L^2(0, T; H_0^1(\Omega))$ such that

$$S_m^N \rightharpoonup S \in L^2(0, T; H_0^1(\Omega)). \quad (5.22)$$

In addition, the apriori estimate in Lemma 5.12 implies that $\partial_t S \in L^2(0, T; H_0^1(\Omega))$. Thus, we have the weak convergence result

$$S_m^N \rightharpoonup S \in H^1(0, T; H_0^1(\Omega)). \quad (5.23)$$

The Rellich Kondrachov compactness theorem 2.22 implies the compact embedding $H^1(0, T; H_0^1(\Omega)) \Subset L^6(\Omega_T)$ for the space dimension $n = 3$ of the domain Ω_T . Hence, the boundedness of the domain Ω_T yields that $H^1(0, T; H_0^1(\Omega))$ is compactly embedded in $L^2(\Omega_T)$. Thus, from the weak convergence result (5.23), we extract the strong convergence

$$S_m^N \rightarrow S \in L^2(\Omega_T). \quad (5.24)$$

This strong convergence and the apriori estimate in Lemma 5.11 implies that the limit S satisfies

$$S, \partial_t S \in L^\infty(0, T; H_0^1(\Omega)). \quad (5.25)$$

Moreover, Theorem 2.19 in Chapter 2 implies the continuity of the function S in the time interval $[0, T]$,

$$S \in C([0, T]; L^2(\Omega)). \quad (5.26)$$

The next step in the proof is to show that the function $S \in L^2(0, T; H_0^1(\Omega))$ with $\partial_t S \in L^2(0, T; H_0^1(\Omega))$ and $S \in C([0, T]; L^2(\Omega))$ fulfills the conditions in Definition 5.4. Thus, we consider an arbitrary test function $\phi \in L^2(0, T; V_m(\Omega))$ such that for a fixed integer M and for almost all $t \in (0, T)$ is given as

$$\phi(t) = \sum_{i=1}^M c_i(t) w_i, \quad (5.27)$$

where $c_i \in L^\infty(0, T)$, $i = 1, \dots, M$, are given functions and $w_i \in H_0^1(\Omega)$, $i = 1, \dots, M$, belong to the orthonormal basis of the subspace $V_m(\Omega)$. Choosing $M < m$, multiplying equation (5.10) by $c_i(t)$, summing for $i = 1, \dots, M$, and then integrating with respect to time yields

$$\begin{aligned}
& \frac{1}{\Delta t} \int_0^T \int_\Omega (S_m^N(t) - S_m^N(t - \Delta t)) \phi \, dx \, dz \, dt \\
& - \int_0^T \int_\Omega U[S_m^N] f(S_m^N) \partial_x \phi \, dx \, dz \, dt - \int_0^T \int_\Omega W[S_m^N] f(S_m^N) \partial_z \phi \, dx \, dz \, dt \\
& + \int_0^T \int_\Omega \nabla S_m^N \cdot \nabla \phi + \frac{\beta}{\Delta t} \nabla (S_m^N(t) - S_m^N(t - \Delta t)) \cdot \nabla \phi \, dx \, dz \, dt \\
& = 0.
\end{aligned} \tag{5.28}$$

In the following we show that this equation converges as $M, N \rightarrow \infty$ to the corresponding equation in Definition 5.4.

The strong convergence (5.24) and the Lipschitz continuity of f and λ_{tot} imply

$$\begin{aligned}
\|f(S_m^N) - f(S)\|_{L^2(\Omega_T)} & \leq L \|S_m^N - S\|_{L^2(\Omega_T)} \rightarrow 0, \\
\|\lambda_{tot}(S_m^N) - \lambda_{tot}(S)\|_{L^2(\Omega_T)} & \leq L \|S_m^N - S\|_{L^2(\Omega_T)} \rightarrow 0.
\end{aligned} \tag{5.29}$$

Jensen's inequality and Fubini's theorem imply

$$\begin{aligned}
& \int_0^T \int_0^1 \left| \int_0^1 \lambda_{tot}(S_m^N(t)(x, z)) \, dz - \int_0^1 \lambda_{tot}(S(t)(x, z)) \, dz \right|^2 \, dx \, dt \\
& \leq \int_0^T \int_0^1 \int_0^1 |\lambda_{tot}(S_m^N(x, z, t)) - \lambda_{tot}(S(x, z, t))|^2 \, dz \, dx \, dt, \\
& = \int_0^T \int_\Omega |\lambda_{tot}(S_m^N(x, z, t)) - \lambda_{tot}(S(x, z, t))|^2 \, dx \, dz \, dt,
\end{aligned}$$

where we used that the measure of the interval $[0, 1]$ in the first inequality is unity. This inequality and the strong convergence of $\lambda_{tot}(S_m^N)$ in (5.29) implies that

$$\int_0^1 \lambda_{tot}(S_m^N(\cdot, z, \cdot)) \, dz \rightarrow \int_0^1 \lambda_{tot}(S(\cdot, z, \cdot)) \, dz \quad \text{in } L^2((0, 1) \times (0, T)). \tag{5.30}$$

Note that the sequence $\int_0^1 \lambda_{tot}(S_m^N(\cdot, z, \cdot)) \, dz$ is constant in the z -direction. Hence, we have

$$\int_0^1 \lambda_{tot}(S_m^N(\cdot, z, \cdot)) \, dz \rightarrow \int_0^1 \lambda_{tot}(S(\cdot, z, \cdot)) \, dz \quad \text{in } L^2(\Omega_T). \tag{5.31}$$

To prove the strong convergence $U[S_m^N] \rightarrow U[S]$ in $L^2(\Omega_T)$, we use the notation $A[S_m^N(x, t)] := \int_0^1 \lambda_{tot}(S_m^N(x, z, t)) dz$ and $A[S(x, t)] := \int_0^1 \lambda_{tot}(S(x, z, t)) dz$ for almost all $x \in (0, 1)$ and $t \in (0, T)$. Then, we have

$$\begin{aligned} & \|U[S_m^N] - U[S]\|_{L^2(\Omega_T)} \\ &= \left\| \frac{\lambda_{tot}(S_m^N)}{A[S_m^N]} - \frac{\lambda_{tot}(S)}{A[S]} \right\|_{L^2(\Omega_T)}, \\ &= \left\| \frac{\lambda_{tot}(S_m^N)(A[S] - A[S_m^N])}{A[S_m^N]A[S]} + \frac{(\lambda_{tot}(S_m^N) - \lambda_{tot}(S))A[S_m^N]}{A[S_m^N]A[S]} \right\|_{L^2(\Omega_T)}, \\ &\leq \left\| \frac{\lambda_{tot}(S_m^N)(A[S] - A[S_m^N])}{A[S_m^N]A[S]} \right\|_{L^2(\Omega_T)} + \left\| \frac{(\lambda_{tot}(S_m^N) - \lambda_{tot}(S))A[S_m^N]}{A[S_m^N]A[S]} \right\|_{L^2(\Omega_T)}. \end{aligned}$$

Note that $A[S_m^N]A[S] > a^2 > 0$ using Assumption 5.3(4) on the total mobility λ_{tot} . Thus, we have

$$\|U[S_m^N] - U[S]\|_{L^2(\Omega_T)} \leq \frac{M}{a^2} \left(\|A[S] - A[S_m^N]\|_{L^2(\Omega_T)} + \|\lambda_{tot}(S_m^N) - \lambda_{tot}(S)\|_{L^2(\Omega_T)} \right).$$

Then, the strong convergence of λ_{tot} in (5.29) and of $A[S_m^N]$ in (5.31) yield

$$\|U[S_m^N] - U[S]\|_{L^2(\Omega_T)} \rightarrow 0. \quad (5.32)$$

Lemma 5.11 and the growth condition on the velocity component W in Lemma 5.7.3 imply the boundedness of $W[S_m^N]$ in $L^2(\Omega_T)$. Hence, up to a subsequence, there exists a function $k \in L^2(\Omega_T)$ such that

$$\int_0^T \int_{\Omega} W[S_m^N] \partial_z \phi dx dz dt \rightarrow \int_0^T \int_{\Omega} k \partial_z \phi dx dz dt, \quad (5.33)$$

for all test functions $\phi \in L^2(0, T; V_m(\Omega))$ as $m, N \rightarrow \infty$. Since $\bigcup_{m \in \mathbb{N}} V_m(\Omega)$ is dense in $H_0^1(\Omega)$, (5.33) holds for all test functions $\phi \in L^2(0, T; H_0^1(\Omega))$. To identify the weak limit k , we take $\phi \in L^2(0, T; C_0^2(\Omega))$ such that $\phi(x, z, t) = 0$ for $x \geq 1 - \Delta x$ and $x \leq \Delta x$, $z \in (0, 1)$, and almost all $t \in (0, T)$ with $\Delta x > 0$ is spatial step size in the x -direction. Note that the spatial derivatives in the discrete equation (5.10) correspond to the centered difference quotient. Thus, applying summation by parts

to the left side of (5.33) yields

$$\begin{aligned}
\int_0^T \int_{\Omega} W[S_m^N] \partial_z \phi \, dx \, dz \, dt &= - \int_0^T \int_{\Omega} \left(\partial_x \int_0^z U[S_m^N(t)(x, r)] \, dr \right) \partial_z \phi \, dx \, dz \, dt, \\
&= \int_0^T \int_{\Omega} \left(\int_0^z U[S_m^N(t)(x, r)] \, dr \right) \partial_{zx}^2 \phi \, dx \, dz \, dt \\
&\quad - \int_0^T \int_0^1 \int_{1-\Delta x}^{1+\Delta x} \left(\int_0^z U[S_m^N(t)(x, r)] \, dr \right) \partial_z \phi \, dx \, dz \, dt \\
&\quad + \int_0^T \int_0^1 \int_{-\Delta x}^{\Delta x} \left(\int_0^z U[S_m^N(t)(x, r)] \, dr \right) \partial_z \phi \, dx \, dz \, dt.
\end{aligned}$$

The second and the third term on the right side of the above equation vanish by the choice of the test function ϕ . We show in the following that the first term on the same side converges to $\int_0^T \int_{\Omega} \left(\int_0^z U[S(t)(x, r)] \, dr \right) \partial_{zx}^2 \phi \, dx \, dz \, dt$. For this, we use Hölder's inequality, Fubini's theorem, and the strong convergence of $U[S_m^N]$ in (5.32) as follows

$$\begin{aligned}
&\int_0^T \int_{\Omega} \left(\int_0^z U[S_m^N](x, r, t) - U[S](x, r, t) \, dr \right) \partial_{zx}^2 \phi \, dx \, dz \, dt \\
&\leq \|\partial_{zx}^2 \phi\|_{L^\infty(\Omega_T)} \int_0^T \int_{\Omega} \int_0^z |U[S_m^N](x, r, t) - U[S](x, r, t)| \, dr \, dx \, dz \, dt, \\
&\leq \|\partial_{zx}^2 \phi\|_{L^\infty(\Omega_T)} \int_0^1 \int_0^T \int_0^z \int_0^1 |U[S_m^N](x, r, t) - U[S](x, r, t)| \, dx \, dr \, dt \, dz, \\
&= \|\partial_{zx}^2 \phi\|_{L^\infty(\Omega_T)} \int_0^T \int_{\Omega} |U[S_m^N](x, r, t) - U[S](x, r, t)| \, dx \, dz \, dt, \\
&\rightarrow 0.
\end{aligned}$$

Thus, we have

$$\begin{aligned}
\int_0^T \int_{\Omega} W[S_m^N(t)(x, z)] \partial_z \phi \, dx \, dz \, dt \\
\rightarrow \int_0^T \int_{\Omega} \left(\int_0^z U[S(t)(x, r)] \, dr \right) \partial_{zx}^2 \phi \, dx \, dz \, dt, \quad (5.34)
\end{aligned}$$

for all test functions $\phi \in L^2(0, T; H_0^1(\Omega))$ as $m, N \rightarrow \infty$. Combining the results (5.33) and (5.34) yields

$$\int_0^T \int_{\Omega} k(x, z, t) \partial_z \phi \, dx \, dz \, dt = \int_0^T \int_{\Omega} \left(\int_0^z U[S(t)(x, r)] \, dr \right) \partial_{zx}^2 \phi \, dx \, dz. \quad (5.35)$$

Thus, Definition 2.6 of weak derivatives in Chapter 2 imply that

$$k(x, z, t) = -\partial_x \int_0^z U[S(x, r, t)] dr = W[S(x, z, t)] \in L^2(\Omega_T), \quad (5.36)$$

for almost all $(x, z) \in \Omega$ and $t \in (0, T)$. Substituting the above equation into (5.33) yields the required convergence

$$\int_0^T \int_{\Omega} W[S_m^N] \partial_z \phi \, dx \, dz \rightarrow \int_0^T \int_{\Omega} W[S] \partial_z \phi \, dx \, dz \, dt. \quad (5.37)$$

Now, we prove the strong convergence of the product $U[S_m^N]f(S_m^N)$ using the strong convergence of $U[S_m^N]$ and $f(S_m^N)$ as follows,

$$\begin{aligned} & \|U[S_m^N]f(S_m^N) - U[S]f(S)\|_{L^2(\Omega_T)} \\ &= \|U[S] (f(S_m^N) - f(S)) + f(S_m^N) (U[S_m^N] - U[S])\|_{L^2(\Omega_T)}, \\ &\leq \|U[S] (f(S_m^N) - f(S))\|_{L^2(\Omega_T)} + \|f(S_m^N) (U[S_m^N] - U[S])\|_{L^2(\Omega_T)}. \end{aligned} \quad (5.38)$$

The boundedness of U in the space $L^\infty(\Omega_T)$ by Lemma 5.7(1) and the strong convergence of f in (5.29) imply

$$\|U[S] (f(S_m^N) - f(S))\|_{L^2(\Omega_T)} \leq \frac{M}{a} \|f(S_m^N) - f(S)\|_{L^2(\Omega_T)} \rightarrow 0. \quad (5.39)$$

The boundedness of f in $L^\infty(\Omega_T)$ by Assumption 5.3(3) and the strong convergence of U in (5.31) imply

$$\|f(S_m^N) (U[S_m^N] - U[S])\|_{L^2(\Omega_T)} \leq M \|U[S_m^N] - U[S]\|_{L^2(\Omega_T)} \rightarrow 0. \quad (5.40)$$

Substituting (5.39) and (5.40) into (5.38) yields

$$U[S_m^N]f(S_m^N) \rightarrow U[S]f(S) \quad \text{in } L^2(\Omega_T).$$

Thus, the limit S satisfies the first part in the first condition in Definition 5.4.

We also prove that the product $W[S_m^N]f(S_m^N) \in L^2(\Omega_T)$. The boundedness of the fractional flow function $f \in L^\infty(\Omega_T)$, the growth condition on W in Lemma 5.7(3), and Lemma 5.11 imply the existence of a constant $C \geq 0$ such that

$$\|W[S_m^N]f(S_m^N)\|_{L^2(\Omega_T)} \leq \frac{2M^2L}{a^2} \|\partial_x S_m^N\|_{L^2(\Omega_T)} \leq C.$$

Hence, there exists a function $q \in L^2(\Omega_T)$ such that, up to a subsequence,

$$\int_0^T \int_{\Omega} W[S_m^N] f(S_m^N) \phi \, dx \, dz \, dt \rightarrow \int_0^T \int_{\Omega} q \phi \, dx \, dz \, dt, \quad (5.41)$$

for all test functions $\phi \in L^2(0, T; V_m(\Omega))$ as $m, N \rightarrow \infty$. Since $\cup_{m \in \mathbb{N}} V_m(\Omega)$ is dense in $H_0^1(\Omega)$, (5.41) holds for all test functions $\phi \in L^2(0, T; H_0^1(\Omega))$. To identify q , we take a test function $\phi \in L^\infty(0, T; C_0^1(\Omega))$ in (5.41). Then we have

$$\begin{aligned} & \int_0^T \int_{\Omega} (W[S_m^N] f(S_m^N) - W[S] f(S)) \phi \, dx \, dz \, dt \\ &= \int_0^T \int_{\Omega} \left(W[S_m^N] (f(S_m^N) - f(S)) + f(S) (W[S_m^N] - W[S]) \right) \phi \, dx \, dz \, dt. \end{aligned} \quad (5.42)$$

The choice of the test function implies $\phi \in L^\infty(\Omega_T)$. Thus, the growth condition on W in Lemma 5.7.3, Lemma 5.11, Hölder's inequality, and the strong convergence of f in (5.29) lead to

$$\begin{aligned} & \int_0^T \int_{\Omega} W[S_m^N] (f(S_m^N) - f(S)) \phi \, dx \, dz \, dt \\ & \leq \|\phi\|_{L^\infty(\Omega_T)} \|W[S_m^N]\|_{L^2(\Omega_T)} \|f(S_m^N) - f(S)\|_{L^2(\Omega_T)}, \\ & \rightarrow 0. \end{aligned} \quad (5.43)$$

The weak convergence of W in (5.37) implies

$$\int_0^T \int_{\Omega} f(S) \phi (W[S_m^N] - W[S]) \, dx \, dz \, dt \rightarrow 0. \quad (5.44)$$

Substituting (5.43) and (5.44) into (5.42) yields

$$\int_0^T \int_{\Omega} W[S_m^N] f(S_m^N) \phi \, dx \, dz \, dt \rightarrow \int_0^T \int_{\Omega} W[S] f(S) \phi \, dx \, dz \, dt. \quad (5.45)$$

By the uniqueness of the limit we obtain $q = W[S] f(S) \in L^2(\Omega_T)$. Thus, the limit S satisfies also the second part in the first condition in Definition 5.4.

The existence of a function $S \in L^2(0, T; H_0^1(\Omega))$ with $\partial_t S \in L^2(0, T; H_0^1(\Omega))$ and the convergence results (5.23), (5.32), and (5.45) imply that equation (5.28)

convergences as $m, N \rightarrow \infty$ to

$$\begin{aligned} \int_0^T \int_{\Omega} \partial_t S \phi \, dx \, dz \, dt - \int_0^T \int_{\Omega} U[S] f(S) \partial_x \phi \, dx \, dz \, dt - \int_0^T \int_{\Omega} W[S] f(S) \partial_z \phi \, dx \, dz \, dt \\ + \int_0^T \int_{\Omega} \nabla S \cdot \nabla \phi + \beta \nabla \partial_t S \cdot \nabla \phi \, dx \, dz \, dt = 0, \end{aligned} \quad (5.46)$$

for all test function $\phi \in L^2(0, T; H_0^1(\Omega))$. Hence, the function S satisfies the first condition in Definition 5.4.

Now, we show that the function $S \in H^1(0, T; H_0^1(\Omega))$ satisfies the weak incompressibility equation in Definition 5.4. We choose a test function $\phi \in C_0^2(\Omega_T)$, then using (5.36), we have

$$\int_0^T \int_{\Omega} W[S] \partial_z \phi \, dx \, dz \, dt = - \int_0^T \int_{\Omega} \partial_x \int_0^z U[S(x, r, t)] \, dr \partial_z \phi \, dx \, dz \, dt. \quad (5.47)$$

Applying Gauss' theorem to the right side of the above equation twice yields

$$\begin{aligned} \int_0^T \int_{\Omega} W[S] \partial_z \phi \, dx \, dz \, dt &= \int_0^T \int_{\Omega} \int_0^z U[S(x, r, t)] \, dr \partial_{zx}^2 \phi \, dx \, dz \, dt, \\ &= - \int_0^T \int_{\Omega} \partial_z \int_0^z U[S(x, r, t)] \, dr \partial_x \phi \, dx \, dz \, dt. \end{aligned} \quad (5.48)$$

However, using summation by parts, we have that

$$\begin{aligned} \int_0^T \int_{\Omega} \int_0^z \frac{U[S(x, r + \Delta z, t)] - U[S(x, r - \Delta z, t)]}{\Delta z} \, dr \partial_x \phi \, dx \, dz \, dt, \\ = \int_0^T \int_{\Omega} \left(\frac{1}{\Delta z} \int_{z-\Delta z}^{z+\Delta z} U[S(x, r, t)] \, dr - \frac{1}{\Delta z} \int_{-\Delta z}^{\Delta z} U[S(x, r, t)] \, dr \right) \partial_x \phi \, dx \, dz \, dt. \end{aligned}$$

We set the horizontal velocity component $U := 0$ in the subdomain $\{x\} \times (-\Delta z, \Delta z)$, as it corresponds to the impermeable lower boundary of the medium. Then, letting $\Delta z \rightarrow 0$ in the above equation and using Lebesgue's Differentiation theorem [25] yield

$$\int_0^T \int_{\Omega} \partial_z \int_0^z U[S(x, r, t)] \, dr \partial_x \phi \, dx \, dz \, dt = \int_0^T \int_{\Omega} U[S(x, z, t)] \partial_x \phi \, dx \, dz \, dt. \quad (5.49)$$

Substituting (5.49) into (5.48) yields the required weak incompressibility equation as in Definition 5.4.

Finally, we show that $S(0) = S^0$ almost everywhere. To do this, we choose a test function $\phi \in C^1([0, T], H_0^1(\Omega))$ in (5.46) such that $\phi(T) = 0$. Then, applying Gauss' theorem to the first term in equation (5.46) yields

$$\begin{aligned} & \int_0^T \int_{\Omega} S \partial_t \phi \, dx \, dz \, dt - \int_0^T \int_{\Omega} U[S] f(S) \partial_x \phi \, dx \, dz \, dt - \int_0^T \int_{\Omega} W[S] f(S) \partial_z \phi \, dx \, dz \, dt \\ & + \int_0^T \int_{\Omega} \nabla S \cdot \nabla \phi + \beta \nabla \partial_t S \cdot \nabla \phi \, dx \, dz \, dt = \int_{\Omega} S(0) \phi(0) \, dx \, dz. \end{aligned} \quad (5.50)$$

Applying summation by parts to the first term in equation (5.28) yields

$$\begin{aligned} & \frac{1}{\Delta t} \int_0^T \int_{\Omega} (\phi(t) - \phi(t - \Delta t)) S_m^N \, dx \, dz \, dt \\ & - \int_0^T \int_{\Omega} U[S_m^N] f(S_m^N) \partial_x \phi \, dx \, dz \, dt - \int_0^T \int_{\Omega} W[S_m^N] f(S_m^N) \partial_z \phi \, dx \, dz \, dt \\ & + \int_0^T \int_{\Omega} \nabla S_m^N \cdot \nabla \phi + \frac{\beta}{\Delta t} (\nabla \phi(t) - \nabla \phi(t - \Delta t)) \cdot \nabla S_m^N \, dx \, dz \, dt \\ & = \int_{\Omega} S_m^0 \phi(0) \, dx \, dz. \end{aligned} \quad (5.51)$$

Letting $m, N \rightarrow \infty$ in equation (5.51) yields, up to a subsequence, that

$$\begin{aligned} & \int_0^T \int_{\Omega} S \partial_t \phi \, dx \, dz \, dt - \int_0^T \int_{\Omega} U[S] f(S) \partial_x \phi \, dx \, dz \, dt - \int_0^T \int_{\Omega} W[S] f(S) \partial_z \phi \, dx \, dz \, dt \\ & + \int_0^T \int_{\Omega} \nabla S \cdot \nabla \phi + \beta \nabla \partial_t S \cdot \nabla \phi \, dx \, dz \, dt = \int_{\Omega} S^0 \phi(0) \, dx \, dz, \end{aligned} \quad (5.52)$$

since $S_m^0 \rightarrow S^0$ in $L^2(\Omega)$ as $m \rightarrow \infty$. As $\phi(0)$ is arbitrarily chosen, comparing equation (5.50) and (5.52) yields that $S(0) = S^0$ almost everywhere. Hence, the function S satisfies the second condition in Definition 5.4, which implies that S is a weak solution of the Brinkman VE-model (5.1), (5.2). \square

5.4 Boundedness of Weak Solutions in $L^\infty(\Omega_T)$

In this section, we show the boundedness of the weak solutions for the Brinkman VE-model, $S \in L^\infty(\Omega_T)$. This boundedness is expected from the numerical examples in Chapter 4. However, proving it requires the property that $\partial_x S \in L^r(\Omega_T)$ for any $r \in (2, \infty)$. In the following we assume that this property holds as it is still unfeasible to prove it, due to the second-order convective term in the model.

To prove the boundedness of weak solutions for the Brinkman VE-model $S \in L^\infty(\Omega_T)$, we follow [27] and reformulate the Brinkman VE-model (5.1) and (5.2)

as

$$\begin{aligned}\partial_t S + \partial_x(f(S)U[S]) + \partial_z(f(S)W[S]) &= \Delta p, \\ p &= S + \beta \partial_t S,\end{aligned}\tag{5.53}$$

The second equation in (5.53) can be rewritten as

$$\partial_t S = \frac{p - S}{\beta}.\tag{5.54}$$

Substituting (5.54) into the first equation in (5.53) yields

$$p - \beta \Delta p = S - \beta \partial_x(f(S)U[S]) - \beta \partial_z(f(S)W[S]).$$

Coupling this equation with the first equation in (5.53), we obtain the system

$$\begin{aligned}\partial_t S + \partial_x(f(S)U[S]) + \partial_z(f(S)W[S]) &= \Delta p, \\ p - \beta \Delta p &= S - \beta \partial_x(f(S)U[S]) - \beta \partial_z(f(S)W[S]).\end{aligned}\tag{5.55}$$

To avoid confusion between a weak solution S for problem (5.1), (5.2) and a solution pair for the other two equivalent formulation given in (5.53) and (5.55), we denote saturation by \bar{S} . Then, the problem of finding weak solutions of problem (5.53) and (5.55) with the incompressibility relation (5.3) and the initial and boundary condition (5.4) is given as in the following two problems:

Problem P_1 . Find $\bar{S} \in H_0^1(0, T; L^2(\Omega))$ and $p \in L^2(0, T; H_0^1(\Omega))$ such that

$$\begin{aligned}\int_0^T \int_{\Omega} \partial_t \bar{S} \phi - f(\bar{S})U[\bar{S}]\partial_x \phi - f(\bar{S})W[\bar{S}]\partial_z \phi + \nabla p \nabla \phi \, dx \, dz \, dt &= 0, \\ \int_0^T \int_{\Omega} p \psi \, dx \, dz \, dt - \int_0^T \int_{\Omega} (\bar{S} + \beta \partial_t \bar{S}) \psi \, dx \, dz \, dt &= 0, \\ \int_0^T \int_{\Omega} (U[\bar{S}]\partial_x \phi + W[\bar{S}]\partial_z \phi) \, dx \, dz \, dt &= 0, \\ \bar{S}(\cdot, \cdot, 0) &= S^0 \text{ almost everywhere,}\end{aligned}$$

for any $\phi \in L^2(0, T; H_0^1(\Omega))$ and $\psi \in L^2(0, T; L^2(\Omega))$.

Problem P_2 . Find $\bar{S} \in H_0^1(0, T; L^2(\Omega))$ and $p \in L^2(0, T; H_0^1(\Omega))$ such that

$$\begin{aligned} \int_0^T \int_{\Omega} \partial_t \bar{S} \phi - f(\bar{S})U[\bar{S}]\partial_x \phi - f(\bar{S})W[\bar{S}]\partial_z \phi + \nabla p \nabla \phi \, dx \, dz \, dt &= 0, \\ \int_0^T \int_{\Omega} p \psi + \beta \nabla p \cdot \nabla \psi \, dx \, dz \, dt &= \beta \int_0^T \int_{\Omega} (f(\bar{S})U[\bar{S}]\partial_x \psi + f(\bar{S})W[\bar{S}]\partial_z \psi) \, dx \, dz \, dt \\ &\quad + \int_0^T \int_{\Omega} \bar{S} \psi \, dx \, dz \, dt, \\ \int_0^T \int_{\Omega} (U[\bar{S}]\partial_x \phi + W[\bar{S}]\partial_z \phi) \, dx \, dz \, dt &= 0, \\ \bar{S}(\cdot, \cdot, 0) &= S^0 \text{ almost everywhere,} \end{aligned}$$

for any $\phi \in L^2(0, T; H_0^1(\Omega))$ and $\psi \in L^2(0, T; H_0^1(\Omega))$.

Proposition 5.14. *Let $S \in H^1(0, T; H_0^1(\Omega))$ be a weak solution for the Brinkman VE-model (5.1), (5.2), (5.3), and (5.4) as defined in Definition 5.4. Let also $(\bar{S}, p) \in H_0^1(0, T; L^2(\Omega)) \times L^2(0, T; H_0^1(\Omega))$ be a weak solution for Problem P_1 and P_2 . Then, $S = \bar{S}$ is a weak solution for the Brinkman VE-model (5.1), (5.2), (5.3), and (5.4) and, conversely, the pair (\bar{S}, p) with $\bar{S} = S$ and $p = S + \beta \partial_t S$ is a weak solution to Problem P_1 and P_2 .*

Proof. If the velocity \mathbf{V} in the Brinkman VE-model and its reformulations (5.53), and (5.55) is constant, then they reduce to those model considered in [27] and Theorem 2.1. in [27] (page 89) states their equivalence. Since the proof of this theorem does not depend on the convective term, it applies also for Brinkman VE-model and its reformulations (5.53) and (5.55) with the velocity \mathbf{V} defined as in (5.2). \square

Lemma 5.15. *Let Assumption 5.3 be satisfied and the initial condition satisfies $S^0 \in C^{0,\alpha}(\bar{\Omega})$ for some $\alpha \in (0, 1]$, where $\bar{\Omega}$ is the closure of Ω . Assume also that weak solutions for the Brinkman VE-model (5.1), (5.2), (5.3), and (5.4) satisfy $\partial_x S(t) \in L^r(\Omega)$ for any $r \in (2, \infty)$, for almost all $t \in (0, T)$. Then, it holds $S \in L^\infty(\bar{\Omega} \times (0, T])$.*

Proof. As shown in Section 5.3, if S is a weak solution of the Brinkman VE-model then it satisfies $S \in L^\infty(0, T; H_0^1(\Omega))$ and $\partial_t S \in L^\infty(0, T; H_0^1(\Omega))$. Thus, Proposition 5.14 implies that $p \in L^\infty(0, T; H_0^1(\Omega))$.

For almost all $t \in [0, T]$ and given $S \in L^\infty(0, T; H_0^1(\Omega))$, the second equation in model (5.55) is a linear elliptic equation in p

$$p - \beta \Delta p = S - \beta \partial_x (f(S)U[S]) - \beta \partial_z (f(S)W[S]).$$

Note that $S \in L^2(\Omega)$ and $f(S)U[S] \in L^\infty(\Omega)$ for almost all $t \in (0, T)$. Moreover, we have $f(S)W[S] \in L^r(\Omega)$, $2 < r < \infty$ using the boundedness of f , the definition of W and the assumption $\partial_x S \in L^r(\Omega)$, $2 < r < \infty$. Thus, Theorem 13.1, page 199 in [38], implies the existence of a constant $C > 0$ such that

$$\|p\|_{L^\infty(0, T; C^{0, \alpha}(\bar{\Omega}))} \leq C. \quad (5.56)$$

Following [12], we show now that S has the same regularity as $p \in L^\infty(0, T; C^{0, \alpha}(\bar{\Omega}))$. For almost all $t \in (0, T]$ and for almost all $\mathbf{x}_1 := (x_1, z_1)$, $\mathbf{x}_2 := (x_2, z_2) \in \Omega$, $\mathbf{x}_1 \neq \mathbf{x}_2$, using the second equation in (5.53) we have

$$\frac{p(\mathbf{x}_1, t) - p(\mathbf{x}_2, t)}{|\mathbf{x}_1 - \mathbf{x}_2|^\alpha} = \frac{S(\mathbf{x}_1, t) - S(\mathbf{x}_2, t)}{|\mathbf{x}_1 - \mathbf{x}_2|^\alpha} + \beta \partial_t \frac{S(\mathbf{x}_1, t) - S(\mathbf{x}_2, t)}{|\mathbf{x}_1 - \mathbf{x}_2|^\alpha}. \quad (5.57)$$

Now, we define $w = \frac{S(\mathbf{x}_1, t) - S(\mathbf{x}_2, t)}{|\mathbf{x}_1 - \mathbf{x}_2|^\alpha}$. Then (5.57) is given as

$$\beta \partial_t w + w = \frac{p(\mathbf{x}_1, t) - p(\mathbf{x}_2, t)}{|\mathbf{x}_1 - \mathbf{x}_2|^\alpha}. \quad (5.58)$$

Multiplying (5.58) by w , integrating from 0 to an arbitrary $\tau \in (0, T]$, then applying Cauchy's inequality (2.19) (with $\epsilon = \frac{1}{8}$) gives

$$\begin{aligned} \frac{\beta}{2} w^2(\cdot, \tau) + \int_0^\tau w^2 dt &= \int_0^\tau \frac{p(\mathbf{x}_1, t) - p(\mathbf{x}_2, t)}{|\mathbf{x}_1 - \mathbf{x}_2|^\alpha} w dt + \frac{1}{2} (w(\cdot, 0))^2, \\ &\leq \frac{1}{8} \int_0^\tau \left(\frac{p(\mathbf{x}_1, t) - p(\mathbf{x}_2, t)}{|\mathbf{x}_1 - \mathbf{x}_2|^\alpha} \right)^2 dt + 2 \int_0^\tau w^2 dt + \frac{1}{2} (w(\cdot, 0))^2. \end{aligned}$$

The assumption $S^0 \in C^{0, \alpha}(\bar{\Omega})$ and estimate (5.56) imply the existence of a constant $C > 0$ such that

$$\beta w^2(\cdot, \tau) \leq C + \int_0^\tau w^2 dt. \quad (5.59)$$

Thus, Gronwall's inequality implies

$$w^2 \leq C \quad \text{for all } \tau \in (0, T]. \quad (5.60)$$

This implies that

$$\frac{|S(\mathbf{x}_1, t) - S(\mathbf{x}_2, t)|}{|\mathbf{x}_1 - \mathbf{x}_2|^\alpha} \leq C, \quad \text{for almost all } \mathbf{x}_1, \mathbf{x}_2 \in \Omega \text{ and all } t \in (0, T]. \quad (5.61)$$

In the following, we show that (5.61) holds everywhere in Ω . For this, we choose $\Omega_c \subset \Omega$ such that (5.61) holds everywhere in Ω_c . Clearly, the set $\Omega \setminus \Omega_c$ is of measure zero. For any $\mathbf{x} \in \Omega \setminus \Omega_c$, there exists a sequence $\{\mathbf{x}_n\}_{n \in \mathbb{N}} \subset \Omega_c$ converging to \mathbf{x} and define $S(\mathbf{x}, t) = \lim_{n \rightarrow +\infty} S(\mathbf{x}_n, t)$. The uniform estimate in (5.61) implies that $S(\mathbf{x}, t)$ is independent of the choice of the sequence $\{\mathbf{x}_n\}_{n \in \mathbb{N}}$. Thus, we have

$$S \in C^{0,\alpha}(\bar{\Omega}). \quad (5.62)$$

The continuity of S and the boundedness of the domain Ω imply that $S \in L^\infty(\Omega_T)$. \square

5.5 Uniqueness of Weak Solutions

In this section, we prove the uniqueness of weak solutions for the Brinkman VE-model when the fractional flow function and the horizontal velocity are linear $f(S) = S$ and $U[S] = S$, respectively. Using the boundedness property of weak solutions $S \in L^\infty(\Omega_T)$, and without loss of generality, we choose $S \in [0, 1]$. Then the Brinkman VE-model reduces to

$$\partial_t S + \partial_x (S U[S]) + \partial_z (S W[S]) - \Delta S - \beta \Delta \partial_t S = 0, \quad (5.63)$$

where

$$U[S] = S, \quad W[S(\cdot, z, \cdot)] = -\partial_x \int_0^z S(\cdot, q, \cdot) dq, \quad (5.64)$$

for all $z \in (0, 1)$. The definition of the velocity components U and W in (5.64) implies that the velocity $\mathbf{V} = (U, W)^T$ is incompressible

$$\nabla \cdot \mathbf{V} = 0. \quad (5.65)$$

The Brinkman VE-model (5.63), (5.64), and (5.65) is still associated with the initial and boundary conditions

$$\begin{aligned} S(\cdot, \cdot, 0) &= S^0, & \text{in } \Omega, \\ S &= 0, & \text{on } \partial\Omega \times [0, T]. \end{aligned} \quad (5.66)$$

This model has weak solutions, according to Definition 5.4, using Theorem 5.13. The linear choice of f allows making use of the weak incompressibility relation in the uniqueness proof. However, the simplified choice of the velocity vector implies

that for any $Q_1, Q_2 \in L^2(0, T; H_0^1(\Omega))$, the vertical velocity component W satisfies

$$\|W[Q_1] - W[Q_2]\|_{L^2(\Omega_T)} \leq \|\partial_x(Q_1 - Q_2)\|_{L^2(\Omega_T)}. \quad (5.67)$$

Theorem 5.16. *Let the assumptions in Lemma 5.15 be satisfied. Then, the Brinkman VE-model (5.63), (5.64), (5.65), and (5.66) has a unique weak solution.*

Proof. Assume that $S_1, S_2 \in L^2(0, T; H_0^1(\Omega))$ with $\partial_t S_1, \partial_t S_2 \in L^2(0, T; H_0^1(\Omega))$ are two weak solutions of Brinkman VE-model (5.63) and (5.64) according to Definition 5.4 such that $S_1(0) = S_2(0)$ and $\nabla S_1(0) = \nabla S_2(0)$ almost everywhere. Substituting the two solutions into equation (5.5), subtracting the two equations, and taking the test function $S_1 - S_2$ yield for an arbitrary time $\tau \in [0, T]$ that

$$\begin{aligned} \int_0^\tau \int_\Omega \partial_t(S_1 - S_2)(S_1 - S_2) dx dz dt + \beta \int_0^\tau \int_\Omega \partial_t \nabla(S_1 - S_2) \cdot \nabla(S_1 - S_2) dx dz dt \\ - \int_0^\tau \int_\Omega (U[S_1]S_1 - U[S_2]S_2) \partial_x(S_1 - S_2) dx dz dt \\ - \int_0^\tau \int_\Omega (W[S_1]S_1 - W[S_2]S_2) \partial_z(S_1 - S_2) dx dz dt \\ + \int_0^\tau \int_\Omega |\nabla S_1 - \nabla S_2| dx dz dt = 0. \end{aligned} \quad (5.68)$$

Since $(S_1 - S_2)(0) = 0$, the first term on the left side of (5.68) simplifies to

$$\begin{aligned} \int_0^\tau \int_\Omega \partial_t(S_1 - S_2)(S_1 - S_2) dx dz dt &= \frac{1}{2} \int_0^\tau \int_\Omega \partial_t(S_1 - S_2)^2 dx dz dt, \\ &= \frac{1}{2} \int_\Omega ((S_1 - S_2)(\cdot, \cdot, \tau))^2 dx dz. \end{aligned} \quad (5.69)$$

Since $\nabla S_1(0) - \nabla S_2(0) = 0$, the second term on the left side of (5.68) simplifies to

$$\int_0^\tau \int_\Omega \partial_t \nabla(S_1 - S_2) \nabla(S_1 - S_2) dx dz dt = \frac{1}{2} \int_\Omega |\nabla(S_1 - S_2)(\cdot, \cdot, \tau)|^2 dx dz. \quad (5.70)$$

The third term on the left side of (5.68) satisfies

$$\begin{aligned} \int_0^\tau \int_\Omega (U[S_1]S_1 - U[S_2]S_2) \partial_x(S_1 - S_2) dx dz dt \\ = \int_0^\tau \int_\Omega U[S_1](S_1 - S_2) \partial_x(S_1 - S_2) dx dz dt \\ + \int_0^\tau \int_\Omega S_2(U[S_1] - U[S_2]) \partial_x(S_1 - S_2) dx dz dt. \end{aligned} \quad (5.71)$$

The fourth term on the left side of (5.68) satisfies

$$\begin{aligned}
& \int_0^\tau \int_\Omega (W[S_1]S_1 - W[S_2]S_2) \partial_z(S_1 - S_2) dx dz dt \\
&= \int_0^\tau \int_\Omega W[S_1](S_1 - S_2) \partial_z(S_1 - S_2) dx dz dt \\
&+ \int_0^\tau \int_\Omega S_2(W[S_1] - W[S_2]) \partial_z(S_1 - S_2) dx dz dt. \tag{5.72}
\end{aligned}$$

Summing the first term on the right side of equation (5.71) to the first term on the right side of equation (5.72), then using the weak incompressibility property in Definition 5.4 with $\phi = (S_1 - S_2)^2$ yields

$$\begin{aligned}
& \int_0^\tau \int_\Omega U[S_1](S_1 - S_2) \partial_x(S_1 - S_2) + W[S_1](S_1 - S_2) \partial_z(S_1 - S_2) dx dz dt \\
&= \frac{1}{2} \int_0^\tau \int_\Omega U[S_1] \partial_x(S_1 - S_2)^2 dx dz dt + \frac{1}{2} \int_0^\tau \int_\Omega W[S_1] \partial_z(S_1 - S_2)^2 dx dz dt, \\
&= 0. \tag{5.73}
\end{aligned}$$

Using the boundedness of S_2 by Lemma 5.15, Lemma 5.7.2, Hölder's Inequality, and Cauchy's inequality, the second term on the right side of (5.71) satisfies

$$\begin{aligned}
& \int_0^\tau \int_\Omega S_2(U[S_1] - U[S_2]) \partial_x(S_1 - S_2) dx dz dt \\
&\leq \|S_2\|_{L^\infty(\Omega_T)} \int_0^\tau \|S_1 - S_2\|_{L^2(\Omega)} \|\partial_x(S_1 - S_2)\|_{L^2(\Omega)} dt, \\
&\leq \|S_2\|_{L^\infty(\Omega_T)} \int_0^\tau (\|S_1 - S_2\|_{L^2(\Omega)} \|\nabla(S_1 - S_2)\|_{L^2(\Omega)}) dt, \\
&\leq \|S_2\|_{L^\infty(\Omega_T)} \int_0^\tau \left(\|S_1 - S_2\|_{L^2(\Omega)}^2 + \|\nabla(S_1 - S_2)\|_{L^2(\Omega)}^2 \right) dt.
\end{aligned}$$

Using Poincaré inequality, there exists a constant $c > 0$ such that

$$\begin{aligned}
& \int_0^\tau \int_\Omega (U[S_1])S_1 - U[S_2]S_2 \partial_x(S_1 - S_2) dx dz dt \\
&\leq \|S_2\|_{L^\infty(\Omega_T)}(1 + c) \int_0^\tau \|\nabla(S_1 - S_2)\|_{L^2(\Omega)}^2 dt. \tag{5.74}
\end{aligned}$$

Using the boundedness of S_2 by Lemma 5.15 and assumption (5.67), the second term on the right side of equation (5.72) satisfies

$$\begin{aligned}
& \int_0^\tau \int_\Omega S_2 (W[S_1] - W[S_2]) \partial_z (S_1 - S_2) \, dx \, dz \, dt \\
& \leq \|S_2\|_{L^\infty(\Omega_T)} \int_0^\tau \int_\Omega |\partial_x (S_1 - S_2)| |\partial_z (S_1 - S_2)| \, dx \, dz \, dt, \\
& \leq \|S_2\|_{L^\infty(\Omega_T)} \int_0^\tau \|\nabla (S_1 - S_2)\|_{L^2(\Omega)}^2 \, dt. \tag{5.75}
\end{aligned}$$

Substituting (5.69), (5.70), (5.71), (5.72), (5.73), (5.74), and (5.75) into (5.68) yields

$$\begin{aligned}
& \|(S_1 - S_2)(\cdot, \cdot, \tau)\|_{L^2(\Omega)}^2 + \|\nabla (S_1 - S_2)(\cdot, \cdot, \tau)\|_{L^2(\Omega)}^2 + \|\nabla (S_1 - S_2)\|_{L^2(0, \tau; L^2(\Omega))}^2 \\
& \leq C \int_0^\tau \|\nabla (S_1 - S_2)\|_{L^2(\Omega)}^2 \, dt, \tag{5.76}
\end{aligned}$$

for some constant $C > 0$. Thus, Gronwall's inequality implies that

$$\|\nabla (S_1 - S_2)(\cdot, \cdot, \tau)\|_{L^2(\Omega)}^2 = 0. \tag{5.77}$$

Substituting (5.77) into (5.76), and as $\tau \in [0, T]$ is arbitrarily chosen, we obtain

$$\|(S_1 - S_2)(\cdot, \cdot, \tau)\|_{L^2(\Omega)}^2 = 0, \quad \text{for all } \tau \in [0, T].$$

This implies the uniqueness of the weak solution. \square

Proving uniqueness of weak solutions for the Brinkman VE-model (5.1) and (5.2) requires that weak solutions satisfy $\partial_x S \in L^\infty(\Omega_T)$, as clarified in the following remark. However, proving this property is still unfeasible as the regularization theory in [30, 38] is not applicable.

Remark 5.17. *Let $Q_1, Q_2 \in L^2(0, T; H_0^1(\Omega))$. Then, there exists constants $C_1, C_2, C_3 > 0$ such that the vertical velocity component W in (5.2) satisfies the property*

$$\begin{aligned}
\|W[Q_1] - W[Q_2]\|_{L^2(\Omega_T)} & \leq C_1 \|\partial_x (Q_1 - Q_2)\|_{L^2(\Omega_T)} + C_2 \|\partial_x Q_1 (Q_1 - Q_2)\|_{L^2(\Omega_T)} \\
& \quad + C_3 \|\partial_x Q_2 (Q_1 - Q_2)\|_{L^2(\Omega_T)}.
\end{aligned}$$

With this property, the estimate in (5.75) is then given as

$$\begin{aligned}
& \int_0^\tau \int_\Omega S_2 (W[S_1] - W[S_2]) \partial_z (S_1 - S_2) \, dx \, dz \, dt \\
& \leq \|S_2\|_{L^\infty(\Omega_T)} \int_0^\tau \int_\Omega |\partial_x (S_1 - S_2)| |\partial_z (S_1 - S_2)| \, dx \, dz \, dt \\
& \quad + \|S_2\|_{L^\infty(\Omega_T)} \int_0^\tau \int_\Omega |\partial_x S_1| |(S_1 - S_2)| |\partial_z (S_1 - S_2)| \, dx \, dz \, dt \\
& \quad + \|S_2\|_{L^\infty(\Omega_T)} \int_0^\tau \int_\Omega |\partial_x S_2| |(S_1 - S_2)| |\partial_z (S_1 - S_2)| \, dx \, dz \, dt.
\end{aligned}$$

The triple product in the second and the third terms on the right side of the above inequality produces the difficulty that weak solutions of the model must satisfy $\partial_x S \in L^\infty(\Omega_T)$ to get an estimate as in (5.75), which is still unfeasible as the regularization theory in [30, 38] is not applicable.

5.6 Conclusion

We proved in this chapter the existence of weak solutions for the Brinkman VE-model (5.1) and (5.2) in a bounded domain $\Omega \times (0, T)$, where $\Omega \subset \mathbb{R}^2$. To do this, we approximated the time derivatives in the model using the backward difference quotient, then applied Galerkin's method to the resulting elliptic problem. We proved a set of a priori estimates on the sequence of discrete solutions of the approximated problem. These estimates implied a strong convergence of the sequence of discrete solutions in the space $L^2(\Omega \times (0, T))$. Then, we proved that the limit of the sequence is a weak solution of the model.

We proved the boundedness of weak solutions $S \in L^\infty(\Omega \times (0, T])$ for the Brinkman VE-model (5.1) and (5.2), under the assumption that $\partial_x S(t) \in L^r(\Omega)$ for any $r \in (2, \infty)$ and almost all $t \in [0, T]$. Then, we proved the uniqueness of weak solutions for the Brinkman VE-model with linear fractional flow function $f = f(S)$ and horizontal velocity $U = U(S)$.

Chapter 6

Gravity-Driven Water Infiltration into Unsaturated Zone

This chapter studies the process of fluid infiltration through the unsaturated zone due to gravity. This process is an important part of the hydrological cycle as it represents many crucial examples, like the flow of rain water or waste fluids into water aquifers and the flow of salt-water into coastal aquifers. These infiltration processes are usually described using Richards' model [6].

Recent experiments on fluid infiltration show that, even in homogeneous porous media, an initially planar front does not remain planar. The fluids infiltrate in preferential flow paths taking the shape of fingers with different widths and velocities. As most of the fluid channelizes in the fingers with high velocity, this may have crucial effects on the environment as it reduces the time needed for a contaminant to reach the underground water. Experiments also show that constant flux infiltration into homogeneous porous media leads to higher saturation at the wetting front than behind the front. This natural behavior has been called saturation overshoots and is believed to cause the gravity-driven fingering [19, 22].

Richards' model is unable to describe saturation overshoots, because it is a second-order parabolic differential equation fulfilling the maximum principle. Moreover, it is unable to predict fingered flows, as nonlinear stability analysis shows that the model is unconditionally stable for all conditions [24, 42]. Therefore, many approaches have been suggested to modify Richards' model [17, 32, 46]. In this chapter we focus on a particular fourth-order model,

$$\partial_t S(p) + \nabla \cdot (K_f(S(p)) (\mathbf{e}_3 - \nabla p)) + \gamma \Delta \nabla \cdot (K_f(S(p)) \nabla p) = 0, \quad (6.1)$$

that violates the maximum principle. This model is related to the fourth-order model proposed in [17]. However, equation (6.1) has the benefit that both second- and fourth-order terms can be linearized using Kirchhoff's transformation, which is more convenient for the analysis later.

The aim of this chapter is to prove the well-posedness of the fourth-order model (6.1) equipped with initial and boundary conditions. To do this, we apply Kirchhoff's transformation to the model, which transfers the nonlinearities from the second- and fourth-order term in (6.1) to the term with time derivative. After approximating the time derivative using the backward difference quotient, we apply Galerkin's method to the approximated model. Then, we show the existence of a sequence of weak solutions for the discrete model that satisfies a set of a priori estimates. Using these estimates and compactness theorems, we prove the weak convergence of the sequence of discrete solutions in the space $L^2(0, T; H_0^2(\Omega))$ to a weak solution of the transformed model. After that, we prove the uniqueness of the weak solution of the transformed model. We also improve the regularity of the weak solution of the transformed model. Then, we prove the well-posedness of the fourth-order model (6.1) by applying the inverse of Kirchhoff's transformation to the transformed problem.

This chapter has the following structure: Section 6.1 presents Richards' equation and the fourth-order extension proposed in [17]. Section 6.2 introduces the fourth-order model (6.1). In Section 6.3, Kirchhoff's transformation is applied to the fourth-order model (6.1) as a preparation step for the analysis in the following section, then a list of assumptions is provided. In Section 6.4, we prove the well-posedness of the transformed fourth-order model. In Section 6.5, we improve the regularity of the weak solution. In Section 6.6 we prove the well-posedness of the fourth-order model (6.1). Finally, Section 6.7 summarizes the chapter.

6.1 Background

In this section, we present two models that describe fluid flows in the unsaturated zone. First, we present the classical Richards' model, then the fourth-order extension proposed by Cueto-Felgueroso and Juanes in [17].

6.1.1 Richards' model

We consider a bounded domain Ω in the unsaturated zone, where gas occupies most of the pores. Since gas in this zone is naturally connected to the atmospheric air, its pressure is constant and equals the atmospheric air pressure. Assuming that

water infiltrates through the medium Ω under the effect of gravity and capillary forces, the two-phase flow model for the infiltrating water is a combination of the mass conservation equation and Darcy's law

$$\begin{aligned}\phi\partial_t S + \nabla \cdot \mathbf{v} &= 0, \\ \mathbf{v} &= -K_f(S) \left(\frac{\nabla p}{\rho g} - \mathbf{e}_3 \right),\end{aligned}\tag{6.2}$$

respectively. Here, S , \mathbf{v} , and p are saturation, averaged velocity, and pressure of the infiltrating water phase, respectively. The porosity ϕ is assumed to be constant, water density is $\rho = 1$, g is the gravitational acceleration, and $\mathbf{e}_3 = (0, 0, 1)^T$. We also consider the closure relation

$$p_c = p_g - p,\tag{6.3}$$

where $p_g = p_{\text{air}}$ is constant. Then, using the van Genuchten parameterization [51] of the capillary pressure $p_c = p_c(S)$, equation (6.2) simplifies to **Richards' equation**

$$\phi\partial_t S + \nabla \cdot \left(K_f(S) \left(\mathbf{e}_3 + \frac{\nabla p_c(S)}{g} \right) \right) = 0.\tag{6.4}$$

6.1.2 Fourth-Order Model of Cueto-Felgueroso and Juanes

Cueto-Felgueroso and Juanes [17] proposed an extension of Richards' equation that accounts for the apparent surface tension at the wetting front. They redefine the free energy per unit volume of the system as the sum of the gravitational potential \mathcal{E}_{gr} , the capillary potential \mathcal{E}_{cap} and the nonlocal energy potential \mathcal{E}_{nl} ,

$$\mathcal{E} := \mathcal{E}_{gr} + \mathcal{E}_{cap} + \mathcal{E}_{nl} = -\rho g z S + \Psi(S) + \frac{1}{2}\epsilon|\nabla S|^2,\tag{6.5}$$

respectively. The first two terms in (6.5) are local, in contrast to the last term that models the extra energetic cost due to the movement of the water-air interface in regions with large saturation gradients [17, 19]. The coefficient ϵ describes the apparent surface tension associated with the wetting front. The flow potential Φ , defined as the variational derivative of the free energy \mathcal{E} , is then given as

$$\Phi := \frac{\delta \mathcal{E}}{\delta S} = \frac{\partial \mathcal{E}}{\partial S} - \nabla \cdot \frac{\partial \mathcal{E}}{\partial \nabla S} = -\rho g z - p_c(S) - \epsilon \Delta S,\tag{6.6}$$

where $p_c = -\frac{d\Psi}{dS}$. Using equation (6.6), Darcy's law becomes

$$\mathbf{v} = -K_f(S)\nabla\left(-z - \frac{1}{g}p_c(S) - \frac{\epsilon}{g}\Delta S\right). \quad (6.7)$$

Substituting (6.7) into the continuity equation in (6.2) yields the fourth-order model

$$\phi\partial_t S + \nabla \cdot \left(K_f(S) \left(\mathbf{e}_3 + \frac{1}{g}\nabla p_c(S) + \frac{\epsilon}{g}\nabla\Delta S \right) \right) = 0, \quad (6.8)$$

as an extension of Richards' model, where p_c is a decreasing function of water saturation. The fourth-order term in (6.8) describes the non-local forces associated with the displacement of the wetting front in regions of large saturation gradients. If $\epsilon = 0$, the fourth-order model (6.8) reduces to Richards' model.

The fourth-order model (6.8) is similar to the model derived by Huppert [36] that describes thin film flows on inclined planes, where fingered flows and saturation overshoots occur.

6.2 The Fourth-Order Model

Throughout this chapter, we consider a fourth-order extension of Richards's equation by adding a fourth-order regularizing term to Darcy's equation

$$\mathbf{v} = K_f(S)\nabla\left(z + \frac{1}{g}p_c(S)\right) - \frac{\epsilon}{g}\nabla\left(\nabla \cdot (K_f(S)\nabla p_c(S))\right), \quad (6.9)$$

where ϵ is a small parameter. Substituting (6.9) into the continuity equation in (6.2) yields the fourth-order model

$$\partial_t S + \nabla \cdot \left(K_f(S) \left(\mathbf{e}_3 + \frac{1}{g}\nabla p_c(S) \right) \right) - \frac{\epsilon}{g}\Delta\nabla \cdot \left(K_f(S)\nabla p_c(S) \right) = 0. \quad (6.10)$$

This model can also be derived by applying the operator $1 - \epsilon\Delta$ to Richards' equation, which produces

$$\begin{aligned} \partial_t S - \epsilon\Delta\partial_t S + \nabla \cdot \left(K_f(S) \left(\mathbf{e}_3 + \frac{1}{g}\nabla p_c(S) \right) \right) - \epsilon\Delta\nabla \cdot \left(K_f(S)\mathbf{e}_3 \right) \\ - \frac{\epsilon}{g}\Delta\nabla \cdot \left(K_f(S)\nabla p_c(S) \right) = 0, \end{aligned} \quad (6.11)$$

then neglecting the second and fourth terms in equation (6.11).

Since capillary pressure p_c is a strictly monotone decreasing function of saturation S , its inverse is a well-defined function. Thus, we can write saturation S as

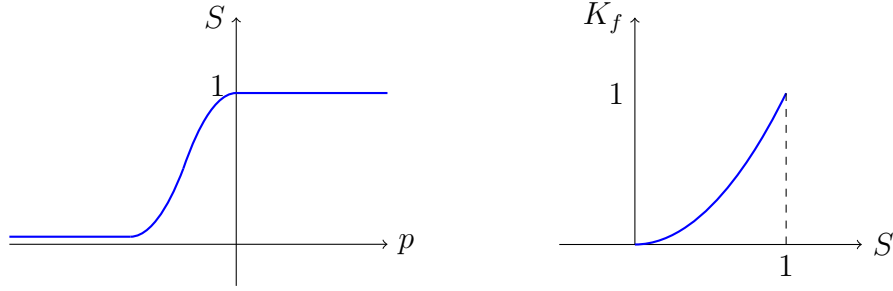


Figure 6.1: Water saturation S as a function $p := -\frac{p_c}{g}$ (left). Conductivity K_f as a function of S (right).

an increasing function of $p := -\frac{p_c}{g}$ such that

$$S(p) = \begin{cases} S(-\frac{p_c}{g}), & p \leq 0, \\ 1, & p > 0. \end{cases}$$

This function is illustrated in Figure 6.1 together with the conductivity $K_f = K_f(S(p))$, which is also a monotone increasing function of S . Using the inverse function p , the fourth order model (6.10) can be written as

$$\partial_t S(p) + \nabla \cdot \left(K_f(S(p)) (\mathbf{e}_3 - \nabla p) \right) + \gamma \Delta \nabla \cdot \left(K_f(S(p)) \nabla p \right) = 0, \quad (6.12)$$

in $\Omega \times (0, T)$ with pressure p is the unknown and $\gamma = \frac{\epsilon}{g}$. The nonlinearity in the fourth-order term in (6.12) is more complex than that in (6.8), but provides the advantage that the second and the fourth-order terms can be simultaneously linearized using Kirchhoff's transformation, which is more convenient to apply Galerkin's method in the next section. Since we are interested in the existence of weak solutions in the space $L^2(0, T; H_0^2(\Omega))$, equation (6.12) is augmented with the initial and boundary conditions

$$\begin{aligned} p(\cdot, 0) &= p^0 && \text{in } \Omega, \\ p &= 0 && \text{on } \partial\Omega \times [0, T], \\ \nabla p \cdot \mathbf{n} &= 0 && \text{on } \partial\Omega \times [0, T], \end{aligned} \quad (6.13)$$

where \mathbf{n} is the outer normal vector at the boundary $\partial\Omega$.

Remark 6.1. *Assuming zero Dirichlet and Neumann boundary conditions in (6.13) simplifies the analysis throughout the chapter. However, the analysis is extendable to more physical boundary conditions that have appropriate regularity and are consistent with the initial condition.*

6.3 Preliminaries and Assumptions

In this section, we apply Kirchhoff's transformation to the fourth-order model (6.12) to linearize the second- and the fourth-order terms. Then, we give a list of assumptions that are imposed to hold throughout the chapter.

Kirchhoff's transformation is a classical transformation used to linearize higher order terms in parabolic equations. It is a continuous monotone increasing map defined as

$$\psi := \begin{cases} \mathbb{R} \rightarrow \mathbb{R} \\ p \mapsto \psi(p) = \int_0^p K_f(S(\tau)) d\tau \end{cases}$$

where $\psi(p)$ is the transformed pressure. We set $u := \psi(p)$. Then, as Figure 6.2 shows, we have $u = p$ for $p \geq 0$, because $K_f(S(p)) = 1$. Moreover, there exists a lower bound $u_l < 0$ of u such that $u_l := \lim_{p \rightarrow -\infty} \psi(p) = -\int_{-\infty}^0 K_f(S(p)) dp$. In other words, the lower bound u_l equals the area under the graph of K_f multiplied by -1 .

Applying the Leibniz rule on the transformed pressure u gives

$$\begin{aligned} \nabla u &= K_f(S(p)) \nabla p, \\ \Delta u &= \nabla \cdot (K_f(S(p)) \nabla p), \\ \partial_t u &= K_f(S(p)) \partial_t p. \end{aligned} \tag{6.14}$$

As the inverse function $\psi^{-1} : (u_l, \infty) \rightarrow \mathbb{R}$ is well-defined, we consider the function

$$b(u) := S(\psi^{-1}(u)),$$

such that

$$b'(u) = \frac{S'(p)}{K_f(S(p))}.$$

Then, the transformed fourth-order model is given as:

$$\partial_t b(u) + \nabla \cdot \left(K_f(b(u)) \mathbf{e}_3 \right) - \Delta u + \gamma \Delta^2 u = 0, \tag{6.15}$$

with the transformed initial and boundary conditions

$$\begin{aligned} u(., 0) &= u^0 && \text{in } \Omega \times \{0\}, \\ u &= 0 && \text{on } \partial\Omega \times (0, T), \\ \nabla u \cdot \mathbf{n} &= 0 && \text{on } \partial\Omega \times (0, T). \end{aligned} \tag{6.16}$$

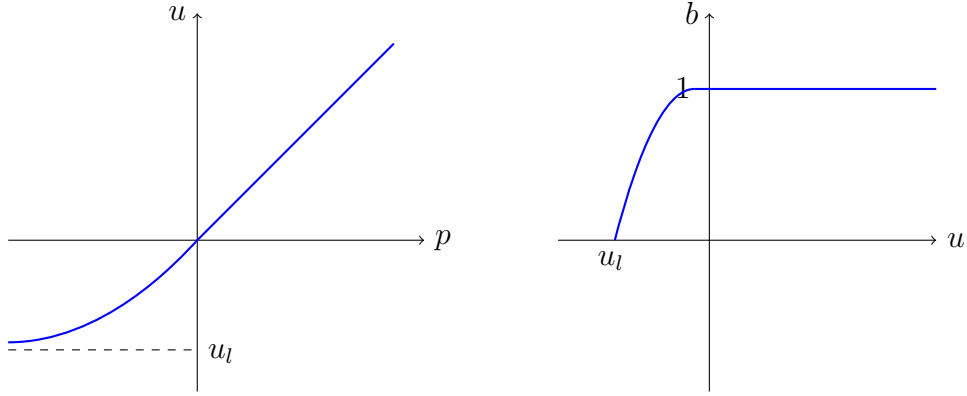


Figure 6.2: An illustration of the transformed pressure $u = \psi(p)$ (left) and transformed saturation $b(u)$ (right).

Due to the nonlinearity of the first term on the left side of equation (6.15), we follow [2] and define the Legendre transform B for the primitive of b ,

$$B := \begin{cases} \mathbb{R} \rightarrow \mathbb{R}^+ \\ z \mapsto B(z) = \int_0^z b(z) - b(s) ds, \end{cases} \quad (6.17)$$

The map B satisfies the following properties:

Lemma 6.2. *If b is a continuous and monotone increasing function, then the Legendre transform B , defined in (6.17), satisfies*

$$B(z) - B(z_0) \geq (b(z) - b(z_0))z_0,$$

$$B(z) - B(z_0) \leq (b(z) - b(z_0))z,$$

for any $z, z_0 \in \mathbb{R}$.

Proof. The continuity and the monotonicity of b imply the existence of a convex function $\phi \in C^1(\mathbb{R}, \mathbb{R})$ such that $b = \phi' := \frac{d\phi}{du}$. The definition of B and the property that $b = \phi'$ give

$$B(z) = \int_0^z (b(z) - \phi'(s)) ds = b(z)z - (\phi(z) - \phi(0)). \quad (6.18)$$

Then, we have

$$B(z) - B(z_0) = b(z)z - b(z_0)z_0 - (\phi(z) - \phi(z_0)).$$

To prove the first inequality, we add and subtract $b(z)z_0$, then we have

$$B(z) - B(z_0) = \left(b(z) - b(z_0)\right)z_0 - \underbrace{b(z)(z_0 - z) - \left(\phi(z) - \phi(z_0)\right)}_{=:M}.$$

The Taylor expansion and the convexity of ϕ imply that $M > 0$, which proves the inequality. The second inequality follows similarly by adding and subtracting $b(z_0)z$. \square

The following assumptions are imposed to hold throughout the chapter:

Assumption 6.3. 1. The domain $\Omega \subset \mathbb{R}^3$ is an open bounded connected region with boundary $\partial\Omega \in C^5$ and $0 < T < \infty$.

2. The initial condition $u^0 \in H_0^2(\Omega)$ satisfies $u^0, b(u^0), B(u^0) \in L^\infty(\Omega)$.

3. The function $b : (u_l, \infty) \rightarrow (0, 1]$ is strictly positive, monotone increasing and Lipschitz continuous.

4. The conductivity function $K_f : (u_l, \infty) \rightarrow (0, 1]$ is Lipschitz continuous, strictly positive, monotone increasing, and there exists a constant $\beta > 0$ such that, for all $z \in \mathbb{R}$, the following growth condition holds

$$\left(K_f(b(z))\right)^2 \leq \beta(1 + B(z)).$$

Remark 6.4. The growth condition on the conductivity function K_f is not a restrictive assumption, because $K_f \in (0, 1]$, as shown in Figure 6.1, and B is nonnegative (by substituting $z_0 = 0$ into the first inequality in Lemma 6.2).

6.4 Well-posedness of the Transformed Fourth-Order Model

In this section, we prove the well-posedness of the transformed fourth-order problem (6.15), (6.16) in an open bounded porous medium $\Omega \subset \mathbb{R}^3$. To do this, we approximate the time derivative using the backward difference quotient then apply Galerkin's method in space. After that, we show the existence of a sequence of weak solutions for the discrete problem. In Section 6.4.1, we prove a set of a priori estimates on this sequence. In Section 6.4.2, we prove the weak convergence of the sequence in the space $L^2(0, T; H_0^2(\Omega))$ to a weak solution of the transformed problem. Finally, we prove in Section 6.4.3 the uniqueness of the weak solution.

Let $N > 0$ be an integer with $\Delta t = T/N$. Approximating $\partial_t b(u)$ in equation (6.15) using the backward difference quotient $\frac{b(u(\cdot, t)) - b(u(\cdot, t - \Delta t))}{\Delta t}$ yields, for almost all $t \in [0, T]$, the biharmonic equation

$$\frac{b(u(\cdot, t)) - b(u(\cdot, t - \Delta t))}{\Delta t} + \nabla \cdot \left(K_f(b(u(\cdot, t))) \mathbf{e}_3 \right) - \Delta u(\cdot, t) + \gamma \Delta^2 u(\cdot, t) = 0. \quad (6.19)$$

Weak solutions of this equation are expected to belong to the Hilbert space $V(\Omega) = H_0^2(\Omega)$. Since $H_0^2(\Omega)$ is separable [1], it has a countable orthonormal basis

$$\{w_i\}_{i \in \mathbb{N}} \subset V(\Omega). \quad (6.20)$$

By applying Galerkin's method to equation (6.19), the solution space $V(\Omega) := H_0^2(\Omega)$ is projected into a finite dimensional space $V_m(\Omega)$ spanned by a finite number of the orthonormal functions w_i , $i = 1, \dots, m$. Thus, for fixed positive integers N, m , we search a function $u_m^N : [0, T] \rightarrow H_0^2(\Omega)$ of the form

$$u_m^N(t) := \sum_{i=1}^m \alpha_{mi}^N(t) w_i, \quad (6.21)$$

where the unknown coefficients $\alpha_{m,i}^N \in L^\infty((0, T))$, $i = 1, \dots, m$, are chosen such that, for almost all $t \in [0, T]$, the equation

$$\begin{aligned} \frac{1}{\Delta t} \int_{\Omega} \left(b(u_m^N(t)) - b(u_m^N(t - \Delta t)) \right) w_i \, d\mathbf{x} + \int_{\Omega} \nabla u_m^N(t) \cdot \nabla w_i + \gamma \Delta u_m^N(t) \Delta w_i \, d\mathbf{x} \\ = \int_{\Omega} K_f(b(u_m^N(t))) \mathbf{e}_3 \cdot \nabla w_i \, d\mathbf{x} \end{aligned} \quad (6.22)$$

holds for all $i = 1, \dots, m$. The initial data is chosen to be

$$u_m^0(t) = u_m^0, \quad \text{for } t \in (-\Delta t, 0], \quad (6.23)$$

where, u_m^0 is the L^2 -projection of the initial data u_0 into the finite dimensional space $V_m(\Omega)$.

Proposition 6.5. *For any $m, N \in \mathbb{N}$, assume that $u_m^N(t - \Delta t) \in V_m(\Omega)$ and*

$$\Delta t \leq \frac{1}{\beta}, \quad (6.24)$$

where $\beta > 0$ is given as in Assumption 6.3(4). Then, equation (6.22) has a solution $u_m^N(t) \in V_m(\Omega)$.

Proof. Before proving the Lemma, we notify that $u_m^N(t - \Delta t)$ for $t \in (0, \Delta t]$ is well-defined by the choice of the initial condition (6.23). Now, we define the vector field $\mathbf{f} : \mathbb{R}^m \rightarrow \mathbb{R}^m$ such that $\mathbf{f} = (f_1, \dots, f_m)$ and the vector $\alpha_m^N = (\alpha_{m,1}^N, \dots, \alpha_{m,m}^N)$ of the unknown coefficients of $u_m^N(t)$ in equation (6.21). Then, we have

$$\begin{aligned} f_i(\alpha_m^N) &:= \frac{1}{\Delta t} \int_{\Omega} (b(u_m^N(t)) - b(u_m^N(t - \Delta t))) w_i \, d\mathbf{x} - \int_{\Omega} K_f(b(u_m^N(t))) \mathbf{e}_3 \cdot \nabla w_i \, d\mathbf{x} \\ &\quad + \int_{\Omega} (\nabla u_m^N(t) \cdot \nabla w_i + \gamma \Delta u_m^N(t) \Delta w_i) \, d\mathbf{x}, \end{aligned} \quad (6.25)$$

for all $i = 1, \dots, m$. Using Assumption 6.3(3) and 6.3(4), the vector field \mathbf{f} is continuous. Moreover, we have

$$\begin{aligned} \mathbf{f}(\alpha_m^N) \cdot \alpha_m^N &= \frac{1}{\Delta t} \int_{\Omega} (b(u_m^N(t)) - b(u_m^N(t - \Delta t))) u_m^N(t) \, d\mathbf{x} - \int_{\Omega} K_f(b(u_m^N(t))) \mathbf{e}_3 \cdot \nabla u_m^N \, d\mathbf{x} \\ &\quad + \int_{\Omega} \nabla u_m^N \cdot \nabla u_m^N \, d\mathbf{x} + \gamma \int_{\Omega} \Delta u_m^N \Delta u_m^N \, d\mathbf{x}. \end{aligned}$$

Applying Lemma 6.2 on the first term of the right side and Cauchy's inequality on the second term yield

$$\begin{aligned} \mathbf{f}(\alpha_m^N) \cdot \alpha_m^N &\geq \frac{1}{\Delta t} \int_{\Omega} (B(u_m^N(t)) - B(u_m^N(t - \Delta t))) \, d\mathbf{x} - \frac{1}{2} \int_{\Omega} (K_f(b(u_m^N(t))))^2 \, d\mathbf{x} \\ &\quad + \frac{1}{2} \int_{\Omega} |\nabla u_m^N|^2 \, d\mathbf{x} + \gamma \int_{\Omega} (\Delta u_m^N)^2 \, d\mathbf{x}. \end{aligned}$$

The growth condition in Assumption 6.3(4), equation (6.21), and the orthonormality of the basis functions w_i , $i = 1, \dots, m$, imply that

$$\begin{aligned} \mathbf{f}(\alpha_m^N) \cdot \alpha_m^N &\geq \frac{1}{\Delta t} \int_{\Omega} (B(u_m^N(t)) - B(u_m^N(t - \Delta t))) \, d\mathbf{x} - \beta \int_{\Omega} (1 + B(u_m^N(t))) \, d\mathbf{x} \\ &\quad + \int_{\Omega} \left(\frac{1}{2} \left| \sum_i^m \alpha_{m,i}^N \nabla w_i \right|^2 + \frac{\gamma}{2} \left(\sum_i^m \alpha_{m,i}^N \Delta w_i \right)^2 \right) \, d\mathbf{x}, \\ &\geq \left(\frac{1}{\Delta t} - \beta \right) \int_{\Omega} B(u_m^N(t)) \, d\mathbf{x} - \left(\beta |\Omega| + \frac{1}{\Delta t} \int_{\Omega} B(u_m^N(t - \Delta t)) \, d\mathbf{x} \right) \\ &\quad + \left(\frac{1}{2} + \frac{\gamma}{2} \right) |\alpha_m^N|^2. \end{aligned}$$

The first term of the right side of above inequality is nonnegative using condition (6.24). Set $r = |\alpha_m^N(t)|$. Since $u_m^N(t - \Delta t) \in V_m(\Omega)$ is known, we have $\mathbf{f}(\alpha_m^N(t)) \cdot \alpha_m^N(t) \geq 0$ provided that r is large enough. Thus, the conditions of Lemma 5.8 are satisfied and we conclude the existence of a point $\alpha_m^N(t) \in \mathbb{R}^m$ such that $\mathbf{f}(\alpha_m^N) = 0$.

Using (6.25), we conclude the existence of a $u_m^N(t)$ as defined in (6.21) that satisfies (6.22). \square

Remark 6.6. *The discrete function u_m^N is a step function in time and, therefore, is defined for all $t \in [0, T]$. This is a result of the structure of equation (6.22), where $u_m^N(t)$, $t \in [(n-1)\Delta t, n\Delta t)$, is determined inductively using the given data $u_m^N(t - \Delta t)$.*

6.4.1 A Priori Estimates

Lemma 6.7. *There exists a constant $c > 0$ such that*

$$\operatorname{ess\,sup}_{t \in [0, T]} \int_{\Omega} (B(u_m^N(t))) \, d\mathbf{x} + \int_0^T \int_{\Omega} |\nabla u_m^N|^2 + \gamma(\Delta u_m^N)^2 \, d\mathbf{x} \, dt \leq c \int_{\Omega} B(u_m^0) \, d\mathbf{x},$$

for all $N, m \in \mathbb{N}$.

Proof. Multiplying equation (6.22) by $\alpha_{m,i}^N$, summing for $i = 1, \dots, m$, and then integrating from 0 to an arbitrary time $\tau \in [0, T]$ yields

$$\begin{aligned} \frac{1}{\Delta t} \int_0^{\tau} \int_{\Omega} (b(u_m^N(t)) - b(u_m^N(t - \Delta t))) u_m^N(t) \, d\mathbf{x} \, dt + \int_0^{\tau} \int_{\Omega} |\nabla u_m^N|^2 \, d\mathbf{x} \, dt \\ + \gamma \int_0^{\tau} \int_{\Omega} (\Delta u_m^N)^2 \, d\mathbf{x} \, dt = \int_0^{\tau} \int_{\Omega} K_f(b(u_m^N)) \mathbf{e}_3 \cdot \nabla u_m^N \, d\mathbf{x} \, dt. \end{aligned} \quad (6.26)$$

Applying the first inequality in Lemma 6.2 to the first term on the left side of equation (6.26) and Cauchy's inequality to the right side yield

$$\begin{aligned} \frac{1}{\Delta t} \int_0^{\tau} \int_{\Omega} (B(u_m^N(t)) - B(u_m^N(t - \Delta t))) \, d\mathbf{x} \, dt + \int_0^{\tau} \int_{\Omega} |\nabla u_m^N|^2 + \gamma(\Delta u_m^N)^2 \, d\mathbf{x} \, dt \\ \leq \frac{1}{2} \int_0^{\tau} \int_{\Omega} (K_f(b(u_m^N)))^2 \, d\mathbf{x} \, dt + \frac{1}{2} \int_0^{\tau} \int_{\Omega} |\nabla u_m^N|^2 \, d\mathbf{x} \, dt. \end{aligned}$$

Applying the growth condition in Assumption 6.3(4) to the first term on the right side of the above equation gives

$$\begin{aligned} \frac{1}{\Delta t} \int_0^{\tau} \int_{\Omega} (B(u_m^N(t)) - B(u_m^N(t - \Delta t))) \, d\mathbf{x} \, dt + \frac{1}{2} \int_0^{\tau} \int_{\Omega} |\nabla u_m^N|^2 \, d\mathbf{x} \, dt \\ + \gamma \int_0^{\tau} \int_{\Omega} (\Delta u_m^N)^2 \, d\mathbf{x} \, dt \leq \beta \int_0^{\tau} \int_{\Omega} (1 + B(u_m^N(t))) \, d\mathbf{x} \, dt. \end{aligned}$$

Applying summation by parts to the first term on the left side of the above equation and noting that u_m^N is a step function in time lead to

$$\begin{aligned} \int_{\Omega} B(u_m^N(\tau)) d\mathbf{x} + \frac{1}{2} \int_0^\tau \int_{\Omega} |\nabla u_m^N|^2 d\mathbf{x} dt + \gamma \int_0^\tau \int_{\Omega} |\Delta u_m^N|^2 d\mathbf{x} dt \\ \leq \beta |\Omega| T + \int_{\Omega} B(u_m^0) d\mathbf{x} + \beta \int_0^\tau \int_{\Omega} B(u_m^N(t)) d\mathbf{x} dt. \end{aligned}$$

Note that $B(u_m^N)$ is nonnegative and summable on $[0, T]$, where the summability results from substituting $z_0 = 0$ into the second inequality in Lemma 6.2, the boundedness of b , and the choice that the coefficients $\alpha_{m,i}^N \in L^\infty((0, T))$. Hence, Gronwall's inequality (2.21) is applicable and implies the existence of a constant $c > 0$ depending on β , $|\Omega|$, and T such that

$$\operatorname{ess\,sup}_{t \in [0, T]} \int_{\Omega} (B(u_m^N(t)) d\mathbf{x} + \int_0^T \int_{\Omega} \left(\frac{1}{2} |\nabla u_m^N|^2 + \gamma (\Delta u_m^N)^2 \right) d\mathbf{x} dt) \leq c \int_{\Omega} B(u_m^0) d\mathbf{x}.$$

□

Corollary 6.8. *It holds that $u_m^N \in L^2(0, T; H_0^2(\Omega))$ for all $m, N \in \mathbb{N}$.*

Proof. Lemma 6.7 and Poincaré's inequality imply the existence of a constant $C > 0$ such that

$$\int_0^T \int_{\Omega} (u_m^N)^2 d\mathbf{x} dt \leq C,$$

for all $N, m \in \mathbb{N}$. Moreover, the biharmonic operator $Lu : \Delta u + \Delta^2 u$ can be written as a combination of two second-order elliptic operators

$$L_1 w = \Delta w + w, \quad \text{and} \quad L_2 u = \Delta u - w.$$

Hence, the basis functions w_i of the biharmonic operator L can be chosen as a combination of the eigenfunctions of the operators L_1 and L_2 . These eigenfunctions belong to the space $C^3(\Omega)$, whenever the boundary $\partial\Omega \in C^5$, [25]. Hence, using Gauss' theorem and Cauchy's inequality, we obtain

$$\begin{aligned} \int_0^T \int_{\Omega} (\partial_{x_i x_j} u_m^N)^2 d\mathbf{x} dt &= - \int_0^T \int_{\Omega} \partial_{x_i} u_m^N \partial_{x_i x_j x_j} u_m^N d\mathbf{x} dt = \int_0^T \int_{\Omega} \partial_{x_i x_i} u_m^N \partial_{x_j x_j} u_m^N d\mathbf{x} dt \\ &\leq \frac{1}{2} \int_0^T \int_{\Omega} (\partial_{x_i x_i} u_m^N)^2 d\mathbf{x} dt + \frac{1}{2} \int_0^T \int_{\Omega} (\partial_{x_j x_j} u_m^N)^2 d\mathbf{x} dt \\ &= \frac{1}{2} \|\Delta u_m^N\|_{L^2(\Omega \times (0, T))}. \end{aligned}$$

for all $i, j, \forall i, j = 1, \dots, d$. Thus we have $D^\beta u \in L^2(\Omega \times (0, T))$ for all index vectors $\beta \in \mathbb{N} \times \mathbb{N} \times \mathbb{N}$ with $|\beta| = 2$. This completes the proof. \square

In the following lemma, we prove an a priori estimate on the backward difference quotient $\frac{b(u_m^N(t)) - b(u_m^N(t - \Delta t))}{\Delta t}$.

Lemma 6.9. *There exists a constant $c > 0$ such that*

$$\frac{1}{\Delta t} \int_0^T \int_\Omega (b(u_m^N(t)) - b(u_m^N(t - \Delta t))) \phi \, d\mathbf{x} \, dt \leq c,$$

for any $\phi \in L^2(0, T; V_m(\Omega))$ and $N, m \in \mathbb{N}$.

Proof. Let $M \leq m$ be a positive integer and choose a function $\phi \in L^\infty(0, T; H_0^2(\Omega))$ such that for almost all $t \in [0, T]$

$$\phi(t) = \sum_{i=1}^M \alpha_i(t) w_i, \tag{6.27}$$

where $\alpha_i \in L^\infty((0, T))$, $i = 1, \dots, M$, are given functions and $w_i \in H_0^2(\Omega)$, $i = 1, \dots, M$, belong to the orthonormal basis of the subspace $V_m(\Omega)$. Choosing $M < m$, multiplying equation (6.22) by $\alpha_i(t)$, summing for $i = 1, \dots, m$, and then integrating from 0 to T yields

$$\begin{aligned} & \frac{1}{\Delta t} \int_0^T \int_\Omega (b(u_m^N(t)) - b(u_m^N(t - \Delta t))) \phi(t) \, d\mathbf{x} \, dt \\ &= \int_0^T \int_\Omega K_f(b(u_m^N(t))) \mathbf{e}_3 \cdot \nabla \phi(t) \, d\mathbf{x} \, dt - \int_0^T \int_\Omega \nabla u_m^N(t) \cdot \nabla \phi(t) \, d\mathbf{x} \, dt \\ & \quad - \gamma \int_0^T \int_\Omega \Delta u_m^N(t) \Delta \phi(t) \, d\mathbf{x} \, dt. \end{aligned}$$

Applying Cauchy's inequality on the terms on the right side of the above equation yields

$$\begin{aligned} & \frac{1}{\Delta t} \int_0^T \int_\Omega (b(u_m^N(t)) - b(u_m^N(t - \Delta t))) \phi(t) \, d\mathbf{x} \, dt \\ & \leq \frac{1}{2} \int_0^T \int_\Omega (K(b(u_m^N(t))))^2 \, d\mathbf{x} \, dt + \int_0^T \int_\Omega |\nabla \phi(t)|^2 \, d\mathbf{x} \, dt + \frac{1}{2} \int_0^T \int_\Omega |\nabla u_m^N|^2 \, d\mathbf{x} \, dt \\ & \quad + \frac{\gamma}{2} \int_0^T \int_\Omega \Delta \phi(t)^2 \, d\mathbf{x} \, dt + \frac{\gamma}{2} \int_0^T \int_\Omega (\Delta u_m^N)^2 \, d\mathbf{x} \, dt. \end{aligned}$$

Now, using the growth condition in Assumption 6.3(4), we obtain

$$\begin{aligned} & \frac{1}{\Delta t} \int_0^T \int_{\Omega} (b(u_m^N(t)) - b(u_m^N(t - \Delta t))) \phi(t) \, d\mathbf{x} \, dt \\ & \leq \frac{\beta}{2} \int_0^T \int_{\Omega} (1 + B(u_m^N(t))) \, d\mathbf{x} \, dt + \int_0^T \int_{\Omega} |\nabla \phi(t)|^2 \, d\mathbf{x} \, dt + \frac{1}{2} \int_0^T \int_{\Omega} |\nabla u_m^N|^2 \, d\mathbf{x} \, dt \\ & \quad + \frac{\gamma}{2} \int_0^T \int_{\Omega} \Delta \phi(t)^2 \, d\mathbf{x} \, dt + \frac{\gamma}{2} \int_0^T \int_{\Omega} (\Delta u_m^N)^2 \, d\mathbf{x} \, dt. \end{aligned}$$

Then, Lemma 6.7 and the choice that $\phi \in L^\infty(0, T; H_0^1(\Omega))$ implies the existence of a constant $c > 0$ such that

$$\frac{1}{\Delta t} \int_0^T \int_{\Omega} (b(u_m^N(t)) - b(u_m^N(t - \Delta t))) \phi(t) \, d\mathbf{x} \, dt \leq c.$$

□

Corollary 6.10. *There exist constants $\delta_0, c > 0$ such that*

$$\frac{1}{\delta} \int_{\delta}^T \int_{\Omega} (b(u_m^N(t)) - b(u_m^N(t - \delta))) (u_m^N(t) - u_m^N(t - \delta)) \, d\mathbf{x} \, dt \leq c,$$

for any $N, m \in \mathbb{N}$ and $\delta \in (0, \delta_0)$.

Proof. Choosing $\phi = u_m^N(t) - u_m^N(t - \Delta t)$ in Lemma 6.9 yields

$$\frac{1}{\Delta t} \int_0^T \int_{\Omega} (b(u_m^N(t)) - b(u_m^N(t - \Delta t))) (u_m^N(t) - u_m^N(t - \Delta t)) \, d\mathbf{x} \, dt \leq c.$$

Using Remark 6.6, u_m^N is a step function in time. Hence, it holds that

$$\frac{1}{\delta} \int_0^T \int_{\Omega} (b(u_m^N(t)) - b(u_m^N(t - \delta))) (u_m^N(t) - u_m^N(t - \delta)) \, d\mathbf{x} \, dt \leq c,$$

for any $\delta > 0$ such that $|\delta - \Delta t|$ is small enough. □

6.4.2 Convergence Results

In this subsection, we show the convergence of the sequence $\{u_m^N\}_{N, m \in \mathbb{N}}$ of discrete solutions of equation (6.22) to a weak solution of the transformed fourth-order problem (6.15) and (6.16). This result is summarized in Theorem 6.12. The proof of the theorem depends on the a priori estimates in Section 6.4.1 and the following proposition by Alt and Luckhaus [2].

Proposition 6.11 (Alt and Luckhaus [2]). *Assume that the sequence $z_\epsilon \rightharpoonup z$ in $L^2(0, T; H^1(\Omega))$ as $\epsilon \rightarrow 0$ and there exists a constant $C > 0$ such that*

$$\frac{1}{\delta} \int_0^{T-\delta} \int_{\Omega} (b(z_\epsilon(t+\delta)) - b(z_\epsilon(t)))(z_\epsilon(t+\delta) - z_\epsilon(t)) \, d\mathbf{x} \, dt \leq C, \quad (6.28)$$

holds for any small $\delta > 0$ and

$$\int_{\Omega} B(z_\epsilon(t)) \, d\mathbf{x} \leq C, \quad \text{for } 0 < t < T.$$

Then, $b(z_\epsilon) \rightarrow b(z)$ in $L^1(\Omega \times (0, T))$ and $B(z_\epsilon) \rightarrow B(z)$ almost everywhere.

Proof. See [2], page: 322, 323. □

Before we state and prove the first main theorem in this chapter, we remind that the Sobolev space $L^2(0, T; H_0^2(\Omega))$ and its dual $L^2(0, T; H^{-2}(\Omega))$ are equipped with the norms

$$\begin{aligned} \|u\|_{L^2(0, T; H^2(\Omega))} &= \int_0^T \int_{\Omega} (u^2 + |\nabla u|^2 + |D^2 u|^2) \, d\mathbf{x} \, dt, \\ \|L\|_{L^2(0, T; H^{-2}(\Omega))} &= \sup \{L(u) \mid u \in L^2(0, T; H_0^2(\Omega)), \|u\|_{L^2(0, T; H^2(\Omega))} \leq 1\}. \end{aligned} \quad (6.29)$$

Theorem 6.12. *Let Assumption 6.3 be satisfied and $\Delta t \leq \frac{1}{\beta}$. Then, problem (6.15), (6.16) has a weak solution $u \in L^2(0, T; H_0^2(\Omega))$ that satisfies*

1. $K_f(b(u)) \in L^2(\Omega \times (0, T))$, $\partial_t b(u) \in L^2(0, T; H^{-2}(\Omega))$, and

$$\int_0^T \int_{\Omega} \left(\partial_t b(u) \phi - K_f(b(u)) \mathbf{e}_3 \cdot \nabla \phi + \nabla u \cdot \nabla \phi + \gamma \Delta u \Delta \phi \right) \, d\mathbf{x} \, dt = 0, \quad (6.30)$$

for every test function $\phi \in L^2(0, T; H_0^2(\Omega))$.

2. $b(u) \in L^\infty(0, T; L^1(\Omega))$, $\partial_t b(u) \in L^2(0, T; H^{-2}(\Omega))$, and

$$\int_0^T \int_{\Omega} \partial_t b(u) \phi \, d\mathbf{x} \, dt = \int_0^T \int_{\Omega} (b(u) - b^0) \partial_t \phi \, d\mathbf{x} \, dt, \quad (6.31)$$

holds for all test functions $\phi \in L^2(0, T; H_0^2(\Omega))$ with $\partial_t \phi \in L^1(0, T; L^\infty(\Omega))$ and $\phi(\cdot, T) = 0$.

Proof. Using Corollary 6.8, the conditions of the Weak Compactness theorem 2.21 are satisfied. Hence, up to a subsequence, there exists a function $u \in$

$L^2(0, T; H_0^2(\Omega))$ such that

$$u_m^N \rightharpoonup u \quad \text{in } L^2(0, T; H_0^2(\Omega)), \quad (6.32)$$

as $m, N \rightarrow \infty$. The next step in the proof is to show that the function $u \in L^2(0, T; H_0^2(\Omega))$ fulfills the conditions (6.30) and (6.31). Thus, we consider an arbitrary test function $\phi \in L^2(0, T; V_m(\Omega))$ such that for a fixed integer M and for almost all $t \in (0, T)$ is given as

$$\phi(t) = \sum_i^M \alpha_i(t) w_i, \quad (6.33)$$

where $\alpha_i \in L^\infty(0, T)$, $i = 1, \dots, M$, are given functions and $w_i \in H_0^2(\Omega)$, $i = 1, \dots, M$, belong to the orthonormal basis of the subspace $V_m(\Omega)$. Choosing $M < m$, multiplying equation (6.22) by $\alpha_i(t)$, summing for $i = 1, \dots, M$, and then integrating with respect to time yields

$$\begin{aligned} & \frac{1}{\Delta t} \int_0^\tau \int_\Omega (b(u_m^N(t)) - b(u_m^N(t - \Delta t))) \phi(t) \, d\mathbf{x} \, dt + \int_0^\tau \int_\Omega \nabla u_m^N \cdot \nabla \phi \, d\mathbf{x} \, dt \\ & + \gamma \int_0^\tau \int_\Omega \Delta u_m^N \Delta \phi \, d\mathbf{x} \, dt = \int_0^\tau \int_\Omega K_f(b(u_m^N)) \mathbf{e}_3 \cdot \nabla \phi \, d\mathbf{x} \, dt. \end{aligned} \quad (6.34)$$

In the following we show that equation (6.34) converges as $m, N \rightarrow \infty$ to equation (6.30). The weak convergence (6.32), Corollary 6.10, and Proposition 6.11 imply the strong convergences,

$$b(u_m^N) \rightarrow b(u) \quad \text{in } L^1(\Omega \times (0, T)), \quad (6.35)$$

and

$$B(u_m^N) \rightarrow B(u) \quad \text{almost everywhere.}$$

The strong convergence of $B(u_m^N)$ and the estimate in Lemma 6.7 leads to

$$B(u) \in L^\infty(0, T; L^1(\Omega)). \quad (6.36)$$

Hence, Assumption 6.3(2) and the first inequality in Lemma 6.2 with $z_0 = u^0$ imply

$$b(u) \in L^\infty(0, T; L^1(\Omega)). \quad (6.37)$$

The Lipschitz continuity of the conductivity function and the strong convergence in (6.35) imply

$$K_f(b(u_m^N)) \rightarrow K_f(b(u)) \quad \text{in } L^1(\Omega \times (0, T)).$$

Consequently, we have

$$K_f(b(u_m^N)) \rightarrow K_f(b(u)) \quad \text{almost everywhere.} \quad (6.38)$$

However, we need to prove at least a weak convergence of $K_f(b(u_m^N))$ in $L^2(\Omega \times (0, T))$. For this, we use the growth condition on K_f and (6.36). Then, we have

$$(K_f(b(u)))^2 \leq \beta(1 + B(u)) \in L^\infty(0, T; L^1(\Omega)).$$

This implies the existence of a constant $C > 0$ such that

$$\|K_f(b(u))\|_{L^2(\Omega \times (0, T))} \leq C. \quad (6.39)$$

This estimate, the almost everywhere convergence in (6.38), the boundedness of the domain $\Omega \times (0, T)$, and Egorov's theorem imply the weak convergence

$$K_f(b(u_m^N)) \rightharpoonup K_f(b(u)) \quad \text{in } L^2(\Omega \times (0, T)). \quad (6.40)$$

The last step in the proof is to show that

$$\frac{b(u_m^N(t)) - b(u_m^N(t - \Delta t))}{\Delta t} \rightharpoonup \partial_t b(u) \quad \text{in } L^2(0, T; H_0^{-2}(\Omega)).$$

To do this, we consider the estimate in Lemma 6.9,

$$\int_0^T \int_\Omega \frac{b(u_m^N(t)) - b(u_m^N(t - \Delta t))}{\Delta t} \phi(t) \, d\mathbf{x} \, dt \leq C, \quad (6.41)$$

for any $\phi \in L^2(0, T; V_m)$. This uniform estimate implies the existence of a sequence of functionals v_m^N in the dual space $L^2(0, T; V_m^*(\Omega))$ such that

$$\int_0^T \langle v_m^N, \phi \rangle \, dt = \int_0^T \int_\Omega \frac{b(u_m^N(t)) - b(u_m^N(t - \Delta t))}{\Delta t} \phi \, d\mathbf{x} \, dt \leq C. \quad (6.42)$$

Hence, there exists a limit $v \in L^2(0, T; H_0^{-2}(\Omega))$ such that

$$\int_0^T \langle v_m^N, \phi \rangle dt \rightarrow \int_0^T \langle v, \phi \rangle dt \quad (6.43)$$

for all $\phi \in L^2(0, T; V_m(\Omega))$ as $N, m \rightarrow \infty$. Since $\bigcup_{m \in \mathbb{N}} V_m$ is dense in $H_0^2(\Omega)$, the convergence result in (6.43) holds also for all $\phi \in L^2(0, T; H_0^2(\Omega))$. To identify the limit v , we consider the test function $\phi \in L^2(0, T; H_0^2(\Omega))$ with $\partial_t \phi \in L^1(0, T; L^\infty(\Omega))$ and $\phi(t) = 0$ for all $t \in (T - \Delta t, T]$. Applying summation by parts to the left side of (6.41) yields

$$\int_0^T \int_\Omega \frac{b(u_m^N(t)) - b(u_m^N(t - \Delta t))}{\Delta t} \phi \, d\mathbf{x} \, dt \quad (6.44)$$

$$\begin{aligned} &= -\frac{1}{\Delta t} \int_{-\Delta t}^0 \int_\Omega b(u_m^N) \phi \, d\mathbf{x} \, dt - \int_0^T \int_\Omega b(u_m^N(t)) \frac{\phi(t) - \phi(t - \Delta t)}{\Delta t} \, d\mathbf{x} \, dt, \\ &= \int_0^T \int_\Omega (b(u_m^0) - b(u_m^N(t))) \frac{\phi(t) - \phi(t - \Delta t)}{\Delta t} \, d\mathbf{x} \, dt, \end{aligned} \quad (6.45)$$

where we get the last equality using $\frac{1}{\Delta t} \int_{-\Delta t}^0 \phi \, dt = -\int_0^T \frac{\phi(t) - \phi(t - \Delta t)}{\Delta t} \, dt$. Letting $N, m \rightarrow \infty$ and using the strong convergence (6.35), we have

$$\int_0^T \int_\Omega v \phi \, d\mathbf{x} \, dt = \int_0^T \int_\Omega (b(u^0) - b(u) \partial_t \phi), \quad (6.46)$$

for all $\phi \in L^2(0, T; H_0^2(\Omega))$ with $\partial_t \phi \in L^1(0, T; L^\infty(\Omega))$ and $\phi(T) = 0$. The right side of (6.46) corresponds to the definition of the time derivative of $b(u)$ in the distributional sense as in Definition 2.6. Hence, we have $v = \partial_t b(u)$ and we conclude

$$\frac{b(u_m^N(t)) - b(u_m^N(t - \Delta t))}{\Delta t} \rightharpoonup \partial_t b(u) \quad \text{in } L^2(0, T; H_0^{-2}(\Omega)). \quad (6.47)$$

The existence of a function $u \in L^2(0, T; H_0^2(\Omega))$, the convergence results (6.40), and (6.47) imply that equation (6.34) convergences as $m, N \rightarrow \infty$ to equation (6.30) for all test function $\phi \in L^2(0, T; H_0^1(\Omega))$. Hence, the function u satisfies the first condition in Theorem 6.12. Clearly, the second condition in Theorem 6.12 is also satisfied using equations (6.46) and (6.47).

□

6.4.3 Uniqueness

In this subsection, we prove the uniqueness of the weak solution of the transformed problem (6.15), (6.16).

Theorem 6.13. *Let Assumption 6.3 be satisfied and the transformed saturation b be strictly monotone increasing, i.e. there exists a constant $a > 0$ such that*

$$\min(b'(\cdot)) > a > 0.$$

Then, problem (6.15) and (6.16) has a unique weak solution that satisfies the properties (6.30) and (6.31).

Proof. Assume that u_1 and u_2 are two weak solutions of problem (6.15) with the initial and boundary conditions (6.16) that satisfy the properties (6.30) and (6.31). Define also

$$g := b(u_1) - b(u_2). \quad (6.48)$$

Then, property (6.31) implies that $g \in L^\infty(0, T; H_0^{-2}(\Omega))$ and consequently $g \in L^2(0, T; H_0^{-2}(\Omega))$, where $L^2(0, T; H_0^{-2}(\Omega))$ is the space of all bounded functional L equipped with the norm (6.29). Thus, Riesz Representation theorem implies the existence of a unique function $w \in L^2(0, T; H_0^2(\Omega))$ such that for any time $\tau \in [0, T]$

$$\int_0^\tau \langle g, \phi \rangle dt = \int_0^\tau \langle w, \phi \rangle dt, \quad (6.49)$$

for all $\phi \in L^2(0, T; H_0^2(\Omega))$, where

$$\langle w, \phi \rangle := \int_\Omega \nabla w \cdot \nabla \phi \, d\mathbf{x} + \gamma \int_\Omega \Delta w \Delta \phi \, d\mathbf{x}. \quad (6.50)$$

Substituting the solutions u_1 and u_2 into equation (6.30), using the test function $w \in L^2(0, T; H_0^2(\Omega))$, subtracting the two equations, and using (6.48) gives

$$\begin{aligned} \int_0^\tau \int_\Omega \partial_t g w \, d\mathbf{x} \, dt + \int_0^\tau \int_\Omega (\nabla(u_1 - u_2) \cdot \nabla w + \gamma \Delta(u_1 - u_2) \Delta w) \, d\mathbf{x} \, dt \\ = \int_0^\tau \int_\Omega (K_f(b(u_1)) - K_f(b(u_2))) \mathbf{e}_3 \cdot \nabla w \, d\mathbf{x} \, dt. \end{aligned} \quad (6.51)$$

Approximating the first term on the left side of (6.51) using the backward difference quotient then applying summation by parts yields

$$\begin{aligned} \int_0^\tau \int_\Omega \frac{g(t) - g(t - \Delta t)}{\Delta t} w(t) \, d\mathbf{x} \, dt &= - \int_0^\tau \int_\Omega g(t) \frac{w(t) - w(t - \Delta t)}{\Delta t} \, d\mathbf{x} \, dt \\ &+ \frac{1}{\Delta t} \int_{\tau - \Delta t}^\tau \int_\Omega g(t) w(t) \, d\mathbf{x} \, dt - \frac{1}{\Delta t} \int_{-\Delta t}^0 \int_\Omega g(t) w(t) \, d\mathbf{x} \, dt. \end{aligned} \quad (6.52)$$

Using equations (6.49) and (6.50), the first term on the right side of (6.52) satisfies

$$\begin{aligned} \int_0^\tau \int_\Omega g(t) \frac{w(t) - w(t - \Delta t)}{\Delta t} \, d\mathbf{x} \, dt &= \int_0^\tau \int_\Omega \nabla w \cdot \frac{\nabla w(t) - \nabla w(t - \Delta t)}{\Delta t} \, d\mathbf{x} \, dt \\ &+ \gamma \int_0^\tau \int_\Omega \Delta w \frac{\Delta w(t) - \Delta w(t - \Delta t)}{\Delta t} \, d\mathbf{x} \, dt. \end{aligned}$$

Applying summation by parts to the right side of the above equation yields

$$\begin{aligned} \int_0^\tau \int_\Omega g(t) \frac{w(t) - w(t - \Delta t)}{\Delta t} \, d\mathbf{x} \, dt &= \frac{1}{2\Delta t} \int_{\tau - \Delta t}^\tau \int_\Omega |\nabla w|^2 + \gamma(\Delta w)^2 \, d\mathbf{x} \, dt \\ &- \frac{1}{2\Delta t} \int_{-\Delta t}^0 \int_\Omega |\nabla w|^2 + \gamma(\Delta w)^2 \, d\mathbf{x} \, dt. \end{aligned} \quad (6.53)$$

The second term on the right side of (6.52), using equations (6.49) and (6.50), satisfies

$$\frac{1}{\Delta t} \int_{\tau - \Delta t}^\tau \int_\Omega g(t) w(t) \, d\mathbf{x} \, dt = \frac{1}{\Delta t} \int_{\tau - \Delta t}^\tau \int_\Omega |\nabla w|^2 + \gamma(\Delta w)^2 \, d\mathbf{x} \, dt. \quad (6.54)$$

Similarly, the third term on the right side of (6.52) satisfies

$$\frac{1}{\Delta t} \int_{-\Delta t}^0 \int_\Omega g(t) w(t) \, d\mathbf{x} \, dt = \frac{1}{\Delta t} \int_{-\Delta t}^0 \int_\Omega |\nabla w|^2 + \gamma(\Delta w)^2 \, d\mathbf{x} \, dt \quad (6.55)$$

Substituting equation (6.53), (6.54), and (6.55) into equation (6.52) gives

$$\begin{aligned} \int_0^\tau \int_\Omega \frac{g(t) - g(t - \Delta t)}{\Delta t} w(t) \, d\mathbf{x} \, dt &= \frac{1}{2\Delta t} \int_{\tau - \Delta t}^\tau \int_\Omega |\nabla w|^2 + \gamma(\Delta w)^2 \, d\mathbf{x} \, dt \\ &- \frac{1}{2\Delta t} \int_{-\Delta t}^0 \int_\Omega |\nabla w|^2 + \gamma(\Delta w)^2 \, d\mathbf{x} \, dt. \end{aligned} \quad (6.56)$$

Using equation (6.49) and the initial choice (6.23), the second term on the right side of (6.56) satisfies

$$\int_{-\Delta t}^0 \int_{\Omega} |\nabla w|^2 + \gamma(\Delta w)^2 \, d\mathbf{x} \, dt = \int_{-\Delta t}^0 \int_{\Omega} gw \, d\mathbf{x} \, dt = 0.$$

Hence, letting $\Delta t \rightarrow 0$ in equation (6.56), we get that for almost all $\tau \in [0, T]$,

$$\int_0^{\tau} \int_{\Omega} \partial_t g w \, d\mathbf{x} \, dt = \frac{1}{2} \int_{\Omega} |\nabla w(\tau)|^2 + \gamma(\Delta w(\tau))^2 \, d\mathbf{x}. \quad (6.57)$$

Using (6.49) with $\phi = u_1 - u_2$, the second term on the left side of (6.51) satisfies

$$\begin{aligned} & \int_0^{\tau} \int_{\Omega} \nabla(u_1 - u_2) \cdot \nabla w + \gamma \Delta(u_1 - u_2) \Delta w \, d\mathbf{x} \, dt \\ &= \int_0^{\tau} \int_{\Omega} (u_1 - u_2) g \, d\mathbf{x} \, dt = \int_0^{\tau} \int_{\Omega} (u_1 - u_2) (b(u_1) - b(u_2)) \, d\mathbf{x} \, dt. \end{aligned} \quad (6.58)$$

The Lipschitz continuity of K_f and b imply the existence of a constant $L > 0$ such that $\max(b'(\cdot)), \max(K_f'(\cdot)) \leq L$. Using this property and Cauchy's inequality (2.19) with $\epsilon = \frac{1}{2L^2}$, the first term on the right side of equation (6.51) simplifies to

$$\begin{aligned} & \int_0^{\tau} \int_{\Omega} (K(b(u_1)) - K(b(u_2))) \mathbf{e}_3 \cdot \nabla w \, d\mathbf{x} \, dt \\ & \leq L \int_0^{\tau} \int_{\Omega} |(b(u_1) - b(u_2)) \mathbf{e}_3 \cdot \nabla w| \, d\mathbf{x} \, dt \\ & \leq \frac{1}{2L} \int_0^{\tau} \int_{\Omega} (b(u_1) - b(u_2))^2 \, d\mathbf{x} \, dt + \frac{L^3}{2} \int_0^{\tau} \int_{\Omega} |\nabla w|^2 \, d\mathbf{x} \, dt \\ & \leq \frac{1}{2} \int_0^{\tau} \int_{\Omega} |(b(u_1) - b(u_2))(u_1 - u_2)| \, d\mathbf{x} \, dt + \frac{L^3}{2} \int_0^{\tau} \int_{\Omega} |\nabla w|^2 \, d\mathbf{x} \, dt. \end{aligned}$$

As the function b is monotone increasing, it follows that

$$\begin{aligned} & \int_0^{\tau} \int_{\Omega} (K(b(u_1)) - K(b(u_2))) \mathbf{e}_3 \cdot \nabla w \, d\mathbf{x} \, dt \\ & \leq \frac{1}{2} \int_0^{\tau} \int_{\Omega} (b(u_1) - b(u_2))(u_1 - u_2) \, d\mathbf{x} \, dt + \frac{L^3}{2} \int_0^{\tau} \int_{\Omega} |\nabla w|^2 \, d\mathbf{x} \, dt. \end{aligned} \quad (6.59)$$

Substituting (6.57), (6.58), and (6.59) into (6.51) yields, for almost all $\tau \in [0, T]$,

$$\begin{aligned} & \frac{1}{2} \int_{\Omega} |\nabla w(\tau)|^2 \, d\mathbf{x} + \frac{1}{2} \int_{\Omega} (\Delta w(\tau))^2 \, d\mathbf{x} + \frac{1}{2} \int_0^{\tau} \int_{\Omega} (b(u_1) - b(u_2))(u_1 - u_2) \, d\mathbf{x} \, dt \\ & \leq \frac{L^3}{2} \int_0^{\tau} \int_{\Omega} |\nabla w|^2 \, d\mathbf{x} \, dt. \end{aligned} \quad (6.60)$$

Since b is a monotone increasing function, the third term on the left side of equation (6.60) is nonnegative. Thus, applying Gronwall's inequality to the first term on the left side gives

$$\int_{\Omega} |\nabla w(\tau)|^2 d\mathbf{x} = 0, \quad (6.61)$$

for any $\tau \in [0, T]$. Substituting (6.61) in equation (6.60) yields

$$\int_0^\tau \int_{\Omega} (b(u_1) - b(u_2))(u_1 - u_2) d\mathbf{x} dt = 0. \quad (6.62)$$

Using the strict monotonicity of b , equation (6.62) implies that $u_1 = u_2$.

□

6.5 Regularity

In this section, we improve the regularity of the weak solution from $u \in L^2(0, T; H_0^2(\Omega))$ to $u \in H^1(\Omega \times (0, T)) \cap L^2(0, T; H_0^2(\Omega))$. For this, it is sufficient to prove that $\partial_t u \in L^2(\Omega \times (0, T))$.

Lemma 6.14. *Let Assumption 6.3 be satisfied and the transformed saturation b be strictly monotone increasing, i.e. there exists a constant $a > 0$ such that $\min(b'(\cdot)) > a > 0$. Then, the weak solution $u \in L^2(0, T; H_0^2(\Omega))$ of the transformed problem (6.15) and (6.16) satisfies the property that $\partial_t u \in L^2(\Omega \times (0, T))$.*

Proof. Multiplying equation (6.22) by $\frac{\alpha_{m,i}^n - \alpha_{m,i}^{n-1}}{\Delta t}$, summing for $i = 1, \dots, m$, integrating from 0 to T , and using the Gauss theorem yields

$$\begin{aligned} & \frac{1}{(\Delta t)^2} \int_0^T \int_{\Omega} (b(u_m^N(t)) - b(u_m^N(t - \Delta t))) (u_m^N(t) - u_m^N(t - \Delta t)) d\mathbf{x} dt \\ & + \int_0^T \int_{\Omega} \nabla u_m^N(t) \cdot \frac{\nabla u_m^N(t) - \nabla u_m^N(t - \Delta t)}{\Delta t} + \gamma \Delta u_m^N(t) \frac{\Delta u_m^N(t) - \Delta u_m^N(t - \Delta t)}{\Delta t} d\mathbf{x} dt \\ & = - \int_0^T \int_{\Omega} \nabla \cdot (K_f(b(u_m^N(t))) \mathbf{e}_3) \frac{u_m^N(t) - u_m^N(t - \Delta t)}{\Delta t} d\mathbf{x} dt. \end{aligned} \quad (6.63)$$

Using the strict positivity of b' , there exists a constant $a > 0$ such that $\min(b'(\cdot)) > a > 0$. Thus, the first term on the left side of (6.63) satisfies

$$\begin{aligned} & \frac{1}{(\Delta t)^2} \int_0^T \int_{\Omega} (b(u_m^N(t)) - b(u_m^N(t - \Delta t))) (u_m^N(t) - u_m^N(t - \Delta t)) \, d\mathbf{x} \, dt \\ & \leq a \int_0^T \int_{\Omega} \left(\frac{u_m^N(t) - u_m^N(t - \Delta t)}{\Delta t} \right)^2 \, d\mathbf{x} \, dt. \end{aligned} \quad (6.64)$$

Applying summation by parts to the second term on the left side of (6.63) yields

$$\begin{aligned} & 2 \int_0^T \int_{\Omega} \nabla u_m^N \cdot \frac{\nabla u_m^N(t) - \nabla u_m^N(t - \Delta t)}{\Delta t} \, d\mathbf{x} \, dt \\ & = \frac{1}{\Delta t} \int_{T-\Delta t}^T \int_{\Omega} |\nabla u_m^N(t)|^2 \, d\mathbf{x} \, dt - \frac{1}{\Delta t} \int_{-\Delta t}^0 \int_{\Omega} |\nabla u_m^N(t)|^2 \, d\mathbf{x} \, dt. \end{aligned}$$

Then, using Remark 6.6, we get

$$\int_0^T \int_{\Omega} \nabla u_m^N \cdot \frac{\nabla u_m^N(t) - \nabla u_m^N(t - \Delta t)}{\Delta t} \, d\mathbf{x} \, dt = \frac{1}{2} \int_{\Omega} |\nabla u_m^N(T)|^2 - |\nabla u_m^0|^2 \, d\mathbf{x}. \quad (6.65)$$

Similarly, the third term on the right side of (6.63) simplifies to

$$\int_0^T \int_{\Omega} \Delta u_m^N \frac{\Delta u_m^N(t) - \Delta u_m^N(t - \Delta t)}{\Delta t} \, d\mathbf{x} \, dt = \frac{1}{2} \int_{\Omega} (\Delta u_m^N(T))^2 - (\Delta u_m^0)^2 \, d\mathbf{x}. \quad (6.66)$$

The Lipschitz continuity of K_f and b implies the existence of a constant $L > 0$ such that $\max(b'(\cdot)), \max(K_f'(\cdot)) \leq L$. Using this property and Cauchy's inequality with $\epsilon = \frac{L^2}{a}$, the right side of (6.63) gives

$$\begin{aligned} & \int_0^T \int_{\Omega} \left| \nabla \cdot (K_f(b(u_m^N)) \mathbf{e}_3) \frac{u_m^N(t) - u_m^N(t - \Delta t)}{\Delta t} \right| \, d\mathbf{x} \, dt \\ & \leq L^2 \int_0^T \int_{\Omega} \left| \nabla u_m^N \frac{u_m^N(t) - u_m^N(t - \Delta t)}{\Delta t} \right| \, d\mathbf{x} \, dt \\ & \leq \frac{L^4}{a} \int_0^T \int_{\Omega} |\nabla u_m^N|^2 \, d\mathbf{x} \, dt + \frac{a}{4} \int_0^T \int_{\Omega} \left(\frac{u_m^N(t) - u_m^N(t - \Delta t)}{\Delta t} \right)^2 \, d\mathbf{x} \, dt. \end{aligned} \quad (6.67)$$

Substituting (6.64), (6.65), (6.66), and (6.67) into inequality (6.63) gives

$$\begin{aligned} & \frac{3a}{4} \int_0^T \int_{\Omega} \left(\frac{u_m^N(t) - u_m^N(t - \Delta t)}{\Delta t} \right)^2 d\mathbf{x} dt + \frac{1}{2} \int_{\Omega} |\nabla u_m^N(T)|^2 + \gamma (\Delta u_m^N(T))^2 d\mathbf{x} \\ & \leq \frac{1}{2} \int_{\Omega} |\nabla u_m^0|^2 + \gamma (\Delta u_m^0)^2 d\mathbf{x} + \frac{L^4}{a} \int_0^T \int_{\Omega} |\nabla u_m^N|^2 d\mathbf{x} dt. \end{aligned}$$

Then, Lemma 6.7 implies the existence of a constant $c > 0$ such that

$$\int_0^T \int_{\Omega} \left(\frac{u_m^N(t) - u_m^N(t - \Delta t)}{\Delta t} \right)^2 d\mathbf{x} dt \leq c.$$

This uniform estimate implies that, up to a subsequence,

$$\frac{u_m^N(t) - u_m^N(t - \Delta t)}{\Delta t} \rightharpoonup \partial_t u \quad \text{in } L^2(\Omega \times (0, T)). \quad (6.68)$$

This completes the proof. \square

Corollary 6.15. *Let the assumptions of Theorem 6.13 be satisfied. Then, we have the strong convergence*

$$u_m^n \rightarrow u \quad \text{in } L^2(\Omega \times (0, T)).$$

Proof. The proof follows using the estimates in Lemma 6.7 and 6.14 together with Rellich Kondrachov Compactness theorem 2.22 with dimension $n = 4$ of the domain $\Omega \times (0, T)$. \square

Corollary 6.16. *Let the assumptions of Theorem 6.13 be satisfied. Then, the transformed saturation b satisfies*

$$b(u) \in C([0, T]; L^2(\Omega)),$$

and the initial condition satisfies

$$b(u(0)) = b(u^0) \quad \text{almost everywhere.}$$

Proof. The Lipschitz continuity of the transformed saturation b and Lemma 6.14 imply that

$$\partial_t b(u) = b'(u) \partial_t u \in L^2(\Omega \times (0, T)). \quad (6.69)$$

Then, Theorem 2.19 in Chapter 2 yields that

$$b(u) \in C([0, T]; L^2(\Omega)). \quad (6.70)$$

To prove that $b(u(0)) = b(u^0)$ almost everywhere, we choose a test function $\phi \in C^1([0, T], H_0^2(\Omega))$ in equation (6.30) with $\phi(T) = 0$. Then, Gauss' theorem gives

$$\begin{aligned} \int_0^T \int_{\Omega} \left(b(u) \partial_t \phi - K_f(b(u)) \mathbf{e}_3 \cdot \nabla \phi + \nabla u \cdot \nabla \phi + \gamma \Delta u \Delta \phi \right) d\mathbf{x} dt \\ = \int_{\Omega} b(u(0)) \phi(0) d\mathbf{x}. \end{aligned} \quad (6.71)$$

Applying summation by parts to the first term in equation (6.34) yields

$$\begin{aligned} \frac{1}{\Delta t} \int_0^{\tau} \int_{\Omega} b(u_m^N(t)) (\phi(t) - \phi(t - \Delta t)) d\mathbf{x} dt + \int_0^{\tau} \int_{\Omega} \nabla u_m^N \cdot \nabla \phi d\mathbf{x} dt \\ + \gamma \int_0^{\tau} \int_{\Omega} \Delta u_m^N \Delta \phi d\mathbf{x} dt - \int_0^{\tau} \int_{\Omega} K_f(b(u_m^N)) \mathbf{e}_3 \cdot \nabla \phi d\mathbf{x} dt \\ = \int_{\Omega} b(u_m^0) \phi(0) dx dz. \end{aligned} \quad (6.72)$$

Letting $m, N \rightarrow \infty$ in equation (6.72) yields, up to a subsequence, that

$$\begin{aligned} \int_0^{\tau} \int_{\Omega} \partial_t \phi b(u(t)) d\mathbf{x} dt + \int_0^{\tau} \int_{\Omega} \nabla u \cdot \nabla \phi d\mathbf{x} dt + \gamma \int_0^{\tau} \int_{\Omega} \Delta u \Delta \phi d\mathbf{x} dt \\ - \int_0^{\tau} \int_{\Omega} K_f(b(u)) \mathbf{e}_3 \cdot \nabla \phi d\mathbf{x} dt = \int_{\Omega} b(u^0) \phi(0) dx dz. \end{aligned} \quad (6.73)$$

since $u_m^0 \rightarrow u^0$ in $L^2(\Omega)$ as $m \rightarrow \infty$. As $\phi(0)$ is arbitrarily chosen, comparing equation (6.71) and (6.73) yields that $b(u(0)) = b(u^0)$ almost everywhere. This completes the proof. \square

6.6 Well-posedness of the Fourth-Order Model

In this section, we utilize the well-posedness of the transformed problem (6.15) and (6.16) to prove the well-posedness of the fourth-order model (6.12) and (6.13). For this, we stress that the coefficients S, S', K_f are strictly positive. Then, we apply the inverse of Kirchhoff's transformation to the weak solution of the transformed problem (6.15) and (6.16).

Definition 6.17. *We call $p \in H^1(\Omega \times (0, T))$ a weak solution of the fourth-order problem (6.12) and (6.13) if it satisfies the conditions*

1. $K_f(S(p)) \in L^2(\Omega \times (0, T))$, $\partial_t S(p) \in L^2(\Omega \times (0, T))$ and $\nabla \cdot (K_f(S(p))\nabla p) \in L^2(\Omega \times (0, T))$ such that

$$\int_0^T \int_{\Omega} \left(\partial_t S(p)\phi - K_f(S(p))\mathbf{e}_3 \cdot \nabla \phi + K_f(S(p))\nabla p \cdot \nabla \phi \right) d\mathbf{x} dt + \gamma \int_0^T \int_{\Omega} \nabla \cdot (K_f(S(p))\nabla p) \Delta \phi d\mathbf{x} dt = 0,$$

for every test function $\phi \in L^2(0, T; H_0^2(\Omega))$.

2. $S(p(0)) = S(p^0)$ almost everywhere.

Theorem 6.18. *Assume that the initial condition in (6.13) satisfies $p^0 \in H_0^2(\Omega)$ and the saturation function $S \in C^1(\mathbb{R})$ is bounded, strictly positive, and strictly monotone increasing. Assume also that the conductivity function $K_f \in C^1(\mathbb{R})$ is strictly positive, bounded, and monotone increasing. Let $u \in H^1(\Omega \times (0, T)) \cap L^2(0, T; H_0^2(\Omega))$ be the weak solution of the transformed problem (6.15) and (6.16) and $p = \psi^{-1}(u) \in H^1(\Omega \times (0, T))$, where ψ is Kirchhoff's transformation. Then, p is the unique weak solution of the fourth-order problem (6.12) and (6.13) according to Definition 6.17.*

Proof. Using equation (6.14), Lemma 6.14, the boundedness and the strict positivity of K_f , we have

$$\begin{aligned} \nabla p &= \frac{\nabla u}{K_f(S(\psi^{-1}(u)))} \in L^2(\Omega \times (0, T)), \\ \partial_t p &= \frac{\partial_t u}{K_f(S(\psi^{-1}(u)))} \in L^2(\Omega \times (0, T)), \end{aligned} \tag{6.74}$$

where there exists a constant $\delta > 0$ such that $K_f > \delta$. These estimates and Poincaré's inequality imply that $p \in H^1(\Omega \times (0, T))$. In addition to this, we have

$$\begin{aligned} \nabla \cdot (K_f(S(p))\nabla p) &= \Delta u \in L^2(\Omega \times (0, T)), \\ S(p) &= b(\Psi^{-1}(u)) \in L^\infty(0, T; L^1(\Omega)), \end{aligned} \tag{6.75}$$

The Lipschitz continuity of the saturation S and the second equation in (6.74) imply

$$\partial_t S(p) = S'(p)\partial_t p \in L^2(\Omega \times (0, T)).$$

These estimates imply that p satisfies the conditions in Definition 6.17 and, thus, is a weak solution of the fourth-order model (6.12) and (6.13). In the

same way, if $p \in H^1(\Omega \times (0, T))$ is a weak solution of the fourth-order problem (6.12) and (6.13) as in Definition 6.17, then the Kirchhoff-transformed $u = \psi(p) \in L^2(0, T; H_0^2(\Omega))$ is a weak solution of the transformed fourth-order problem (6.15) and (6.16). This implies that the fourth-order problem (6.12), (6.13) and the transformed fourth-order problem (6.15) and (6.16) are equivalent. This equivalency, the uniqueness of the weak solution u of the transformed problem by Theorem 6.13, and the strict monotonicity of Kirchhoff's transformation imply the uniqueness of the weak solution p of the fourth-order problem (6.12) and (6.13). This completes the proof. \square

6.7 Conclusion

We studied the vertical infiltration of water through unsaturated soils and the formation of saturation overshoots. We proposed an extension of Richards' equation that violates the maximum principle. The proposed model (6.12) is related to the fourth-order model in [17], for which numerical investigations show the ability to describe saturation overshoots [18].

We proved the well-posedness of our proposed fourth-order model (6.12) in three main steps:

1. We applied Kirchhoff's transformation to the fourth-order model (6.12) and (6.13) such that the nonlinearities in the second- and fourth-order terms are transformed to the term with time derivative.
2. We proved the well-posedness of the transformed fourth-order model by approximating the time derivative in the transformed model using the backward difference quotient, then applying Galerkin's method. After proving a set of a priori estimates on the sequence of discrete solutions, we obtained a weak convergence in the space $L^2(0, T; H_0^2(\Omega))$. Then, we proved that the weak limit of this sequence is the weak solution of the transformed model. Finally, we improved the regularity of the weak solution.
3. We proved the well-posedness of the original fourth-order model (6.12) and (6.13) using the inverse of Kirchhoff's transformation and the well-posedness of the transformed model.

Chapter 7

Summary and Outlook

7.1 Summary

In this thesis, we proposed mathematical models to describe transport processes of incompressible fluids in saturated and unsaturated media in the subsurface. Understanding these processes is crucial for many environmental and industrial applications, such as the infiltration of contaminants or rain water through the soil into aquifers and the flow of extracted oil from reservoirs. In modeling these transport processes, three aspects were taken into account: firstly, reducing models' complexity based on natural properties of the transport process, secondly, describing more physical properties such as vertical dynamics and saturation overshoots, thirdly, proving models' well-posedness.

In saturated media, fluid flows are typically described using the two-phase flow model, which is a coupled system of two unknowns. This coupled structure of the model and the large volume of saturated media lead to very high computational complexity. However, saturated media are in general flat with small thickness, such that fluid flows are almost horizontal. Based on this natural behavior of the flows, several approaches have been suggested to reduce the complexity of the two-phase flow model [13, 28, 29, 39, 43, 53]. We are interested in a model reduction approach that reduces the number of unknowns [53]. Assuming negligible gravity and capillary pressure forces, the reduced model is a nonlinear transport equation of the unknown saturation, which we call the VE-model.

To demonstrate the validity and numerical efficiency of the VE-model, we first present a set of classical and recently derived models that also describe almost horizontal flows in saturated media. These models are the two-phase flow model, a vertically averaged model, and a multiscale model proposed in [31]. Then, we performed several numerical tests that compare the VE-model to these models.

These tests show: first, numerical solutions of the two-phase flow model converge to the corresponding solution of the VE-model as the geometrical parameter $\gamma = \frac{\text{domain thickness}}{\text{domain length}}$ approaches zero. Additionally, the computational complexity of the VE-model is significantly reduced over that of the two-phase flow models. Second, fluids' spreading speed is well-estimated using the VE-model in contrast to the vertically integrated model. Third, the VE-model is equivalent to the multiscale model. However, the computational complexity of the VE-model is notably reduced over that of the multiscale algorithm proposed in [31].

Motivated by the numerical efficiency of the VE-model, we proposed an extension to describe almost horizontal flows in macroscopically heterogeneous media as well as in media with high porosity, where fluids' velocity is often described using Brinkman's equation instead of Darcy's law. The extended model is a third-order pseudo-parabolic equation of saturation only, which we call the Brinkman VE-model. To clarify the numerical advantages to this model, we executed a set of numerical experiments that compare the Brinkman VE-model to the Brinkman two-phase flow model and the VE-model. These experiments show the reduced computational complexity of our proposed Brinkman VE-model. Additionally, the Brinkman VE-model is able to describe saturation overshoots in contrast to the VE-model.

We investigated the well-posedness of the Brinkman VE-model. First, we proved the existence of weak solutions for the model by discretizing the time derivatives in the model, then applying Galerkin's method. After proving a priori estimates on the sequence of weak solutions for the approximated problem, we concluded a strong convergence. Then, we proved that the limit of the convergent sequence is a weak solution of the Brinkman VE-model. Second, we proved the uniqueness of weak solutions for a special case of the Brinkman VE-model where the fractional flow function and the horizontal velocity are assumed to be linear.

In unsaturated media, like the soil, fluids infiltrate vertically under the effect of gravity. Such infiltration processes are described using Richards' equation, which is a second-order parabolic equation of saturation. This equation is unable to describe the phenomenon of saturation overshoots, as it satisfies the maximum principle. Therefore, different extensions have been proposed [17, 32, 46]. We proposed a fourth-order extension of Richards' equation. We also proved the well-posedness of our extended model in three steps: first, we applied Kirchhoff's transformation to linearize the higher-order terms in the model. Second, we proved the well-posedness of the transformed model. Third, we applied the inverse of Kirchhoff's transformation to prove the well-posedness of the original model.

7.2 Outlook

In the following, we give a list of future work that we are interested in:

- The VE-model is derived by Yortsos [53] to describe almost unidirectional flows in a two-dimensional vertical cross section of a three-dimensional reservoirs. For future work, we recommend extending the model into three-dimensional reservoirs where fluid flows are axisymmetric.
- We showed a numerical convergence of the Brinkman two-phase flow model to the Brinkman VE-model, as the geometrical parameter γ approaches zero. Since the existence of weak solution for the Brinkman two-phase flow model (4.3) is proved in [15] and we proved the existence of weak solutions for the Brinkman VE-model in Theorem 5.13. Hence, we recommend finding error estimates of the form,

$$|S^\gamma - S| \leq C \gamma^r,$$

for some constants $C, r > 0$, where S^γ is a weak solution of the dimensionless Brinkman two-phase flow model (4.20) and $S := \lim_{\gamma \rightarrow 0} S^\gamma$ is a weak solution of Brinkman VE-model (4.30), (4.31), and (4.32).

- The accuracy of the Brinkman VE-model (and the VE-model) depends on the viscosity ratio M of the fluids flowing in the medium. For future work, we recommend extending the derivation of the Brinkman VE-model (and the VE-model) such that the asymptotic analysis depends also on the viscosity parameter M .
- Richards' equation is a second-order parabolic equation that describes the vertical infiltration of fluids into unsaturated soil due to gravity. This equation satisfies the maximum principle and, consequently, is unable to predict saturation overshoots. In contrast to this, the fourth-order extension of Richards' equation (6.10) violates the maximum principle and saturation overshoots is expected. However, saturation overshoots is mathematically identified by undercompressive traveling wave solutions, which arise only when the flux function in the model is nonconvex [9]. For future work, we recommend investigating the existence (or nonexistence) of undercompressive traveling waves of the fourth-order extension (6.10).

The convex convective term in Richards' equation corresponds to the gravity force only and neglects the effect of viscous forces. Since the displaced fluid

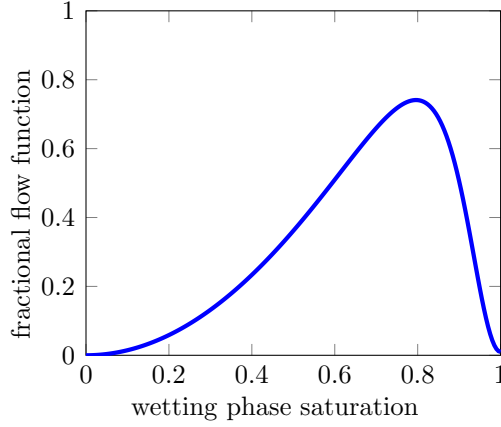


Figure 7.1: The flux function $f(S)v - Gr\bar{\lambda}$ in a fourth-order extension of Richards' equations after taking the effect of viscous forces into account.

in the process of water infiltration is the less viscous gas, we expect that the viscous force influences the flow in the opposite direction to the driving gravity force. This interaction between the two forces yields a nonconvex flux function similar to that in the model describing thin film flows [9]. Thus, we suggest taking the viscous force into account in the fourth-order model (6.12) such that the model is reformulated in the fractional flow formulation,

$$\begin{aligned} \phi \partial_t S + \partial_z (f(S)v - Gr\bar{\lambda}(S)) + \frac{1}{g} \nabla \cdot (K_f(S) \nabla p_c(S)) \\ - \frac{\epsilon}{g} \Delta \nabla \cdot (K_f(S) \nabla p_c(S)) = 0, \end{aligned} \quad (7.1)$$

where

$$Gr = \frac{K_3 g (\rho_n - \rho_w)}{q}, \quad (7.2)$$

$\bar{\lambda}$ is the diffusion function defined in equation (2.7), K_3 is the intrinsic permeability in the vertical direction, q is the speed at the inflow boundary, and ϵ is a small parameter. The flux function in this model is nonconvex as illustrated in Figure 7.1, where the parameters for water and gas phases are given as $\mu_w = 10^{-3}$, $\mu_n = 1.7 \times 10^{-5}$, $\rho_w = 10^3$, $\rho_n = 1.2$. We also considered the parameters $g = 9.81$, $K_3 = 1.5 \times 10^{-9}$, $q = 10^{-2}$, and $v = 10^{-2}$.

For future work, we recommend performing numerical examples that compare the formation of saturation overshoots using the fourth-order extension (6.10), with a convex flux function, and the fourth-order extension (7.1) with a nonconvex flux function.

Bibliography

- [1] R. A. Adams and J. J. F. Fournier. *Sobolev spaces*, volume 140 of *Pure and Applied Mathematics*. Elsevier/Academic Press, Amsterdam, second edition, 2003.
- [2] W. H. Alt and S. Luckhaus. Quasilinear elliptic-parabolic differential equations. *Mathematische Zeitschrift*, 183(3):311–341, 1983.
- [3] J. L. Auriault. On the domain of validity of Brinkman’s equation. *Transport in Porous Media*, 79(2):215–223, 2009.
- [4] J. L. Auriault, C. Geindreau, and C. Boutin. Filtration law in porous media with poor separation of scales. *Transport in Porous Media*, 60(1):89–108, 2005.
- [5] J. Bear. *Dynamics of fluids in porous media*. Dover, 1988.
- [6] J. Bear and Y. Bachmat. *Introduction to modeling of transport phenomena in porous media*. Kluwer Academic Publishers, 1991.
- [7] A. Yu. Beliaev and S. M. Hassanizadeh. A theoretical model of hysteresis and dynamic effects in the capillary relation for two-phase flow in porous media. *Transport in Porous Media*, 43(3):487–510, Jun 2001.
- [8] A. L. Bertozzi, A. Munch, and M. Shearer. Undercompressive shocks in thin film flows. *Physica D*, 134:431–464, 1999.
- [9] A. L. Bertozzi and M. Shearer. Existence of undercompressive travelling waves in thin film equations. *SIAM Journal on Mathematical Analysis*, pages 194–213, 2000.
- [10] H. C. Brinkman. A calculation of the viscous force exerted by a flowing fluid on a dense swarm of particles. *Applied Scientific Research*, 1(1):27–34, 1949.
- [11] R. H. Brooks and A. T. Corey. *Hydraulic properties of porous media*. Hydrology Papers. Colorado State University, 1964.
- [12] X. Cao and I.S. Pop. Uniqueness of weak solutions for a pseudo-parabolic equation modeling two phase flow in porous media. *Applied Mathematics Letters*, 46:25–30, 2015.

- [13] H. Class, A. Ebigbo, R. Helmig, H. K. Dahle, J. M. Nordbotten, M. A. Celia, P. Audigane, M. Darcis, J. Ennis-King, Y. Fan, B. Flemisch, S. E. Gasda, M. Jin, S. Krug, D. Labregere, Beni A. N., R. J. Pawar, A. Sbai, S. G. Thomas, L. Trenty, and L. Wei. A benchmark study on problems related to CO₂ storage in geologic formations. *Computational Geosciences*, 13(4):409–434, 2009.
- [14] K. H. Coats, J. R. Dempsey, and J. H. Henderson. The use of vertical equilibrium in two-dimensional dimulation of three-dimensional reservoir performance. *Society of Petroleum Engineers*, 11:63–71, 1971.
- [15] G. M. Coclite, S. Mishra, N. H. Risebro, and F. Weber. Analysis and numerical approximation of Brinkman regularization of two-phase flows in porous media. *Computational Geosciences*, 18(5):637–659, 2014.
- [16] B. Court, K. W. Bandilla, M. A. Celia, A. Janzen, M. Dobossy, and J. M. Nordbotten. Applicability of vertical-equilibrium and sharp-interface assumptions in CO₂ sequestration modeling. *International Journal of Greenhouse Gas Control*, 10:134–147, 2012.
- [17] L. Cueto-Felgueroso and R. Juanes. Nonlocal interface dynamics and pattern formation in gravity-driven unsaturated flow through porous media. *Physical Review Letters*, 101:244504, 2008.
- [18] L. Cueto-Felgueroso and R. Juanes. A phase field model of unsaturated flow. *Water Resources Research*, 45(10), 2009.
- [19] L. Cueto-Felgueroso and R. Juanes. Stability analysis of a phase-field model of gravity-driven unsaturated flow through porous media. *Physical Review Letters*, 79:036301, 2009.
- [20] G. Dal Maso, P. G. LeFloch, and F. Murat. Definition and weak stability of nonconservative products. *Journal des Mathématiques Pures et Appliquées*, 74:483–548, 1995.
- [21] D. A. DiCarlo. Experimental measurements of saturation overshoot on infiltration. *Water Resources Research*, 40(4), 2004.
- [22] D. A. DiCarlo. Stability of gravity-driven multiphase flow in porous media: 40 years of advancements. *Water Resources Research*, 49(6):4531–4544, 2013.
- [23] E. C. Donaldson, G. V. Chilingarian, and T. F. Yen, editors. *Enhanced oil recovery, IIProcesses and Operations*. Elsevier, 1989.
- [24] A. G. Egorov, R. Z. Dautov, J. L. Nieber, and Al. Y. Sheshukov. Stability analysis of gravity-driven infiltrating flow. *Water Resources Research*, 39(9), 2003.
- [25] L. C. Evans. Partial differential equations. *American Mathematical Society*, 2010.

- [26] Y. Fan and I. S. Pop. A class of pseudo-parabolic equations: existence, uniqueness of weak solutions, and error estimates for the Euler-implicit discretization. *Mathematical Methods in the Applied Sciences*, 34(18):2329–2339, 2011.
- [27] Y. Fan and I. S. Pop. Equivalent formulations and numerical schemes for a class of pseudo-parabolic equations. *Journal of Computational and Applied Mathematics*, 246:86–93, July 2013.
- [28] S. E. Gasda, J. M. Nordbotten, and M. A. Celia. Vertical equilibrium with sub-scale analytical methods for geological CO₂ sequestration. *Computational Geosciences*, 13:469–481, 2009.
- [29] S. E. Gasda, J. M. Nordbotten, and M. A. Celia. Vertically averaged approaches for CO₂ migration with solubility trapping. *Water Resources Research*, 47, 2011.
- [30] D. Gilbarg and N. S. Trudinger. *Elliptic partial differential equations of second order*. Springer-Verlag, Berlin, 1977.
- [31] B. Guo, K. W. Bandilla, F. Doster, E. Keilegavlen, and M. A. Celia. A vertically integrated model with vertical dynamics for CO₂ storage. *Water Resources Research*, 50(8):6269–6284, 2014.
- [32] S. M. Hassanizadeh and W. G. Gray. Thermodynamic basis of capillary pressure in porous media. *Water Resources Research*, 29:3389–3406, 1993.
- [33] R. Helmig. *Multiphase flow and transport processes in the subsurface*. Springer-Verlag, 1997.
- [34] D. E. Hill and J.-Y. Parlange. Wetting front instability in layered soils. *Soil Science Society of America Journal*, 36(5):697–702, 1972.
- [35] R. Huber and R. Helmig. Multiphase flow in heterogeneous porous media: A classical finite element method versus an implicit pressure–explicit saturation-based mixed finite element–finite volume approach. *International Journal for Numerical Methods in Fluids*, 29(8):899–920, 1999.
- [36] H. E. Huppert. Flow and instability of a viscous current down a slope. *Nature*, 300:427–429, 1982.
- [37] D. Kröner. *Numerical schemes for conservation laws*. Wiley-Teubner, 1997.
- [38] O. A. Ladyzhenskaya and N. N. Ural'tseva. *Linear and quasilinear elliptic equations: Translated by Scripta Technica. Translation editor: Leon Ehrenpreis*. Academic Press New York, 1968.
- [39] L. W. Lake. *Enhanced oil recovery*. Prentice Hall Englewood Cliffs, N.J, 1989.
- [40] G. Menon and F. Otto. Dynamic scaling in miscible viscous fingering. *Communications in Mathematical Physics*, 257(2):303–317, 2005.

- [41] G. Menon and F. Otto. Fast communication: Diffusive slowdown in miscible viscous fingering. *Communications in Mathematical Sciences*, 4(1):267–273, 2006.
- [42] J. L. Nieber, R. Z. Dautov, A. G. Egorov, and A. Y. Sheshukov. Dynamic capillary pressure mechanism for instability in gravity-driven flows; Review and extension to very dry conditions. *Transport in Porous Media*, 58:147–172, 2005.
- [43] J. M. Nordbotten and M. A. Celia. Similarity solutions for fluid injection into confined aquifers. *Journal of Fluid Mechanics*, 561:307–327, 2006.
- [44] C. Parés and M. L. Muñoz Ruiz. On some difficulties of the numerical approximation of nonconservative hyperbolic systems. *Boletín de la Sociedad Española de Matemática Aplicada*, 2009.
- [45] C. Z. Qin and S. M. Hassanizadeh. Multiphase flow through multilayers of thin porous media: General balance equations and constitutive relationships for a solid–gas–liquid three-phase system. *International Journal of Heat and Mass Transfer*, 70:693–708, 2014.
- [46] B. Schweizer. The Richards equation with hysteresis and degenerate capillary pressure. *Journal of Differential Equations*, 252(10):5594–5612, 2012.
- [47] U. Shavit, G. Bar-Yosef, R. Rosenzweig, and S. Assouline. Modified Brinkman equation for a free flow problem at the interface of porous surfaces: The Cantor-Taylor brush configuration case. *Water Resources Research*, 38(12):56–1–56–13, 2002.
- [48] C. J. van Duijn, Y. Fan, L. A. Peletier, and I. S. Pop. Travelling wave solutions for degenerate pseudo-parabolic equations modelling two-phase flow in porous media. *Nonlinear Analysis: Real World Applications*, 14(3):1361–1383, 2013.
- [49] C. J. van Duijn, L. A. Peletier, and I. S. Pop. A New Class of Entropy Solutions of the Buckley–Leverett Equation. *SIAM Journal on Mathematical Analysis*, 39(2):507–536, 2007.
- [50] C. J. van Duijn, G. J. M. Pieters, and P. A. C. Raats. Steady flows in unsaturated soils are stable. *Transport in Porous Media*, 57(2):215–244, Nov 2004.
- [51] M. T. van Genuchten. A closed-form equation for predicting the hydraulic conductivity of unsaturated soils. *Soil science society of America journal*, 44(5):892–898, 1980.
- [52] Y. Yokoyama and L. W. Lake. *The effects of capillary pressure on immiscible displacements in stratified porous media*. Society of Petroleum Engineers, 1981.
- [53] Y. C. Yortsos. A theoretical analysis of vertical flow equilibrium. *Transport in Porous Media*, 18:107–129, 1995.

- [54] Y. C. Yortsos and D. Salin. On the selection principle for viscous fingering in porous media. *Journal of Fluid Mechanics*, 557:225–236, 2006.
- [55] V. J. Zapata and L. W. Lake. *A theoretical analysis of viscous crossflow*. Society of Petroleum Engineers, 1981.